The Institute of Paper Chemistry

Appleton, Wisconsin

Doctor's Dissertation

An Investigation of the Effect of Fiber Structural Properties on the Compression Response of Fibrous Beds

Robert Lewis Jones

June, 1962

AN INVESTIGATION OF THE EFFECT OF FIBER STRUCTURAL PROPERTIES ON THE COMPRESSION RESPONSE OF FIBROUS BEDS

A thesis submitted by

Robert Lewis Jones

B.Ch.E. 1957, Rensselaer Polytechnic Institute
M.S. 1959, Lawrence College

in partial fulfillment of the requirements
of The Institute of Paper Chemistry
for the degree of Doctor of Philosophy
from Lawrence College,
Appleton, Wisconsin

June, 1962

TABLE OF CONTENTS

PRESENTATION OF THE PROBLEM

The rheological behavior of nonwoven fibrous structures offers an area for study which is of great importance to the paper industry. By far the largest amount of work dealing with mechanical behavior of fibrous structures has been carried out on dry paper in tension. In addition to the work on paper, extensive studies have been made on individual fibers or filaments in tension. However, the behavior of fibrous systems under compressive stress has received much less attention than either of these areas.

There are a number of places in the paper manufacturing operation where compression of fiber structures occurs. In general, these compressive stresses are applied in a direction perpendicular to the plane of the sheet. During pulp washing and sheet formation operations, the application of compressive stress to a fiber network occurs through fluid drag forces built up during the removal of water. Further compression of wet fiber masses takes place through direct application of mechanical compressive stress at the wet presses. Dry papers and boards also undergo compression in calendering and printing operations, but these cases differ markedly from the compression of wet structures because of the presence of a high degree of interfiber bonding in the sheets.

The compression response of unbonded wet fiber webs is an important aspect of the sheet-forming process because it dictates the web void fraction which is a controlling factor in determining the rate of water removal from the sheet. In addition, the compression response of the web influences its final structure and thus the mechanical, optical, and other properties of the dry paper being manufactured.

Compared to the behavior of fibrous masses, the load-deformation behavior of individual filaments is well understood, at least on the macroscopic scale. Filaments exhibit an immediate deformation and also a time-dependent component of deformation. The deformation properties are dependent upon the stress applied and the molecular structure of the material making up the fiber. Fiber networks also exhibit immediate and time-dependent components of deformation. However, the mechanical behavior of a fiber network such as paper is dependent not only upon the properties of the individual fibers making up the network, but also the interactions between the fibers. A deformation stress applied to a fiber network would not develop uniform deformation stresses in all of the fibers. Rather, individual fibers would be subjected to tensile, compressive, bending, and shear stresses even though the applied stress may be entirely tensile or compressive in nature. The response of a fiber network to an applied stress is, therefore, highly dependent upon the nature of the fiber structure and the type of stress applied. Since fiber networks formed by filtration are highly anisotropic in their structure, the direction of stress application is also important.

The largest part of the tensile studies done on paper structures has been done with the tensile stress applied along the plane of a well-bonded sheet. The type of compressive stresses that generally occur in sheet-making operations is that applied perpendicular to the plane of the sheet, and consequently the fibers are found to be preferentially oriented with their length perpendicular to the applied stress. In such a case, an unbonded fiber network will act as a complex system of beams, with each fiber supported by the fibers below it in the fiber mass. Because of

these differences in bonded and unbonded sheets and the direction of application of compressive and tensile stress to fiber structures and also because of the importance of fiber interactions in stress-deformation behavior of fibrous networks, the extensive work done on tensile stress-deformation behavior is not expected to be very helpful in predicting compression response.

The general behavior of fibrous masses in compression is fairly well known, but the details of how the individual fibers behave is not well understood. The work which has been done indicates clearly that the response to compressive stress is a function of not only the applied compressive load, but also the mechanical properties of the individual fibers and the network structure. The type of network structure built up is determined by the method of fiber bed formation as well as the fiber structural properties and fiber surface properties. Since the compression behavior of a wet fiber mass affects both its rate of formation and the properties of the dry bonded structure made from it, it was felt that a careful investigation of fiber bed compression response was desirable. The purpose of this investigation was to study the behavior of fibrous systems in compression as it is related to the network structure of the fibrous mass. It was hoped to obtain a clearer picture of the way in which a fiber bed and its component fibers respond to both stress application and stress relief. In particular, an evaluation of the mechanism through which individual fibers contribute to the over-all deformation was desired.

INTRODUCTORY MATERIAL AND HISTORICAL REVIEW

There have been a number of investigations dealing with the behavior of nonwoven fibrous networks under compressive stress. Many of these have dealt with dry structures, both bonded and unbonded, but very little work has been done on wet, unbonded fiber systems. In considering our current interests, most of this work may be regarded as primarily exploratory in nature. Its implications in terms of mechanisms involved in fibrous bed compression will be discussed below.

It is convenient at this point to divide this introductory material into four sections. The first section will deal with the rheological behavior of materials in general and methods of studying this behavior. This will be followed by a section dealing with the behavior of fibrous systems in compression. Section Three will be devoted to the possible mechanisms that contribute to fibrous bed deformation, and Section Four will deal with mathematical treatments of compressibility data.

RHEOLOGICAL PROPERTIES OF MATERIALS

ELASTIC MATERIALS

The response of a material to a stress depends upon the molecular structure of the material and the magnitude of the stress applied. The method of load application and sample conditions such as moisture content and temperature are also important. Certain solid materials exhibit a strain which is proportional to the magnitude of the applied stress up to a certain limiting value of this stress. This type of behavior where stress is proportional to strain is known as Hookean response. The

deformation which occurs in a sample below this limiting value of stress is all recoverable or elastic in nature. Steel and glass are examples of items which behave in this way. In the elastic region, all of the deformation is recoverable upon release of the applied load. The deformation of these materials is generally complete immediately upon application of the load and is known as immediate elastic deformation. Beyond a limiting value of applied stress, the elastic material deforms more rapidly with increased stress application than before.

VISCOELASTIC MATERIALS

Newtonian liquids deform in such a way that the stress is proportional to rate of strain. Somewhere between the solid and liquid behavior is a group of materials such as rubber, paper, and plastics which exhibit both an immediate elastic and a time-dependent component of deformation. The term "viscoelastic" is commonly applied to materials of this type. A large number of fiber materials such as wood pulp, cotton, nylon, and other synthetics are viscoelastic in their response to stress. Therefore, the networks formed from these fibers are also viscoelastic in nature, but the behavior of the bed may be far more complicated than that of the fibers. Consequently, the behavior of viscoelastic materials deserves additional discussion.

Viscoelastic response is conveniently divided into three parts: immediate elastic deformation, delayed elastic deformation, and nonrecoverable deformation. Delayed elastic deformation is time dependent and approaches a limiting value of deformation asymptotically. As soon as the load is removed, the immediate elastic deformation is recovered.

There is, in addition, a delayed component of recovery which also approaches a limiting value. However, not all the delayed deformation is recoverable, even at infinite time, and there is always a nonrecoverable component of deformation.

Immediate elastic deformation is usually associated with deformation of chemical bonds, but, because of the complications introduced by delayed deformation, it is very difficult to measure. Solid materials are characterized by a number of moduli which are determined from the slope of an appropriate stress-strain curve. The slope of the tensile or compression stress-strain curve is designated as the modulus of elasticity, E. The modulus of elasticity of a material will be highly dependent upon the nature and number of bonds per unit volume. Therefore, crystalline materials generally will exhibit a higher modulus of elasticity than amorphous or less ordered materials when the modulus is determined from deformation measurements. Furthermore, there is a balance between delayed elastic deformation and nonrecoverable deformation which depends to a great extent on the conditions of recovery used. Delayed elastic deformation can often be increased with an attendant decrease in nonrecoverable deformation simply by raising the temperature. In terms of molecular motion, delayed deformation is generally attributed to changes in molecular configuration. Nonrecoverable deformation may be a result of the inability of the molecular structure to return to its original configuration or of actual "viscous" flow and repositioning of the molecules.

When a viscoelastic material is subjected to a number of repeated load-deload cycles, the material soon begins to exhibit little or no

nonrecoverable deformation. This treatment is known as mechanical conditioning. A material is not mechanically conditioned by this process for applied stresses greater than those used in the conditioning cycles since greater stresses may cause further breakdown of the molecular structure and develop more nonrecoverable deformation. Although it is unlikely that wet webs are mechanically conditioned at any point in the paper manufacturing process, it is possible that portions of the web do approach this state through repeated load-deload cycles which occur as a result of table roll action.

During the load-deload cycle on a mechanically conditioned material, a portion of the work done may be dissipated as heat. Although there is no nonrecoverable deformation, the stress-strain curve for loading may differ from that for deloading. This will show up in the stress-strain response as a closed hysteresis loop.

An understanding of the mechanical behavior of materials is important in assessing this investigation and other work on the compression response of fibrous beds. It has also proved to be an important factor in the selection of fibers for this work, a topic which will be dealt with shortly. For a more thorough analysis of the rheological properties of materials, the reader is referred to the literature (1-3). With special reference to the viscoelastic properties of fiber networks and filamentous materials, three pieces of literature are most important. Leaderman (1) has studied the elastic and creep properties of individual fibers, while Brezinski (2) has investigated the tensile creep properties of paper. Of more importance to the present work is the study by Wilder (4) on the compression creep properties of wet pulp mats.

TESTING METHODS

There are four test methods used to investigate the rheological behavior of materials. These are the stress-relaxation test, the creep test, the load-deformation test, and certain dynamic tests. The first two tests are used in studying viscoelastic materials and permit a separation of stress and time or strain and time. The load-deformation test has received wider use in studying materials of all types, but in this case both stress and strain vary with time. For this reason, interpretations concerning viscoelastic materials are more difficult when the load-deformation test is used, and if comparisons are to be made between samples, it is desirable to use the same rate of stress application. These tests are discussed in detail in the literature (1, 2).

The compressibility test, which is a type of load-deformation test, has been chosen for use in the present study. In the compressibility test, the solids concentration of a fibrous bed is measured at arbitrary values of apparent applied stress. The stress is transmitted to the bed through a piston, and the level of stress is controlled mechanically by adding dead weight loads to the piston. The time variable is generally not considered in that the deformation is usually measured at an arbitrary value of time when no further compression can be measured.

Because of its simplicity, the compressibility test is particularly well suited to a study of compressible fiber beds. Fiber beds formed from pulp, nylon, and other viscoelastic materials do exhibit a time-dependent component of deformation which is most likely due to the time-dependent deformation of the individual fibers; such a behavior does

complicate the interpretation of a compressibility test. The magnitude of the time-dependent component of deformation can be compared to the immediate deformation for highly viscoelastic pulp fibers by reference to the work of Wilder (4). By far the largest degree of bed deformation takes place immediately after load application, and further changes of consistency with time may be considered as second order in relation to this. Therefore, although time-dependent components of deformation do complicate the interpretation of compressibility studies, it is still possible to use the test to study gross fiber network behavior of viscoelastic materials under compressive stress.

BEHAVIOR OF FIBROUS SYSTEMS IN COMPRESSION

GENERAL

Information concerning the behavior of fibrous networks under compressive stress may be derived primarily from two sources: the textile industry, where most of the work has been conducted with dry flock, and the paper industry, where some work has been carried out with wet pulp mats. The general rheological behavior of pulp fiber networks in compression has been examined carefully by a series of workers. Seborg, et al. (5, 7) studied the recovery of wet fiber mats from compressive deformation, and Christensen and Barkas (8) loaded and deloaded wet fiber mats through capillary tension forces created by the water held in the beds. Ivarsson (9) investigated the load-deformation behavior of fibrous sheets under constant rate of compressive strain, and Wilder (4) studied the compressive creep characteristics of wet pulp mats. Wilder was the only worker who avoided the complicating influence of surface tension

effects in compression recovery behavior, and he did this by keeping the fiber bed completely submerged in water throughout the testing. The other workers forced water out of the networks during compression and permitted air to enter them during recovery. Although this may have affected the absolute values of the results, it is doubtful that the general behavior was adversely influenced.

The state of our knowledge as a result of the findings of these workers may be summarized as follows:

When a deforming load is placed upon a wet, unbonded fibrous network, there is a large, immediate deformation followed by a smaller amount of time-dependent deformation. The initial rate of deformation at very short times (less than 0.1 sec.) is controlled by the flow of water out of the network. At longer times, the rate of deformation is controlled by the physical properties of the fibers making up the network. When the load is removed, the process is reversed. However, at longer times, the creep recovery of the network is dependent upon the physical properties of the fibers in such a way that the rate of recovery is increased as the duration of the load cycle is increased. At the same time, the nonrecoverable deformation is increased by increasing the duration of loading. The nonrecoverable deformation is also increased by increasing the magnitude of the load applied to the network.

In addition, it has been shown that fiber networks can be mechanically conditioned for both creep and over-all compression. That is to say, not only the network but the fiber making up the network may be mechanically conditioned.

RELATION TO FIBER FLEXIBILITY

The above description of the general behavior of fibrous networks in compression demonstrates that they exhibit both viscoelastic and elastic characteristics. Since the single fibers from which the beds are formed may also exhibit viscoelastic and elastic behavior, the question is raised as to how much of the observed behavior is due to fiber-fiber interaction and how much is due to individual fiber behavior. Some of the earliest work on the compressive behavior of wood pulp fiber was carried out in an effort to develop a test for the flexibility of the fibers making up the bed. Brown (11), Buckingham (12), and Seborg, et al. (5) found that refining decreased the recovery of a pulp mat and concluded that this effect was the result of a decrease in fiber stiffness brought about through refining. On the other hand, Ingmanson and Andrews (10) report that beating over wide ranges did not change the nature of the wet pulp apparent density-compacting pressure relationship for bleached pulps. However, they did find some change for unbleached pulps (14). Seborg, et al. (5-7) also found that a well-cooked pulp recovered less than a high-yield pulp, but that bleaching alone did not affect recovery from compressive deformation. Since they felt that these findings were a result of differences in fiber stiffness, they set about to demonstrate this. Seborg and Simmonds (6) found that individual fiber stiffness measurements made on wet fibers in bending ranked the fibers in the same order as recovery of fibrous beds from compressive deformation. In studying pulp sheets, Ivarsson (9) found that an increase in moisture content increased both the degree of compression at any load and the amount of nonrecoverable deformation. He attributed this behavior to a

decrease in the relative amount of elastic behavior in favor of more plastic flow. These results point to a strong dependence of fiber network compressional behavior upon both the viscoelastic nature and the flexibility of the fibers.

Flexibility may be defined as the reciprocal of the product of the modulus of elasticity, E, and the moment of inertia, I, (the second moment of the cross section), i.e., flexibility = $1/EI$, where EI is defined as the flexural rigidity. The moment of inertia is a function of the cross-section dimensions of the structural member in consideration, and an increase in diameter of a round member would result in decrease in the flexibility. Likewise, an increase in the modulus of elasticity would result in a decrease in flexibility.

IMPORTANCE OF FIBER DIAMETER

In view of the above, one would anticipate that a change in fiber diameter would modify compressional behavior. Information on this point is conflicting. Saxl (13) finds that with dry rayon flock, a high-denier* fiber is harder to compress and recovers to a greater extent than a lower denier. However, Ingmanson (14) has found that there is no difference in the compressional response of water-saturated fiber beds formed from nylon fibers of widely differing denier, and Kolb, et al. (15) reports that compressional recovery of dacron is not dependent on denier. Work, Thorne, and Livingstone (16) make the comment that

*Denier is the weight in grams of 9000 meters of fiber.

recovery from compressive deformation is not dependent upon fiber size. These workers studied celanese and wool. In reference to wool, Van Wyk (17) feels that the effect of fiber diameter may be masked by crimping. It has been pointed out that flexibility is also dependent upon modulus of elasticity. Since elastic modulus was not measured or controlled in these studies of the effect of diameter, it is very likely that the modulus factor is at least partially responsible for the contradictory results reported above. Up to this time, no one has studied carefully the effect of changes in modulus of elasticity on fiber bed compression and recovery.

INTERFIBER FRICTIONAL EFFECTS

Busse (18), and Kolb, et al. (15), in studying the application of high compressive stresses to textile fibers, noted some visual evidence of impression at fiber contact. They found that recovery from 20% elongation ranked fibers in the same order as compressional recovery and took this as proof of the importance of high fiber strains in the compression test. These workers also noted that lubricating the surface of the fiber had little effect on recovery. This led to the conclusion that surface friction is not highly important to compressional response. Several workers have observed a hysteresis in the compression-release cycle for fiber networks, and Van Wyk (17) feels that this may be due in part to frictional effects. Here again, conflicting results are reported, and even similar results are given several interpretations. For example, Pigeon and van Winsen (19) found an increase in both rate and degree of stress relaxation of asbestos as well as cotton fiber with an increase in

moisture content. This was interpreted as a lubrication effect, but Ivarsson (9) attributed similar compression results on pulp fiber to changes in fiber plasticity.

IMPORTANCE OF FIBER LENGTH

Indications are that the behavior of fiber networks during compression is also highly dependent upon the network structure, particularly as it is related to fiber size and orientation. The fiber length is believed to play a primary role in determining the initial mat geometry, and therefore the original number of fiber-to-fiber contact points. This also means that fiber length is important in deciding the initial distance between fiber-to-fiber contact points. Consequently, the fiber length should be an important factor in determining the amount of deformation taking place in an individual fiber, and one would expect a dependence of compressional behavior on fiber length. [As early as 1932, Doughty (45) found that shorter fiber lengths led to dry sheets of paper with higher solid fractions.] In working with wet wood pulps, Seborg (5-7) has found an increase in the percentage of recovery from first compression with an increase in fiber length. Van Wyk (17) found no effects on compression of wool staple due to fiber length at lengths greater than 4 cm. The effects observed at shorter lengths were believed to show the influence of the number of free fiber ends on bending and slippage of individual fibers. Working with dry rayon flock, Saxl (13) found that fiber masses with fibers predominantly below 0.5 mm. in length were harder to compress and had less associated nonrecoverable deformation than longer fibers. This observation on nonrecoverable deformation seems to be at

odds with the findings of Seborg (5-7) who found that recovery increased with increasing fiber length. However, Saxl is talking in terms of absolute values of nonrecoverable deformation and Seborg's results are reported as per cent recovery.

An interesting study of the effect of fiber dimensions on sheet properties has recently been reported by Dadswell and Watson (20), who found that thick-walled wood fibers produced bulky sheets and thin-walled springwood fibers gave dense sheets. Of more interest was the fact that when the average length-to-diameter ratio of the wood fiber increased, the resulting sheet became more bulky.

POSSIBLE MECHANISMS INVOLVED IN MAT COMPRESSION

The investigations reviewed above indicate that the compressibility characteristics of fiber networks depend upon the bulk properties of the fiber, such as:

(a) elasticity and flow properties,

(b) strength and ultimate elongation for tensile, compressive, and shear stresses,

(c) surface properties such as the coefficient of friction, adhesion characteristics, and surface roughness, and

(d) fiber dimensions.

However, when dealing with fiber networks, one cannot ignore the behavior of fibers relative to their nearest neighbors. It seems reasonable that fiber network compressive deformation may be divided into three categories of fiber behavior:

(1) fiber bending,

(2) fiber slippage, and

(3) fiber compression at points of fiber-to-fiber contact.

These categories are based on the interpretation that the fiber is the building unit of the bed. The molecular structure of the fibers is not considered except as it affects the fiber properties, and the deformation of a fibrous bed is viewed as the result of changes in the geometry of the system of fibers making up the bed. Each of the above-mentioned categories of fiber deformation and motion may contribute to both recoverable and nonrecoverable deformation as well as the time dependence of the deformation.

Because no clear-cut distinction can be made between those mechanisms which contribute to recoverable deformation and those which contribute to nonrecoverable deformation, interpretation of available literature in terms of mechanisms is very difficult. In early loading cycles, fibers probably slip past one another until they reach a position of repose for the particular applied load. The result of this repositioning of fibers would be a contribution to nonrecoverable deformation since there would be no forces tending to restore the fiber to its original position. Applications of stress to fiber arrangements involving fibers held rigidly at one end can result in slippage of the free fiber end. Restoring forces set up in the fiber would bring about at least partial recovery upon relief of the deformation stress.

It is also possible that the occurrence of one or two of the three suggested types of deformation may lead to a third. In cases where repeated loadings are being carried out, the variation of stress in the

fiber and changes in relative position of the fiber in the bed brought about by the first cycle can completely change its response to successive loading cycles. When a network is finally mechanically conditioned, no further permanent fiber repositioning would be taking place, but it seems reasonable that rather substantial amounts of reversible slippage could be included in the completely recoverable portion of the bed deformation. In addition, a slipping phenomenon should be dependent on the surface properties of the fiber as well as fiber size and may take a finite time to occur. It is apparent, then, that slippage could contribute to both elastic and viscoelastic deformation of the network as a whole.

When a fiber bed is visualized as a complex network of beams supported at many points, it is possible to visualize the bending of fiber elements between points of support. If the material composing the fiber is entirely elastic, the deformation within a fiber may be expected to be entirely recoverable. However, in a viscoelastic fiber, both nonrecoverable bending deformation and time-dependent bending deformation would occur, so that nonrecoverable components of bending deformation could not be separated from nonrecoverable slippage. Bending and slippage of fibers would also result in the development of new contact points between fibers. Since the load supported by each contact will depend upon the total number and distribution of contact points, the importance of compression of fibers at points of contact will be closely interrelated to both fiber bending and slippage behavior. Here again, the compressive deformation could be entirely elastic and very small, but it could also be viscoelastic, contributing to both nonrecoverable and time-dependent deformation. The single and interrelated mechanisms

discussed above all find support in the literature which has been cited. In addition, the close interrelation of the three categories of deformation as suggested by the above discussion point to the need for simplification and further study of fibrous networks under compressive stresses in order to clarify the mechanisms involved in compressive deformation.

MATHEMATICAL TREATMENTS OF COMPRESSION DATA

EMPIRICAL EQUATIONS

The most widely used correlation for graphical treatment of fiber bed compression data is the empirical "compressibility equation"

$$C = MP^N \qquad (1)$$

where C is the mat solids concentration in mass of dry fiber per unit volume, P is the apparent applied stress, and M and N are constants. Data are plotted as log C vs. log P to yield straight lines of slope N. Although much attention was directed to the use of the equation by Campbell (21), it was actually first applied to wet pulp compression data by Qviller (22).

Equation (1) has been found useful in correlating compressibility data for both wet and dry wood fiber in thick pads (26) or in thin sheets (27). Application of the compressibility equation to nonwoven fibrous beds of glass (23), nylon and dacron (24), orlon (25), and wool staple (17) has been equally successful. The values of the slope N for thick pads of wood pulp range from 0.29 to 0.46. On the other hand, the compressibility data for thin sheets had a slope in the range of 0.24. Slopes for synthetics ranged from 0.20 to 0.25.

Compressibility studies carried out by the Institute staff (24-26) have generally been confined to loads in the range of 10 to 100 g./sq. cm. However, the compressibility studies carried out by Kurath (28), and Ingmanson (14) on wet pulp show that the empirical compressibility equation seems to be applicable up to loads of 6400 g./sq. cm., and possibly up to loads of 25,000 g./sq. cm., if sufficient time is allowed for the major portions of delayed deformation to take place. The data of MacLaurin (27) on thin sheets fit Equation (1) from 350 g./sq. cm. up to loads of 21,000 g./sq. cm., and those of Brown (29) on dry pulp fibers agree fairly well from 35,000 to 910,000 g./sq. cm.

There is some evidence from the work of Van den Akker, et al. (30) that there is an upper limit to the applicability of the compressibility equation. This upper limit occurs where further changes in applied stress do not produce significant changes in the density of the pad. Furthermore, in considering the data reported above, it seems very likely that the mechanisms controlling deformation of thin sheets and of fiber pads at very high loads are far different from those controlling the deformation of thick pads at lower loads. Some of the foregoing discussion of fiber mechanisms and their interrelation may not be applicable to these cases.

Little work has been done to extend static compressibility measurements to loads lower than 10 g./sq. cm. Wilder (4) found that static compressibility of wood pulp gave straight-line log-log plots of C vs. P in the range of 1-60 g./sq. cm., and Ingmanson (14) showed that dynamic compressibility follows $C = MP^{\frac{N}{}}$ down to 0.5 g./sq. cm. He reasons that in all probability, agreement of static tests also extends this low.

The data of Train (31) and Agte and Petrdlik (32) on the compressibility of powder materials (which may be considered an extreme case of fibers of very short length) can also be fitted to Equation (1) with a very low value of N. In these cases, an upper and lower limit to the applicability of the equation was found.

Because of the difference in specific volume, v, of different fiber types, Ingmanson (37) has suggested that it would be easier to compare network behavior of different fibers if the data were expressed as solid fraction, vC, rather than as mat solids concentration, C. Since solid fraction is a dimensionless quantity, this would permit direct comparison of all data on the same basis. A strict application of this principle would at times be quite difficult and somewhat unreliable. For fibers which swell in liquid, a value of the specific volume which is applicable to this situation is difficult to obtain. There is also indirect evidence from drainage studies (14) that compressive loads on pulp fiber beds causes a deswelling of the fiber which would result in a specific volume which varies with load.

Peter Wrist (33) has suggested that fiber bed compression data be treated in terms of the four moduli which may be used to describe an elastic body, i.e., Young's (E), bulk (K), shear (G), and Poisson's ratio (σ). These constants are easily interrelated for elastic materials, but such relationships are very complex for viscoelastic materials. Wrist has attempted to attach theoretical significance to the empirical compressibility equation by deriving it from the basic assumption that the bulk modulus, K, of the fiber bed is proportional to the apparent compacting stress, i.e.,

$$K = -V(dP_2/dV) = kP_2 \qquad (1a)$$

where K is the bulk modulus, V is the bed volume, and k is a constant. P_2 is defined as the sum of the applied stress and the compacting pressure in sedimentation.

From this starting point, he derives the empirical compressibility Equation (1) in the form

$$C = (C_o/P_o^{1/k})P_2^{1/k} \qquad (2)$$

where C_o is the sedimentation consistency of the slurry and P_o is the compacting pressure in sedimentation.

There is a serious shortcoming in an equation of the form $C = MP^N$ in that it requires that the pad concentration be zero at zero compacting pressure. Wrist attempts to avoid this difficulty by defining the stress P as the applied stress plus a compacting stress in sedimentation so that the stress never goes to zero even though the applied stress may do so. In the empirical compressibility equation, P is, of course, merely defined as applied stress. Ingmanson and Whitney (26) have suggested that a more reasonable form of the empirical compressibility equation is

$$C = C_o + MP^N \qquad (3)$$

where C_o is the pad concentration at zero applied stress. Reliable measurements of C_o for pulp fiber have not yet been made, so the applicability of Equation (3) to pulp cannot be checked.

Attempts have been made in this work to measure the value of C_o for synthetics, and this effort will be discussed in the presentation of the

data, together with some thoughts about the significance of the value. However, Wilder (4) found that his creep data could be fitted by an empirical equation of the form

$$C - C_o = (A' + B' \log t)P^N \qquad (4)$$

where C_o, A', and B' are empirically determined constants and t is time.

A number of other equations have been advanced for the treatment of compressibility data. Two of interest are those of Eggert and Eggert (34) which may be rearranged to the form

$$C - C_o = \left(\frac{C_o}{P_o}\right)P \qquad (5)$$

where P_o is the "latent pressure" of the fiber at zero applied load, and that of Bogaty, et al. (35),

$$(P + c')(H - a') = b' \qquad (6)$$

which is an equation of the Van der Waal's type. H is the pad height and a', b', and c' are constants.

THEORETICAL EQUATIONS

Fiber Bending

Although the compression of a mass of fibers is believed to involve several mechanisms, the problem may be considerably simplified when the mass is reduced to a system of bending units. Considering the elements of fibers between contacts with other fibers as simple beams, Van Wyk (17) has developed an equation to relate the volume of the fiber system

to the applied stress. This treatment ignores slippage and compression of individual fibers. An equation for the unsupported fiber length was derived by considering the probability of a spherical particle striking the fibers as it passed down through the bed. All possible orientations of fiber elements were allowed, and no attempt was made to account for changes in orientation during compression. The equations developed were combined with the equation for the deflection of simple beams to obtain the result

$$P = [K'Em^3/\rho^3][1/V^3 - 1/V_o^3] \qquad (7),$$

where V is bed volume, E is Young's modulus, ρ is fiber density, and K' and V_o are constants. Substituting m/C for V, where m is the mass of dry fiber in the bed, one may write

$$C^3 - C_o^3 = [\rho^3/KE]P \qquad (8).$$

By assuming C_o to be very small in comparison to C, one obtains the same form as the empirical compressibility equation,

$$C = [\rho^3/KE]^{1/3}P^{1/3} \qquad (9)$$

with N equal to 1/3.

More recently, Wilder (4) has independently made a similar derivation which is also dependent on all the assumptions implied in using simple beam theory. The original derivation has been improved by both Wilder and this writer. In this case, the fibers are assumed to be randomly oriented in a plane perpendicular to the direction of the applied stress. An equation for the unsupported fiber length is derived by considering the

probability that two fibers will create an intersection when viewed from the top. These fiber elements are mathematically distributed throughout the bed and assumed to change in length in a certain way with a change in solids concentration. When combined with the equation for the deflection of a simple beam, the following expression for the immediate elastic deformation of the bed is obtained

$$C^{4\alpha-1} - C_o'^{4\alpha-1} = \left[\frac{(4\alpha - 1)\pi^8 \rho^5 C_o'^{4\alpha-6}}{9.8 \times 10^4 E}\right] P \qquad (10)$$

where α is a constant. If $\underline{C}^{4\alpha-1}$ is much greater than $\underline{C}_o'^{4\alpha-1}$, the equation can be placed in the form $\underline{C} = \underline{M}\underline{P}^{\underline{N}}$, and if α is assumed to be equal to 1, $\underline{N}$ is also equal to 1/3 as in Van Wyk's derivation.

In both of the simple beam developments, the general form of the equation is highly dependent upon (among other things) the assumption that a relationship exists between the unsupported fiber length and the mat solids concentration. The particular relationship chosen by Wilder (4) is $\underline{b} = \underline{k}/\underline{C}^{\alpha}$ where $\underline{b}$ is the unsupported fiber length and $\underline{k}$ is a constant. The many other assumptions necessary to carry out the derivations seem to affect only the value of the exponent $\underline{N}$ and the form of the constant $\underline{M}$. Up to this time, attempts to rationalize available compressibility data with Wilder's equation have not been particularly rewarding. This, however, is due to a lack of a positive knowledge about the various fiber properties affecting the constant $\underline{M}$.

Compression at Points of Fiber Contact

For fibers of low modulus of elasticity, the compression of fibers at points of fiber contact would also seem to be an important mechanism for deformation. Finch (36) has treated the compression of individual fibers at points of contact both experimentally and theoretically. The Hertzian equations for the shape of the contact area of curved isotropic elastic bodies were written for cylinders in contact at any angle, and these equations were tested for applicability to anisotropic visco-elastic nylon fibers. When the equations developed by Wilder (4) to describe fiber networks are applied to Finch-Hertzian equations for the relationship between the applied load and the distance of approach of two cylinders along a common z axis through their radii, one obtains an equation of the same form as that derived by Wilder and Van Wyk. This solution is also dependent upon the assumption that a relationship exists between the mat solids concentration and the number of contact points.

One might expect a change in controlling bed compression mechanisms from bending to compression at points of contact would appear as a change in slope of a log C vs. log P plot. However, log-log plots are particularly insensitive to small changes, and, since one would not expect a sharp change from one mechanism to another, a noticeable change in slope would probably be difficult to observe. At least, the data available indicate this to be the case.

APPROACH TO THE PROBLEM

The very complex nature of fibrous bed deformation involving both elastic and creep components contributed by several mechanisms makes an analysis of pulp fiber compression data in terms of controlling fiber mechanisms extremely complicated. When such a situation arises, it is often helpful to simplify the system being studied. Since separation of the contributions of all the mechanisms and/or the components of deformation is not feasible, the approach taken was to eliminate as many of these as possible. It was decided insofar as was practical to eliminate the creep component of deformation, the compression of fibers at points of contact, and the irreversible slippage. To accomplish this, a system of glass fibers was selected, since the fiber structural properties of modulus of elasticity, length, and cross section can be carefully measured and controlled with glass.

In order to form reproducible structures, plans were made to form the beds with the fibers preferentially oriented perpendicular to the applied stress. The choice of glass eliminated the complications of creep deformation in the fibers and compression of fiber at points of contact. Mechanically conditioning the beds permitted an analysis of nonrecoverable and recoverable slippage deformation. The purpose of this approach was to set up a system in which the elastic bending of the fibers was the only major mechanism involved in compression. The scope of the information gained was then broadened by studying viscoelastic fibers such as nylon and comparing all of these data to the data obtained on wood pulp fiber systems.

The investigation reported here is primarily phenomenological. The analysis of the literature indicated that there are two major factors controlling fiber bed compression response:

(a) fiber network structure, and

(b) fiber properties.

Fiber length and fiber diameter were indicated to be the most important factors in determining network structure, and fiber diameter and modulus of elasticity were known to be the two important factors in determining fiber flexibility. Therefore, a controlled variation of these three important fiber structural properties has been used as a method of clarifying fiber bed compression-recovery response and of assessing the importance of the three fiber mechanisms suspected to be controlling this response.

FIBER SELECTION AND CHARACTERIZATION

A number of synthetic fiber samples were made available to this writer through the courtesy of several manufacturers. Synthetic fibers for this study were selected from this group in order to set up a pattern of experiments which would permit the modulus of elasticity and the diameter to be varied independently of each other. A further criterion was that the diameter distribution of the fiber be narrow and the modulus of elasticity be uniform from fiber to fiber. A pulp fiber sample was also selected and will be discussed shortly. The techniques used to characterize the synthetics are described below, and the results are tabulated in Table I.

FIBER DENSITIES

A pycnometric density was measured for all fibers. Clean fibers were deaerated in a vacuum desiccator, and pycnometers were filled with air-free fiber slurry by carrying out the filling operation below the water surface. Densities were calculated from the equation

$$\rho = W\rho_w/(W - y) \qquad (11)$$

where

ρ = density of fiber, g./cc.,

$\underline{W}$ = weight of dry fiber, g.,

$\rho_{\underline{w}}$ = density of water at the test temperature, g./cc., and

$\underline{y}$ = difference in weight between the slurry-filled and water-filled pycnometer.

TABLE I

CHARACTERIZATION PROPERTIES OF FIBERS STUDIED

Fiber	Pycnometric Density, g./cc.	Diameter, microns	Modulus of Elasticity, g./sq. cm. x 10^{-7}
Glass			
Standard	2.56	5.12±0.39	72.60±1.66
Standard	2.56	9.12±0.78	71.20±1.36
Standard	2.56	12.86±0.94	74.39±1.28
Beryllia	2.85	9.14±1.35	102.65±4.44
Dacron	1.39	22.72±0.93	14.67±0.67
Nylon			
High modulus	1.14 (41)	77.35±1.32[a]	1.07±0.06[a]
		46.2 (42)	1.27±0.10
		44.75±0.7[a]	1.33±0.76[a]
		16.78±0.76[a]	1.30±0.29[a]
Low modulus		76.76±1.49[a]	0.38±0.03[a]
		43.75±0.94[a]	0.37±0.01[a]
		44.49±4.44[a]	0.31±0.03[a]
		15.08±1.68[a]	0.36±0.09[a]
Pulp	1.60	43.6 (4)	Hydrodynamic specific volume 3.62 cc./g. (4)

[a]Myers (40)

FIBER DIAMETER DISTRIBUTIONS

Diameter distributions for all glass fiber samples were measured microscopically, using a 25X eyepiece and a 97X oil immersion objective. A segment of glass fiber strand was spread out on a glass slide and immersed in a fluid having an index of refraction of 1.48-1.50. In general, 150 fibers were measured, and this constituted approximately 75% of the fibers in a strand. The same technique was used for nylon and dacron fiber, except that a 43X objective was generally employed and virtually all the fibers in the strand were measured.

MODULUS OF ELASTICITY DETERMINATIONS

There are a number of techniques for determining the modulus of elasticity of a filamentous material including the stress-strain technique, the static bending technique, and the resonance frequency technique. For a homogeneous, elastic material the same value will be found by all these methods. For a nonhomogeneous material, the result obtained from a bending test will be different from that obtained in a tensile test. The modulus of elasticity for a viscoelastic material will also depend upon the rate of strain, so that the value obtained from simple bending will be lower, and that obtained from resonance frequency techniques higher, than that obtained from stress-strain measurements.

After fairly extensive preliminary study, the stress-strain technique was chosen for this work because of its simplicity, reproducibility, and reliability. In the stress-strain technique used for glass fibers,

load-elongation curves for single filaments were measured and recorded with the Instron Tensile Tester. The slope of these curves provided the necessary data for the calculation of Young's modulus through the relationship

$$E = F\ell/A_f(\Delta\ell) \qquad (12)$$

where

E = modulus of elasticity, g./sq. cm.,

F = load, g.,

A_f = fiber cross-sectional area, sq. cm.,

$\Delta\ell$ = elongation, in., and

ℓ = initial fiber length, in.

The extreme brittleness of the glass fibers demanded special handling and mounting techniques for the load-elongation tests. Filaments of clean fiber were lifted from water with a dissecting needle and mounted on brass tabs as shown below in Fig. 1.

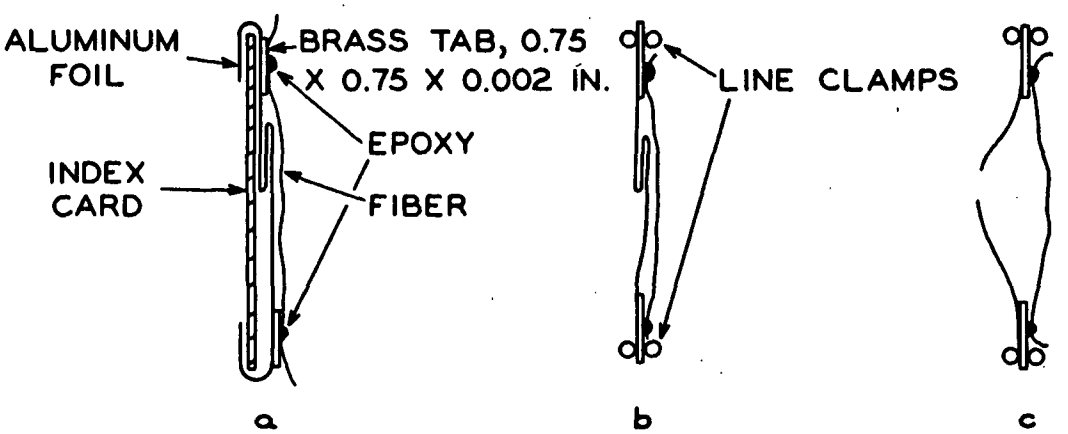

Figure 1. Procedure for Mounting Fibers in the Instron Tensile Tester

The aluminum foil was taped to the index card which provided rigidity for mounting, and the brass tabs were glued to the foil, as in "a". Single fibers were lined up across the center of the brass tabs and fastened with an epoxy resin, Armstrong's Adhesive A-1. To make a run, a single fiber and its mounting were cut from the card. The remaining tab and foil arrangement was mounted in the line clamps of the Instron Tester, which had been preset to a given span length, as in "b". When the aluminum foil was pushed away from the fiber and cut as in "c", a single fiber was left mounted for testing. All fibers were tested at 0.1 in./min. rate of strain. The conditions were 73°F. and 50% R.H.

The load-elongation curves showed only a slight tendency to deviate from a straight line, indicating that the fibers were close to 100% elastic. Resonance frequency studies in this work and simple bending studies of Sinclair (38) verified that the modulus of elasticity for glass is the same in tensile and in bending.

A correction for fiber slack, a tab weight correction, a load, and a corresponding elongation were taken directly from the recorded curve. Fiber cross-sectional area was determined from a diameter measurement on the particular fiber tested. A measurement of the clamp-line-to-glue-line distance was made through microscopic examination of the tabs after break. The initial fiber length was determined by subtracting the clamp-line-to-glue-line distance from the span length and then adding the slack to this value. Test specimens were from 3.2 to 3.4 inches long.

Since moisture is known to have an effect on the modulus of elasticity of nylon, the modulus of elasticity of nylon and dacron samples was

run on filaments submerged in water. This was done using an adaptation of the technique described above and first worked out by Myers (40). According to Myers' technique, the fiber was mounted as shown in Fig. 2 in a glass cell filled with fluid. The fibers were still mounted on tabs, but the lower tab passed through a cork and was held in the lower line clamp of the Instron Tester. There was no aluminum foil backing to be clipped and the fiber was strained while immersed in liquid. All tests were run at 0.1 in./min. rate of strain and 73°F. The fibers were immersed in the fluid for at least 1 hour before testing. It was demonstrated by Myers that the modulus of elasticity of nylon fibers did not change after 1 hour of soaking.

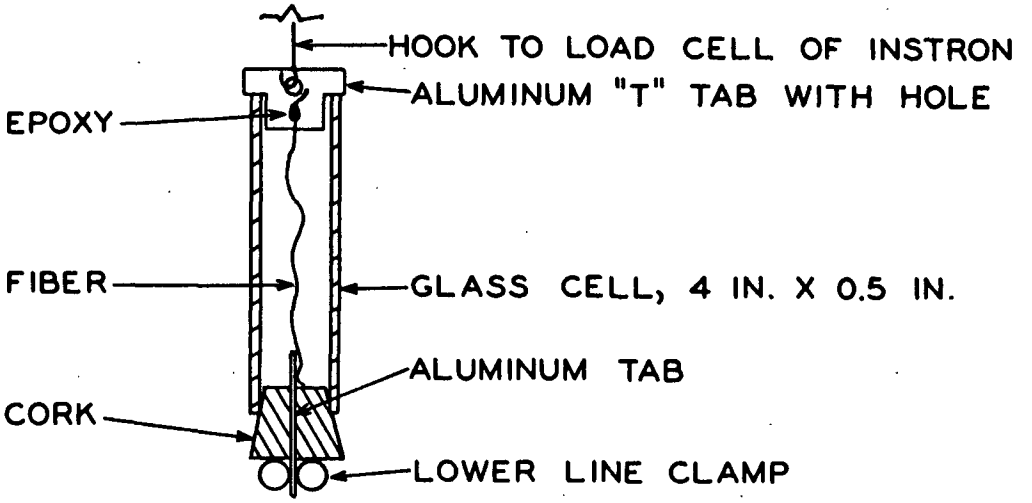

Figure 2. Cell for Determining Modulus of a Fiber Immersed in a Fluid

Although the modulus of elasticity of the nylon and dacron samples was measured on filaments that were under water, the modulus of glass fiber was originally determined on dry glass filaments. The question was then raised as to the effect of a leaching action by the water on

glass fiber modulus of elasticity. Tests made on glass fibers held under water after they had been soaked in water for 8 hours showed that no significant change in modulus of elasticity had occurred.

FIBER PREPARATION

SYNTHETIC FIBERS

All synthetic fibers used in this work were obtained as continuous filament and were cut to desired lengths in the following way. The fiber was unwound from the bobbin and rewound onto a hexagonal wheel about 2 feet in diameter, placing the fibers in parallel alignment on a backing of blotter stock and chipboard. This skein of fiber was glued with Duco cement at several points prior to removing it from the wheel for cutting.

The cutting was accomplished with razor blade gang cutters. These cutters consisted of a number of single-edge razor blades mounted on steel rods and spaced with washers to give the desired fiber length. The cutter was forced through the bundles of fiber with a hydraulic press.

Cutters were prepared to produce five different fiber lengths, as shown in Table II.

TABLE II

FIBER LENGTHS STUDIED FOR SYNTHETIC FIBERS

Average Fiber Length, mm.
0.96 ±0.09
1.68 ±0.34
3.13 ±0.12
4.60 ±0.17
6.30 ±0.13

Fiber length distributions were determined by placing a sample of slurried fiber on a glass slide and projecting the slide at 50X on the Finnish Fiber Length Recorder (38a). A ruler was used to measure the fibers to the nearest 0.1 mm. Approximately 200 fibers were measured. A number of duplicates were analyzed, and this showed that a single cutter would always prepare fiber of the same average length within the limits of error shown in Table II regardless of fiber diameter or type of synthetic. Therefore, all the fiber samples run were not analyzed for length distribution, but rather a fiber length distribution characteristic of a particular cutter was determined.

Nylon and dacron fibers were dispersed in water using 50 to 100 counts on the British Disintegrator. Fibers were not damaged by this procedure. The fiber slurries were then placed in 4000-ml. vacuum flasks and deaerated under vacuum before adding them to the stock tank in the bed formation system.

The individual filaments in the strands of standard glass fiber were held together with a binder that was predominantly starch. The cut glass fibers were cleaned by soaking them in 30% hydrogen peroxide for approximately 4 hours. The hydrogen peroxide was then drawn off and the fibers washed before placing them in hot water for deaerating. Since the surface charges are maintained at a level most favorable for the dispersion of glass fibers at low pH, a small quantity of concentrated hydrochloric acid (1 cc.) was added to the suspension in each flask before deaerating.

The "Hi-Modulus Beryllia" glass fiber was supplied with a different type of binder, and it was found necessary to soak these fibers briefly (~15 min.) in hot 50% sulfuric acid in order to clean them. Following this, the fibers were washed and dispersed in the manner used for standard glass.

PULP FIBERS

The pulp fiber studied in this work was a Virginia loblolly pine (Pinus taeda) summerwood kraft pulp with a lignin content of 5.1%, based on the pulp. It was cooked according to the procedure described by Wilder (4) and classified in the Bauer-McNett classifier. The work reported here was conducted on the fraction retained on a 12-mesh screen.

A portion of the classified pulp was bleached according to the following procedure, using as little mechanical action on the fiber as was possible.

BLEACHING PROCEDURE

First stage	5% chlorine
Second stage	2% caustic extraction
Third stage	0.5% chlorine dioxide
Fourth stage	0.5% chlorine dioxide
Fifth stage	0.5% chlorine dioxide

This procedure reduced the lignin content to 0.3%, based on the pulp.

Finally, a portion of this bleached pulp was reduced in fiber length in the following way:

1. A pad containing 15 g. o.d. pulp was formed on a 6-inch diameter Buchner funnel.

2. The wet pad was cut into 3/16-inch wide strips with a guillotine cutter.

3. Steps 1 and 2 were repeated 10 times.

The fiber obtained in this way had a weighted average fiber length of 1.23 mm. as opposed to 2.84 mm. for the original fiber. The advantage of this procedure was that it altered the mean fiber length and fiber length distribution without causing appreciable fibrillation of the fibers.

The fiber length characteristics of the three samples of pulp fiber studied are shown in Table III. Approximately 1000 fibers were measured in each case.

TABLE III

FIBER LENGTH CHARACTERISTICS OF PULP FIBER SAMPLES

Fiber Sample	Arithmetic Average Fiber Length, mm.	Weighted Average Fiber Length, mm.
Unbleached fiber	2.54	2.84
Bleached fiber	2.57	2.82
Cut fiber	0.72	1.23

The pulp fiber samples were dispersed with 50 counts in the British Disintegrator before deaeration.

APPARATUS: CONSTRUCTION AND OPERATION

GENERAL CONSIDERATIONS

The equipment designed and used by Wilder (4) to study the creep properties of wet pulp mats was adapted for use in the present work. Minor modifications were made to the equipment which included the installation of new forming systems, a new piston strong enough to permit the use of high loads, and a counterbalance system for the piston to permit the use of very low loads.

Several special considerations have been given to the design of the creep-compressibility equipment as a result of extensive preliminary work. Studies made in this investigation and work done by Wilder (4) demonstrated that beds compressed within the confines of a forming tube showed a different response to stress application and stress relief than those pads which were compressed after the forming tube was removed. The apparatus was designed by Wilder to allow for the removal of the forming tube before compression-recovery studies were initiated. It has also been shown in this work that beds formed from badly flocculated glass fibers showed a far different compression response than those beds formed from nonflocculated slurries (see Fig. 3). These results emphasized the need for a reproducible forming and loading technique. All of the work reported here was carried out on fiber beds formed by filtration from extremely dilute fiber suspensions. The consistencies ranged from a maximum of 0.018% for very short fibers to a minimum of 0.0005% for very long fibers. These beds were formed at flow rates which were high enough to cause the fibers to assume a position in the plane of the bed

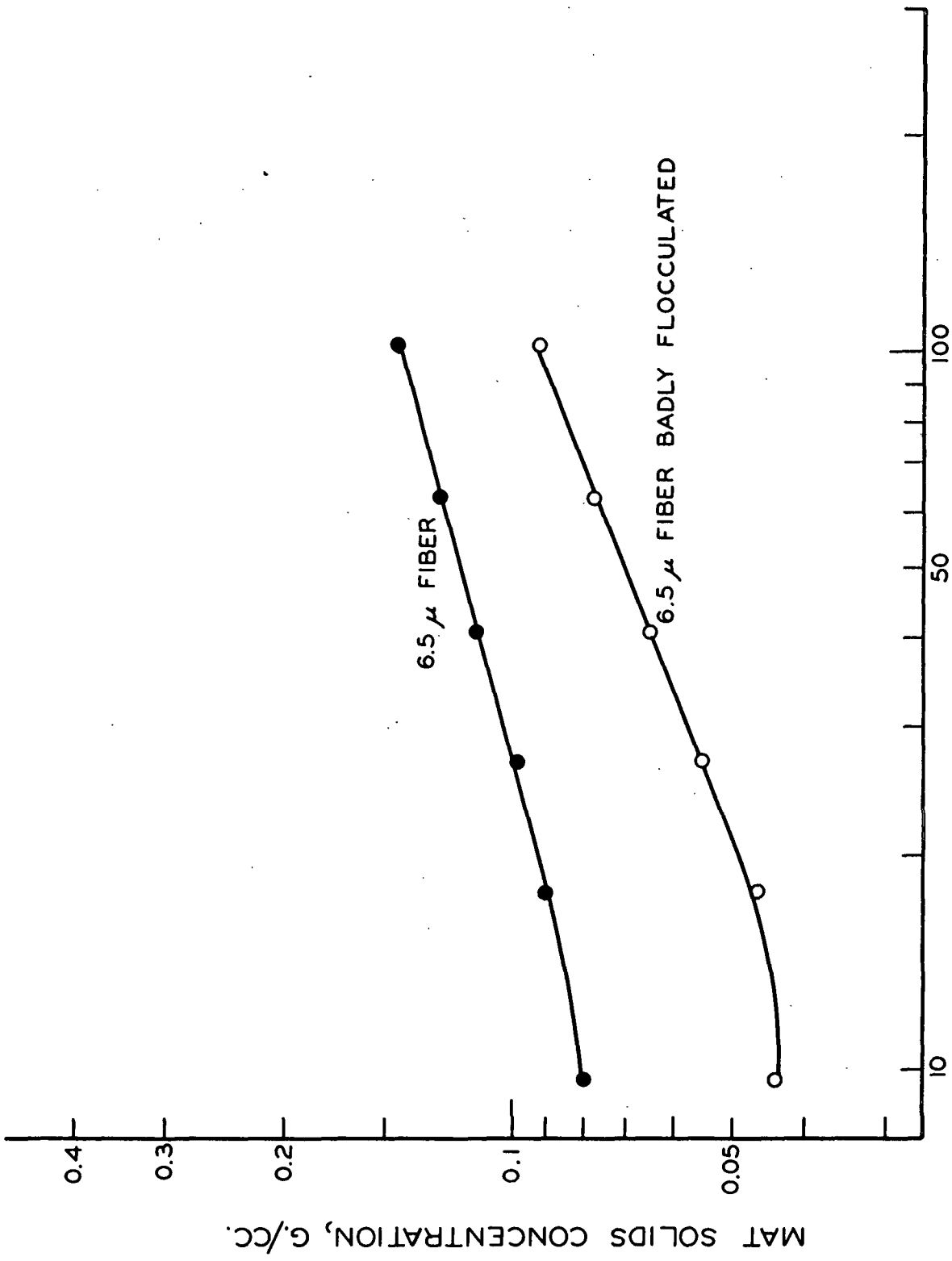

Figure 3. First Compression Curves for Glass Fiber Data Taken with the IPC Compressibility Apparatus

normal to the direction of flow. This made it possible to obtain reproducible fiber beds with the fibers randomly oriented in the x-y plane normal to the direction of fluid flow, but with little orientation in the z direction parallel to the flow (see Fig. 4). It should be pointed out that although flocculation almost assuredly means that some fibers are z-oriented, z orientation can occur without flocculation.

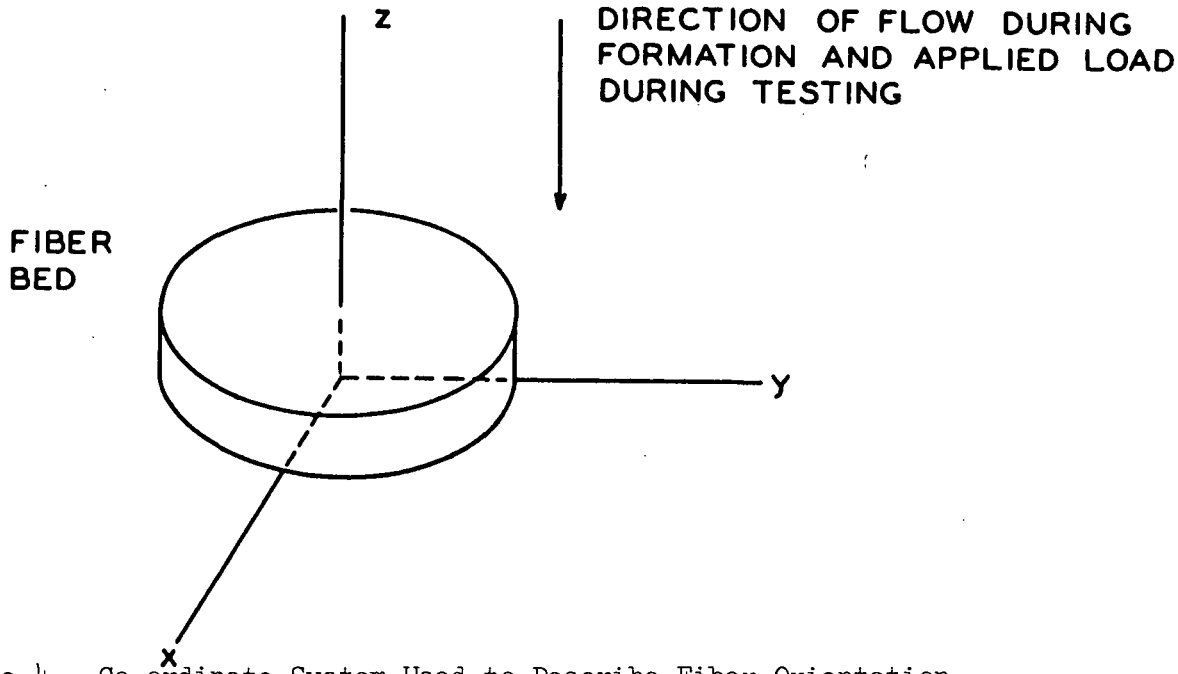

Figure 4. Co-ordinate System Used to Describe Fiber Orientation

The success of this method is demonstrated by Fig. 5 and 6. Figure 5 is a photograph of a typical fiber bed showing random distribution of the fibers in the x-y plane. To obtain this photograph, a thin section was gently lifted from the center of a wet glass fiber bed and placed upon a glass slide. The assumption of little z-direction orientation is shown to be valid in Fig. 6, which is a photograph of the z-y plane of a thin cross section taken from the same fiber bed. In this case, a large portion of a dry glass fiber bed was impregnated with methyl

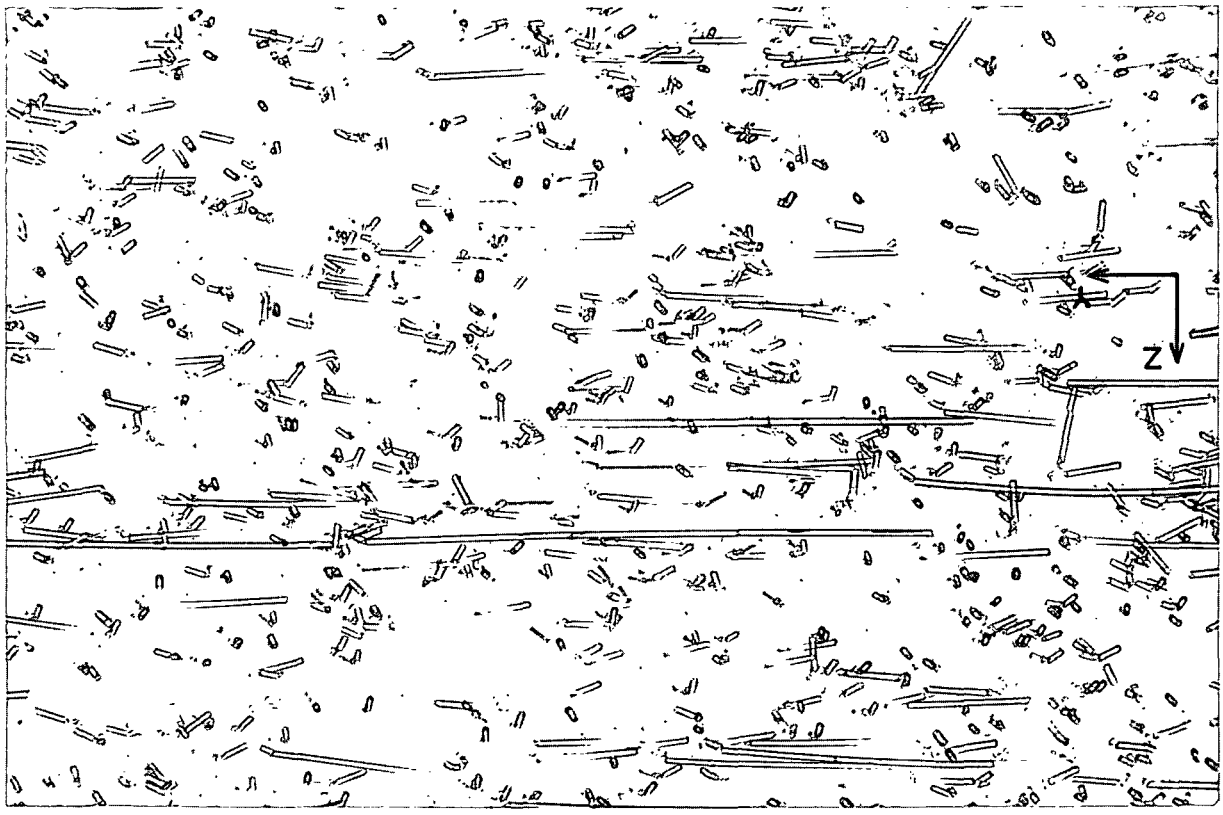

Figure 5. Photomicrograph of the x-y Plane of a Typical Glass Fiber Bed. Fiber Diameter 12.86 microns; Fiber Length 3.13 mm.; Magnification: 80X

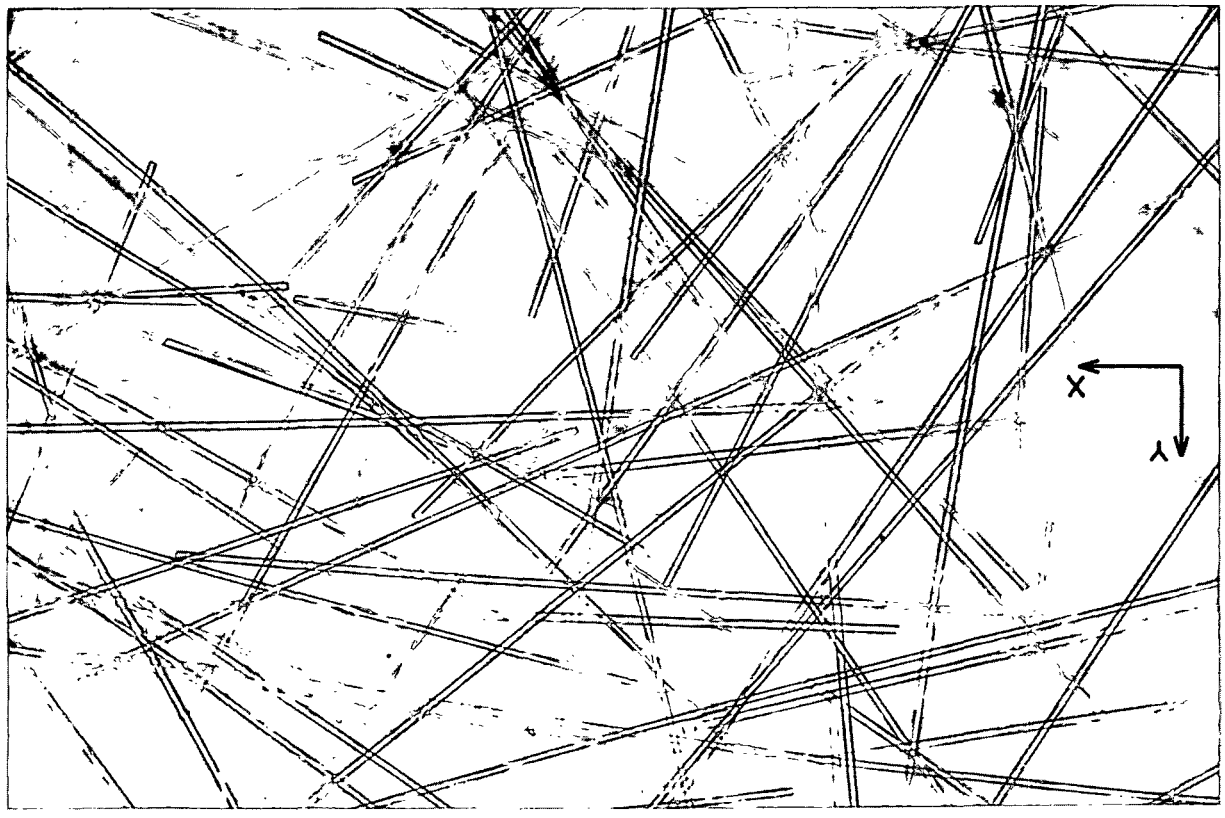

Figure 6. Photomicrograph of the z-y Plane of a 60-μ Thin Section for a Typical Glass Fiber Bed. Fiber Diameter 12.86 μ; Fiber Length 3.13 mm. Mat Solids Concentration Approximately 0.038 g./cc.; Porosity = 0.9847; Magnification: 65X

methacrylate before sectioning. Note that the fibers in the section lie in the x-y plane. The information in this photograph is supported by visual observations of fiber beds during formation and also the observation that fiber beds can be peeled apart after formation. The small pieces of fiber in the photograph which appear to have many possible orientations are almost certainly those which were snapped off by the cutting procedure and spread across the surface of the section. This is supported by the work of Arnold (43). In trying to make microtome sections of embedded glass fibers to study their cross-sectional shape, Arnold found that the microtome popped the small pieces of fiber out of the embedding material.

The type of structure described above was known to exist throughout a large portion of the fibrous bed, but it was also known that some orientation of the fibers in the z direction would occur at the walls of the forming tube. This portion of the bed was assumed to be a negligible part of the whole. However, problems were encountered in obtaining reliable results with glass and dacron fibers. These problems, which were originally thought to be associated with a squeezing-out of the unconfined pad, were later identified with the z-orientation edge effect in the pad structure. During the first compression of glass fiber pads, the fibers at the edge of the pad were forced into a structure of considerable strength and rigidity. Consequently, the edges of the pad did not recover as did the center of the pad in the deloading cycle. This is shown in Fig. 8. Such an edge effect did not occur at all with nylon fiber and therefore is believed to be related to the high stiffness and apparent high interfiber friction characteristics of the glass fibers.

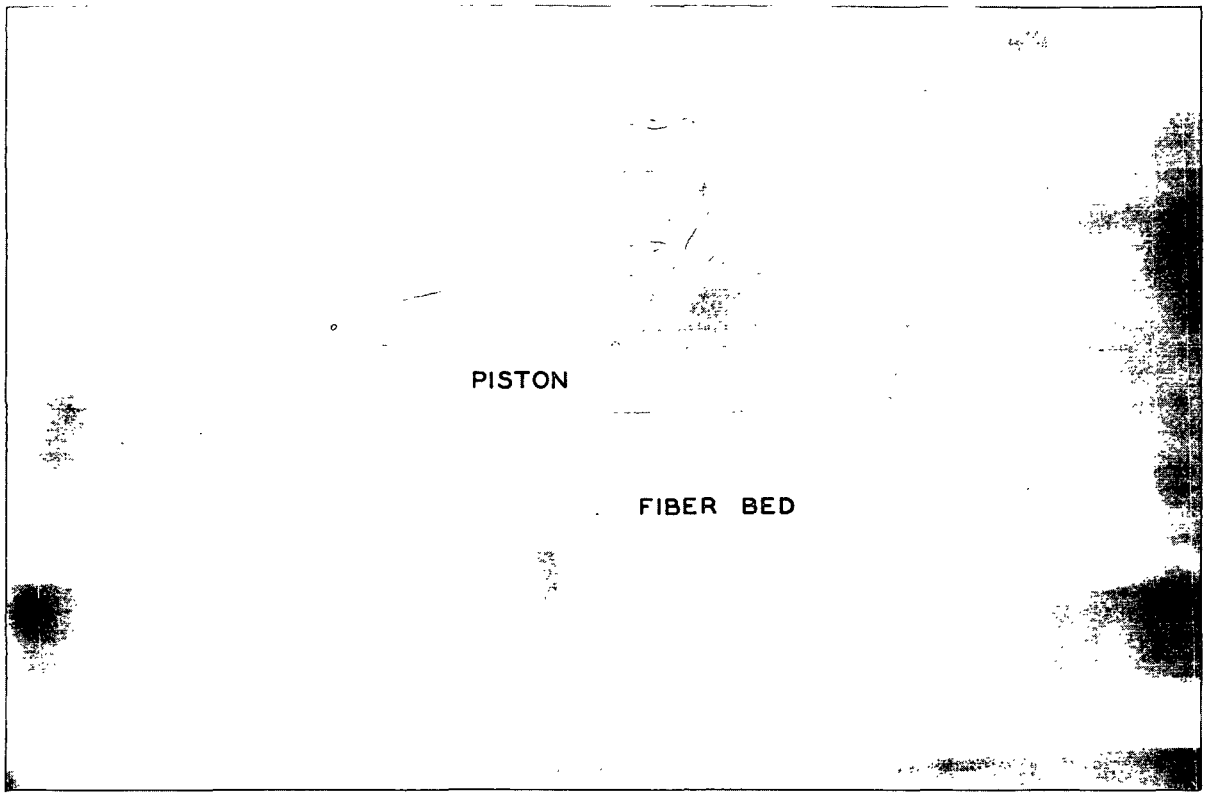

Figure 7. Photograph of a Typical Glass Fiber Bed Made by the Procedure of Forming a 5-in. Diameter Bed and Clipping off the Edge to a 4-in. Diameter Bed Using the Piston as a Template. Applied Stress = 0.111 g./sq. cm.; Fiber Size, $\underline{\ell}$ = 3.13 mm.; $\underline{d}$ = 12.86 microns

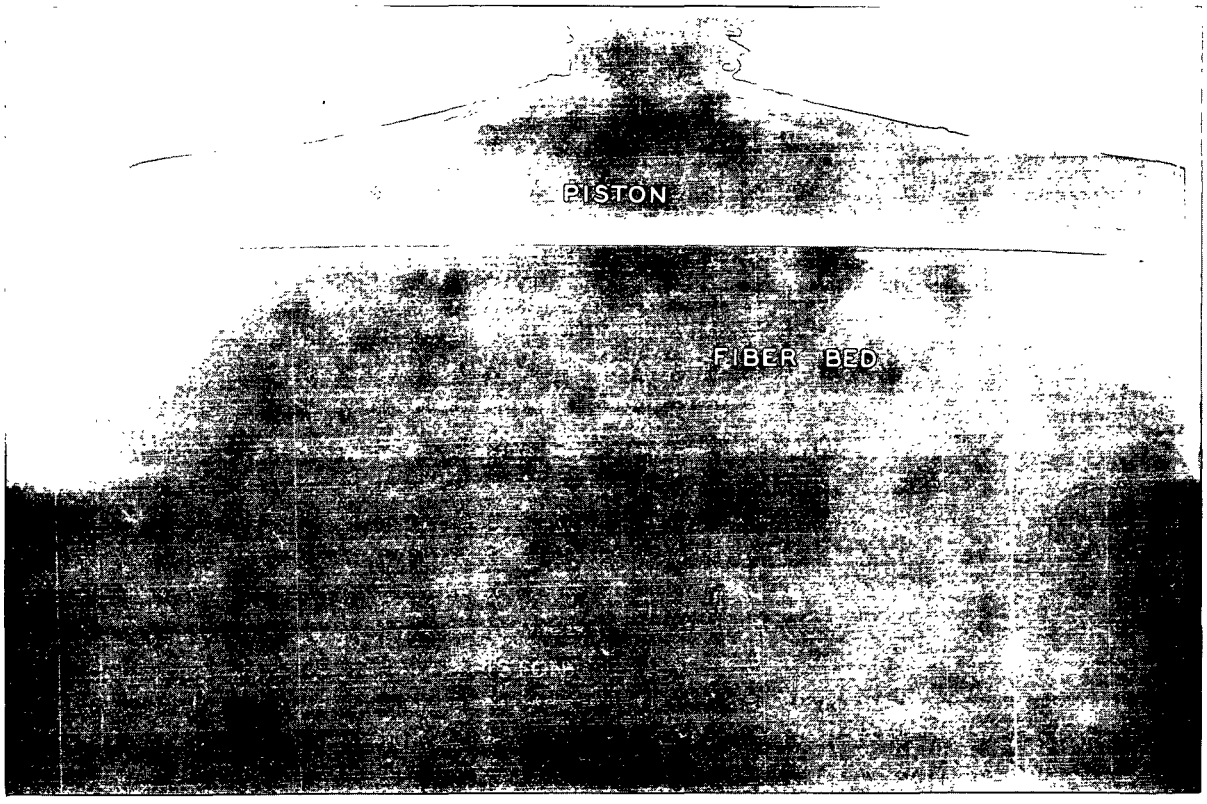

Figure 8. Photograph Showing the Edge Effect for a Glass Fiber Bed Originally Formed 4 in. in Diameter. Applied Stress = 0.039 g./sq. cm. Fiber Size: $\underline{\ell}$ = 3.13 mm.; $\underline{d}$ = 12.86 microns

To rectify this situation, a procedure was developed for making glass fiber beds with diameters greater than the desired test section and then removing the fibers on the edge. The details of this technique will be discussed in a section dealing with bed testing procedures. However, the appearance of a bed so treated can be seen in Fig. 7.

Studies were also made to determine the loads which could be applied to glass fiber beds before individual glass fibers started to break, an important consideration since fiber length was one of the variables to be studied. It was shown that the glass fiber beds used in this work would sustain an applied stress of 150 g./sq. cm. before any appreciable breakage began to occur. This was determined by removing a sample of fiber from a bed mechanically conditioned to that stress and comparing its fiber length distribution to that of the original fiber slurry.

The creep-compressibility equipment as designed by Wilder and modified in this work is a flexible instrument with a number of advantages designed to overcome the problems encountered in the preliminary work. These advantages are:

1. The equipment is versatile in that it permits one to study both compression and recovery using a compressibility test and/or a creep test.

2. It eliminates the edge effects due to mat-forming tube friction or piston-forming tube friction.

3. Using this equipment, a mat can be tested while it is held below the surface of the water in order to avoid surface tension effects.

4. The bed-forming system permits reproducible fiber beds to be formed under any desired pressure drop, beginning as low as 1 cm. of water.

5. Beds can be formed from slurries of any desired consistency.

6. The system permits close temperature regulation of the sample during testing.

7. The equipment provides for a swift and accurate method of measuring bed deformation. Measurements may be made to $\pm$0.0007 in. over a range of 2 in. and to $\pm$0.0001 in. over a selected range of 0.2 in.

8. The equipment is designed to permit the use of dead loads in the range of 1 gram to 52,000 grams.

9. Either 4-in. or 5-in. diameter beds may be formed.

10. Provisions are made for the removal of the mat after testing to permit determination of the bed basis weight.

A description of the mat-forming and testing procedures will be given below, at which time the methods of achieving the features listed above will be clarified.

MAT FORMATION

All fiber beds tested in this investigation were formed by filtration from a closed system with recycle. A schematic diagram of the equipment used during bed formation is shown in Fig. 9. The forming tube and tank were filled from a supply of deaerated water through the septum at the bottom of the forming tubes in order to avoid trapping air in the system. This was done by opening only valves V_1, V_2, and V_3,

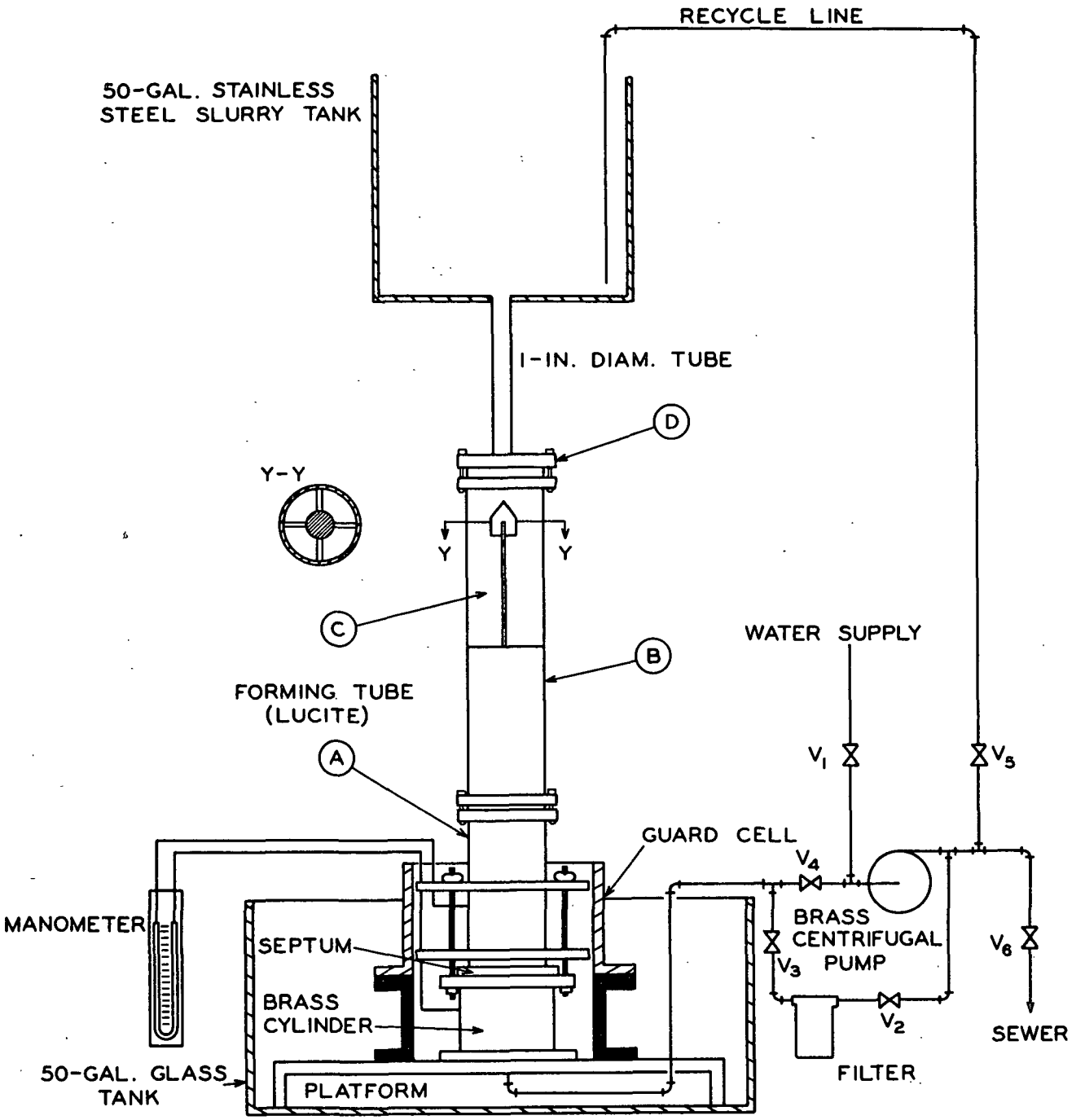

Figure 9. Mat-Forming System

and pumping the supply water through a filter up into the forming tubes and slurry tank. Supply water, free from dissolved gases, was prepared by boiling filtered, deionized water in a 500-gal. water supply tank. The water was cooled before use.

The forming septum was a brass plate drilled with many holes over a circular area 5 inches in diameter to permit water passage. This was covered with a 100-mesh brass screen held tightly in place on the septum by a brass ring. The septum was mounted upon a brass cylinder, and its initial position was measured before the forming system was put together and filled with water. To do this, the piston (E) (see Fig. 10) was placed upon the septum (F). The distance between the micrometer support (G) and the micrometer contact (H) was measured to 0.001 in. and estimated to 0.0002 in. Contact between the micrometer and the piston rod was determined electrically, using a d.c. milliammeter (J) which indicated when the circuit was closed.

The forming tube assembly generally consisted of (1) a 16-in. lower forming tube, A (Fig. 9), which was bolted on top of the septum to the brass cylinder; (2) a 36-in. top forming tube, B, containing a set of baffles, C, to steady out the flow pattern after turbulent mixing had taken place just above section Y-Y; and (3) a 1-in. diameter tube from the slurry tank to the forming tube attached to the latter by flange D.

When a bed was to be formed, deaerated fibers were placed in the slurry tank and gently agitated with a 1/8-H.P. "Lightnin'" mixer. With all other valves shut, Valves V_4 and V_5 were opened and the pump started. The pressure drop across the mat was regulated, using throttling

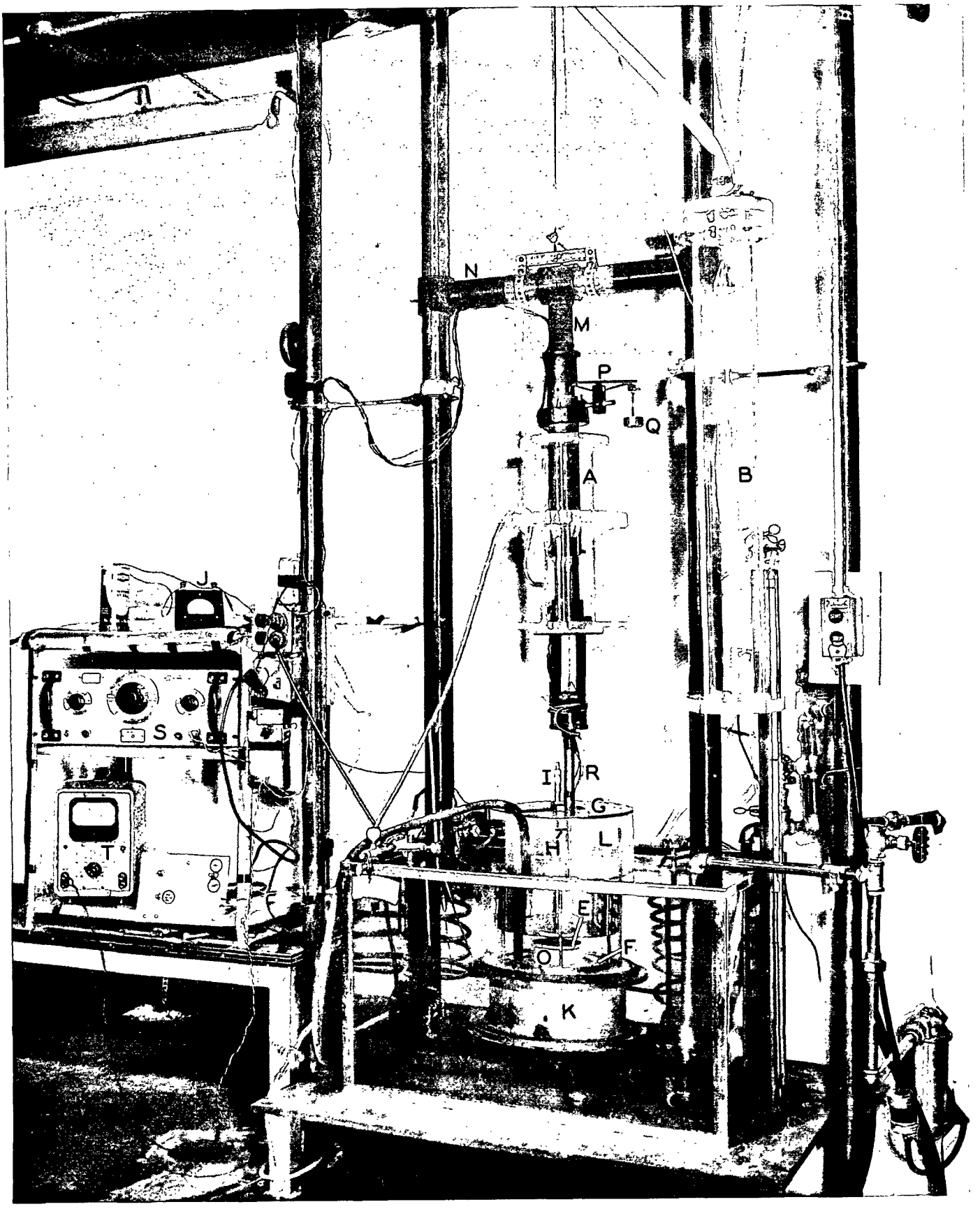

Figure 10. Creep-Compressibility Apparatus

valve V_4 in conjunction with a carbon tetrachloride-water manometer. Additional fibers were added to the slurry tank from time to time until a bed of the desired basis weight was formed.

All the test beds were 4 in. in diameter. In working with nylon fiber, both forming tubes A and B were 4 in. in diameter and the velocity during formation ranged from 0.12 to 0.13 ft. per sec. These velocities are in the laminar flow region, which is desirable in order to prevent continual disturbance of the fibers at the slurry-fiber bed interface. However, the forming tube assembly was not long enough to permit a serious parabolic velocity profile to develop in the slurry before it reached the mat being formed. This is important since a parabolic velocity profile would introduce variables in the bed basis weight from the center to the edge of the pad. Basis weight measurements indicated that the basis weight of the beds did not vary significantly from the center to the edge of the pad.

During formation of glass fiber beds, the A section of the forming tube was replaced with a 5-in. diameter tube of the same length. This permitted a 5-in. diameter bed to be formed so that the edges could be removed. In this case, the flow rates ranged from 0.08 to 0.09 ft. per sec. in the 5-in. diameter section. In all cases, the pH of the glass fiber slurries was adjusted and maintained at 5.5 in order to obtain uniform conditions on the glass fiber surface.

Pulp fiber presented another special case since pulp fiber pads compress a great deal under relatively low loads. In order to avoid excessively high pressure drops during formation of pulp fiber beds,

very low flow rates were used. To accomplish this and still obtain uniform formation, forming tube B was removed from the system and flange D attached to the 4-in. diameter forming tube A. A smaller version of the baffle C was also installed in forming tube A. The pressure drop across the pad during formation was kept below 2.5 cm. of water.

The forming times for the beds studied ranged from 35 minutes to 8 hours, depending upon fiber type, fiber size, desired bed basis weight, and maximum allowable frictional pressure drop.

TEMPERATURE CONTROL

In order to eliminate a possible temperature variable, the entire mat-containing apparatus was placed in a constant-temperature bath. (See both Fig. 9 and 10.) The temperature was maintained at 24.8 $\pm$0.1°C. during all runs. Once the forming tube was removed and the mat was no longer confined, it could not be subjected to the water agitation used to maintain uniform temperature in the constant-temperature bath. For this reason, the fiber bed, septum, and supporting brass cylinder were placed in a guard cell. The lower section of the guard cell (K) was brass to facilitate heat transfer, and the upper section (L) was lucite to permit observation of the bed during testing.

PREPARATION OF BEDS FOR TESTING

The fiber beds formed by filtration have all been formed under positive pressure drops, and these pressure drops across the bed cause some bed compression. Therefore, the first compression results of this investigation are in reality second compression results. The effect of

this small compression during formation on first compression results will be discussed in the presentation of the data.

When bed formation was complete, the water level was lowered to the top of forming tube A and forming tube B was moved aside. The piston held in the end of the piston support bar (M) was lowered down inside tube A by means of the sliding crossbar (N) until the weight of the piston was supported by the mat (O). The piston was held in such a way that it could not fall down out of the support arm but could move up in the support arm freely when contact was made with the bed. The piston served to hold the fiber mat in place so that forming tube A could be lifted from around the bed. To do this, the water levels inside the guard cell and inside the forming tube were adjusted to the same height. Then the forming tube was unbolted and lifted upward, using its extra-large flanges as guides inside the guard cell. The tube was secured to crossbar N. Sufficient time (1 to 3 hours) was allowed for the water inside the guard cell to come to temperature before testing.

BED COMPRESSION AND RECOVERY

The piston used in this work consisted of a 4-in. diameter aluminum disk, 3/16 in. thick at the edge and 5/8 in. thick at the center. This was covered with a 1/16-in. lucite face to prevent corrosion. A 19-inch aluminum piston rod was attached to the piston face. Before compression-recovery measurements were made, the water level in the guard cell was lowered by siphoning to a specified mark on the piston rod about 1 inch above the face of the piston. Allowing for the buoyancy force of the

submerged portion of the piston, the piston alone exerts an applied stress of 2.70 g./sq. cm.

The micrometer system already described was used to determine the initial height of the bed. When this equipment was removed, additional stress could be applied to the bed by placing slotted, circular steel weights gently upon a small support disk, approximately 2 inches above the face of the piston. The rate of addition and removal of loads was controlled by hand. The operation had to be carried out slowly enough to permit the water in the bed to move out through the bottom and sides of the structure without disrupting it. The disk supporting the loads never passed below the surface of the water so that small changes in the buoyancy force on the piston as it settled below the surface were negligible. Stresses less than 2.70 g./sq. cm. were applied to the beds by counterbalancing the piston. The counterbalancing system consisted of a string attached to the top of the piston and passing up through the support bar (M). This was attached to a beam from an analytical balance (P), and small weights (Q) were added to a pan at the opposite end of the beam.

Deformations following the determination of the original bed height under the piston load were measured with a Shavitz 1000SS-L linear variable differential transformer (LVDT). This measuring system consisted of an LVDT (R), a Hewlett-Packard Audio Oscillator Model 200B (S) and a Hewlett-Packard Vacuum Tube Voltmeter Model 400D (T). A circuit diagram is shown in Fig. 11. The audio oscillator was operated at an output of 10 v. and 3530 c.p.s. and was utilized as a power supply

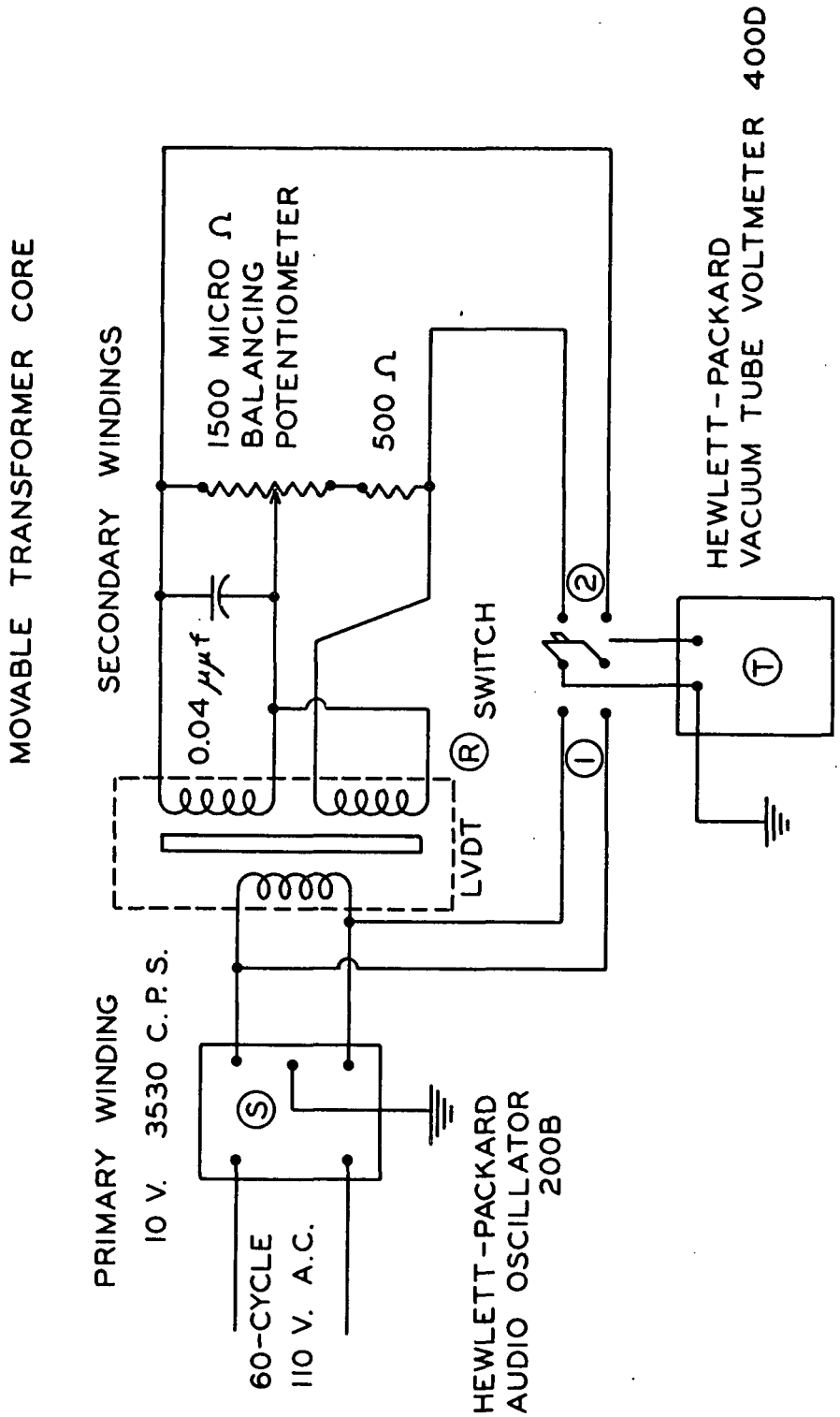

Figure 11. Linear Variable Differential Transformer Circuit

for the LVDT. The iron core of the LVDT was a portion of the piston rod, and the output of the secondary coils of the LVDT was a function of the position of this core. The relationship between the voltage output and the core portion was linear over most of the LVDT's range of $\pm$ 1 in. The output voltage was very nearly zero when the core was positioned in the center of the coils. The LVDT was calibrated by measuring output voltage as a function of core position, using a depth micrometer to position the core accurately. By taking an initial output voltage reading at the same time that the initial bed height was measured with the depth micrometer, further changes in bed height with load application could be followed by measuring output voltage. Before each measurement, the switch (Fig. 11) was placed in position 1 and the input voltage adjusted to 10 volts. Then the switch was placed in position 2 to read the LVDT output voltage on the vacuum tube voltmeter (VTVM).

A piston guide collar was located in the piston support arm just above the LVDT (R). This collar kept the piston properly lined up in the LVDT so that reproducible readings could be obtained. However, this collar was designed as a split ring that could be pulled apart so that there was no friction between the piston and the collar when loads were being added or removed. Deformation due to repeated load addition and removal could be followed step by step with the LVDT circuit through compression-recovery cycles until the beds were mechanically conditioned.

It has already been mentioned that a special technique was devised to prepare 4-in. diameter glass and dacron fiber beds free from the serious edge effects pictured in Fig. 8. This was done by first forming

a 5-in. diameter fiber bed. When the forming was completed, the 4-in. diameter piston was lowered onto the bed, and the bed was taken through a standard first compression. The loading of a 5-in. bed with a 4-in. piston resulted in 4 to 5% error in the first compression data, particularly at the higher loads. This error occurred because the piston received some support from the fibers lying beyond its outside edge. The piston was then locked in its position at maximum load; the excess fiber was carefully clipped away from the pad with a pair of small scissors, utilizing the piston as a template. A new bed height at maximum load was obtained and the rest of the test data were taken on the resulting 4-in. diameter bed. The procedure was very successful in eliminating the edge effect, as is demonstrated in Fig. 7. Note the smoothness of the clipped edges. It has been determined that this clipping procedure can result in a 2.5-3% difference in bed weight between the actual mass of dry fiber under the piston determined by weighing and the mass calculated to be there based on the total weight of the 5-in. diameter bed. In most cases, the error was less and this is felt to be quite good control in view of the techniques used.

MAT REMOVAL

When a compression-recovery run was complete, the water was drained from around the test bed, and the septum together with the fiber bed and piston was removed from the guard cell. Pulp, nylon, and dacron beds were dried at 110°C. for basis weight determinations. The glass fiber beds were first washed briefly with hydrochloric acid to remove any adsorbed hydroxides formed during the filtration operation and then dried

at 1000°C. in a muffle furnace to assure complete removal of binding material.

A sample calculation of mat solids concentration is contained in Appendix I, together with an estimation of attendant errors.

PRESENTATION OF DATA AND DISCUSSION OF RESULTS

INTRODUCTION

The experimental work carried out in this investigation may be conveniently separated into three groups based on the type of fiber studied: (1) the work conducted with perfectly elastic fibers (glass); (2) the studies carried out with viscoelastic fibers (nylon and dacron), and (3) the work conducted with viscoelastic fibers which undergo extreme swelling in water (pulp).

The discussion of this work has been divided into three main topics. First, the scope of the work accomplished with each fiber is presented. Second, there is a graphical presentation and general discussion of the results. Finally, there is a detailed analysis of the data, including a discussion of attempted data treatment techniques and a discussion of the conclusions which may be drawn from the data analysis.

SCOPE OF WORK ACCOMPLISHED

All the work done in this investigation was carried out on relatively thick, water-saturated fiber beds formed by filtration from dilute slurries. In very nearly all runs, data for both the first compression and recovery and the mechanically conditioned compression and recovery were taken. A bed was determined to be mechanically conditioned when two successive compression-recovery cycles were the same. The number of cycles required to mechanically condition the pad was also noted. In addition, an attempt was made to obtain the value of the solids

concentration of a mechanically conditioned bed at zero applied load. This was done by carrying out the final pad recovery to extremely low loads and looking for a point where further reduction in applied stress did not cause a significant change in mat solids concentration.

The extent of the studies made on nylon fiber is shown in Table IV.

TABLE IV

NYLON FIBER STUDIES

Run No.	Fiber Length, mm.	Fiber Diameter, μ	Modulus of Elasticity, g./sq. cm. x 10^{-7}
Length Study			
C26	6.30	46.2	1.27
C27	4.60	46.2	1.27
C25	3.13	46.2	1.27
C24	0.96	46.2	1.27
High Modulus Diameter Study			
C29	4.60	77.4	1.07
C30	4.60	44.8	1.33
C31	4.60	16.8	1.30
Low Modulus Diameter Study			
C43 and C52	4.60	76.8	0.38
C45	4.60	43.8	0.37
C32	4.60	44.5	0.31
Modulus Studies at 2 Diameters			
C29	4.60	77.4	1.07
C43 and C52	4.60	76.8	0.38
C30	4.60	44.8	1.30
C32	4.60	44.5	0.31

The modulus studies are merely a regrouping of the runs made in the two diameter studies and show how the effect of modulus was evaluated, independent of length and diameter considerations.

The series of dacron and glass fibers studied are summarized in Tables V and VI.

Again, the diameter studies are merely regroupings of the data in the modulus and length studies. Taken together, the nylon, dacron, and glass data make it possible to evaluate each of the selected fiber variables: length, diameter, and elastic modulus, independent of the other two.

The carefully selected pulp fiber has been evaluated for comparison to synthetics in order to try to make the information gained from studies of synthetic fiber systems more valuable to an interpretation of the behavior of pulp fiber systems. A sample of the bleached fiber was mechanically conditioned, but in the other tests only first compression and recovery were run. A summary of the fibers tested is shown in Table VII.

TABLE V

DACRON FIBER STUDY

Run No.	Fiber Length, mm.	Fiber Diameter, μ	Modulus of Elasticity, g./sq. cm. x 10^{-7}
C42	4.60	22.7	14.67

TABLE VI

GLASS FIBER STUDIES

Run No.	Fiber Length, mm.	Fiber Diameter, μ	Modulus of Elasticity, g./sq. cm. x 10^{-7}
Length Studies at 2 Diameters			
C54	6.3	12.86	74.39
C53	4.6	12.86	74.39
C56	1.68	12.86	74.39
C57	0.96	12.86	74.39
C51	6.30	5.12	72.60
C50	4.60	5.12	72.60
C49	3.13	5.12	72.60
C48	1.68	5.12	72.60
C47	0.96	5.12	72.60
Moduli Studies at 2 Lengths			
C58	4.60	9.12	71.20
C60	4.60	9.14	102.65
C59	0.96	9.12	71.20
C61	0.96	9.14	102.65
Diameter Studies at 2 Lengths			
C53	4.60	12.86	74.39
C58	4.60	9.12	71.20
C50	4.60	5.12	72.60
C57	0.96	12.86	74.39
C59	0.96	9.12	71.20
C47	0.96	5.12	72.60

TABLE VII

PULP FIBER STUDIES

Run No.	Weighted Average Fiber Length, mm.	Fiber "Diameter," μ	Condition
C64	2.84	43.6 (4)	Unbleached
C62 and C63	2.84		Bleached
C65	1.23		Bleached

The "diameter" given here is an average one measured microscopically without regard to whether a major or minor axis of the cross section was being measured. It is included here merely to give the reader a means of comparing the length-to-diameter ratio of these fibers with those of the synthetics studied.

GENERAL PRESENTATION OF THE RESULTS

This section consists primarily of graphical representations of the compression studies which have already been summarized in Tables IV-VII. Attention will be directed to the obvious trends in the data and similarities between the data taken on different fiber types.

REPRODUCIBILITY OF RESULTS

Duplicate compression-recovery runs have been made with a sample of nylon fiber (Runs C43 and C52). The data are reported graphically in Fig. 12 and demonstrate the excellent reproducibility which may be obtained with the equipment for both first compressions and mechanically conditioned compressions and recoveries. In the present work, all compression and recovery data are reported graphically as double logarithmic plots of the mat solids concentration, C (a bulk density term) vs. the apparent applied stress, P. Note the small scale which indicates the $\pm 1\%$ and $\pm 5\%$ levels of deviation for the data. The majority of the data are reproducible to $\pm 1\%$. Data taken in this investigation substantiate the findings of Wilder (4) in regard to the effect of bed diameter and basis weight on compression recovery studies. Changes in pad basis weight in the range 0.02-0.08 g./sq. cm. and pad diameter at least in the

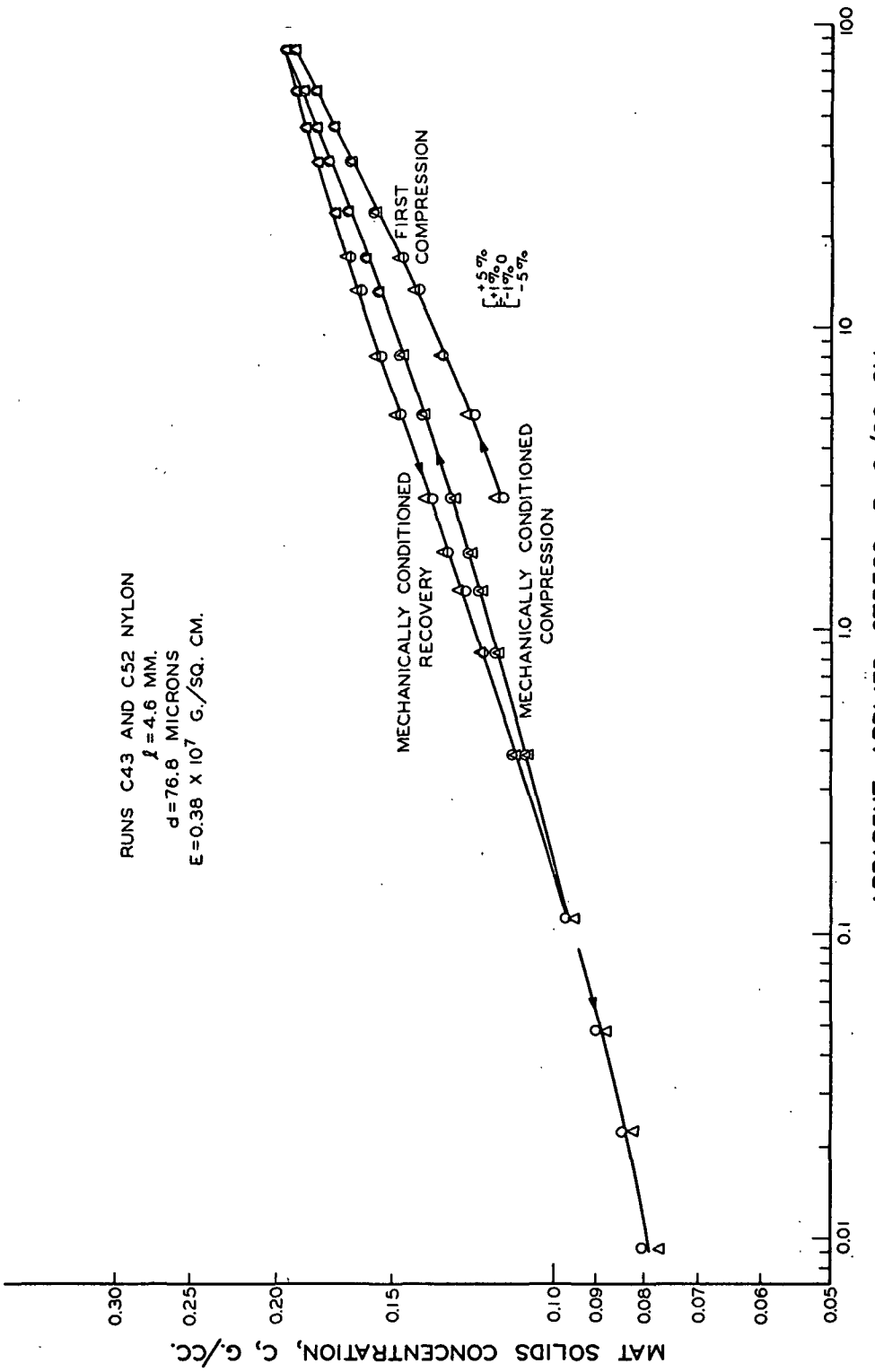

Figure 12. Reproducibility of Compression and Recovery Data

diameter range of 3 to 5 inches do not alter the relationship between C and P for a single fiber type. These findings are based on work with relatively thick pulp fiber pads.

NYLON FIBER STUDIES

The first compression results for the nylon length study appear in Fig. 13. In this part of the work, fiber diameter and elastic modulus were maintained constant. The compression data for the mechanically conditioned beds are to be found in Fig. 14, and those data for the recovery of these beds in Fig. 15. In each case, there is an obvious trend to higher solids concentration at any given stress as the fiber length is decreased. Although the portion of the data at low applied stress tends to be curved, the relationship tends toward a straight line at higher applied stresses. This observation is true of all the nylon first compression curves but will be seen to be more descriptive of mechanically conditioned glass fiber data than of mechanically conditioned nylon fiber data. The slope of the straight-line portion of a log C vs. log P plot has been designated as the limiting slope.

The limiting slope of the first compression curves increases up to about a fiber length of 3 mm. and thereafter, at longer lengths, the slope remains approximately constant. In other words, a given change in applied stress produces a much larger change in solids concentration for long fibers than for short fibers. Consequently, the curves for all lengths tend to converge at higher applied stresses and one expects that at extremely high stresses all the curves would converge to a mat solids concentration very close to the density of nylon.

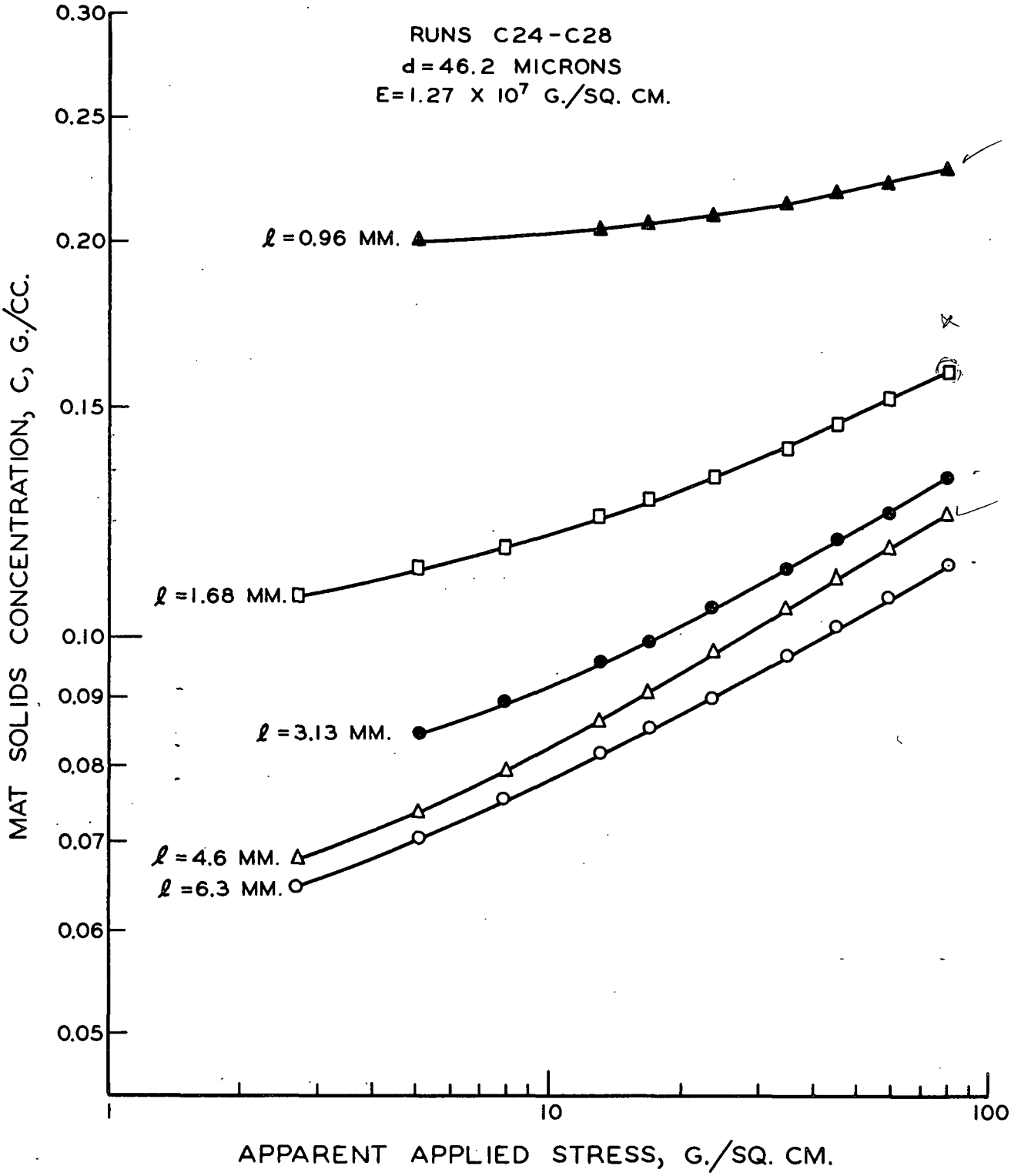

Figure 13. First Compression Data for a Nylon Fiber Length Study

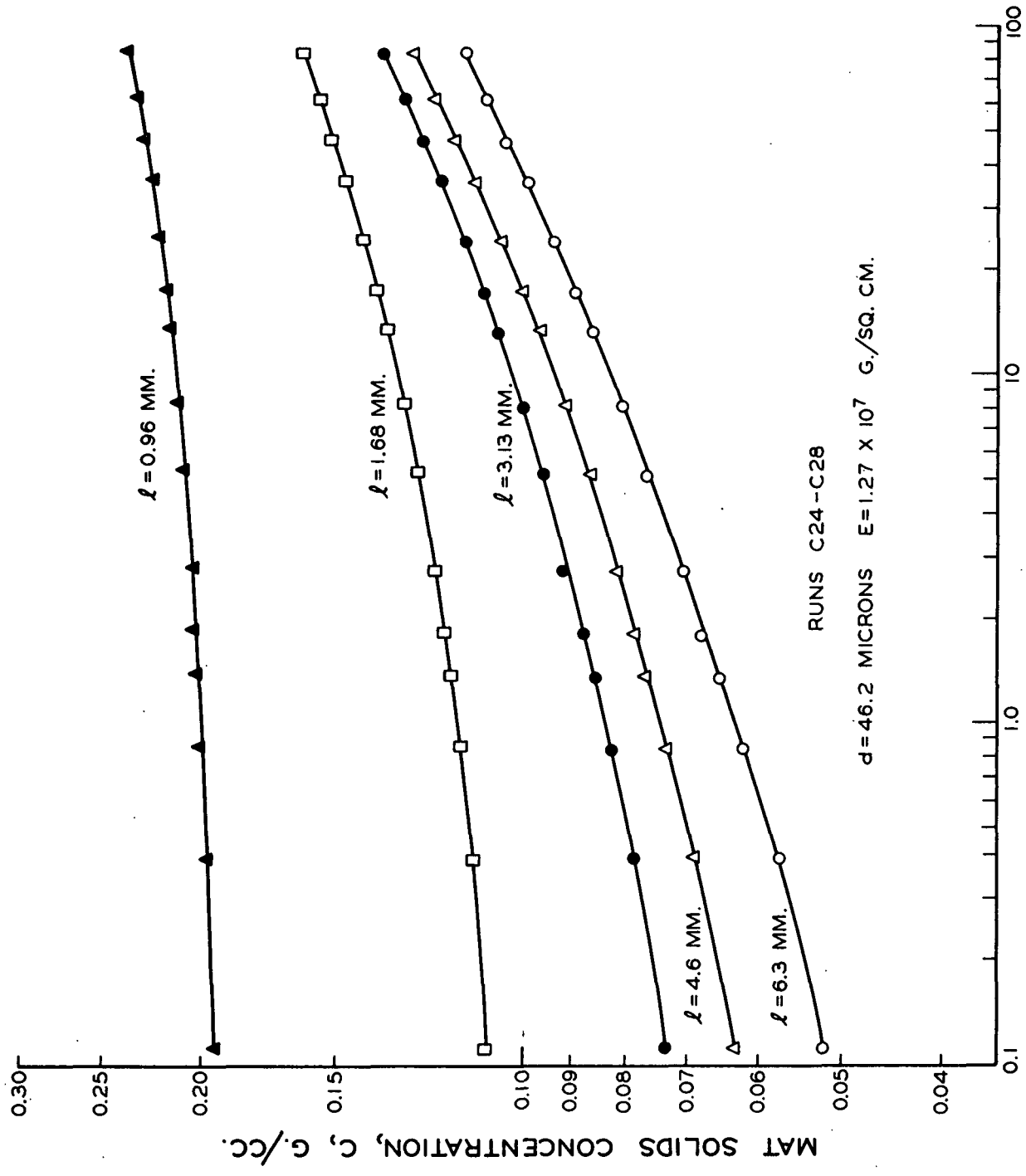

Figure 14. Mechanically Conditioned Compression Data for a Nylon Fiber Length Study

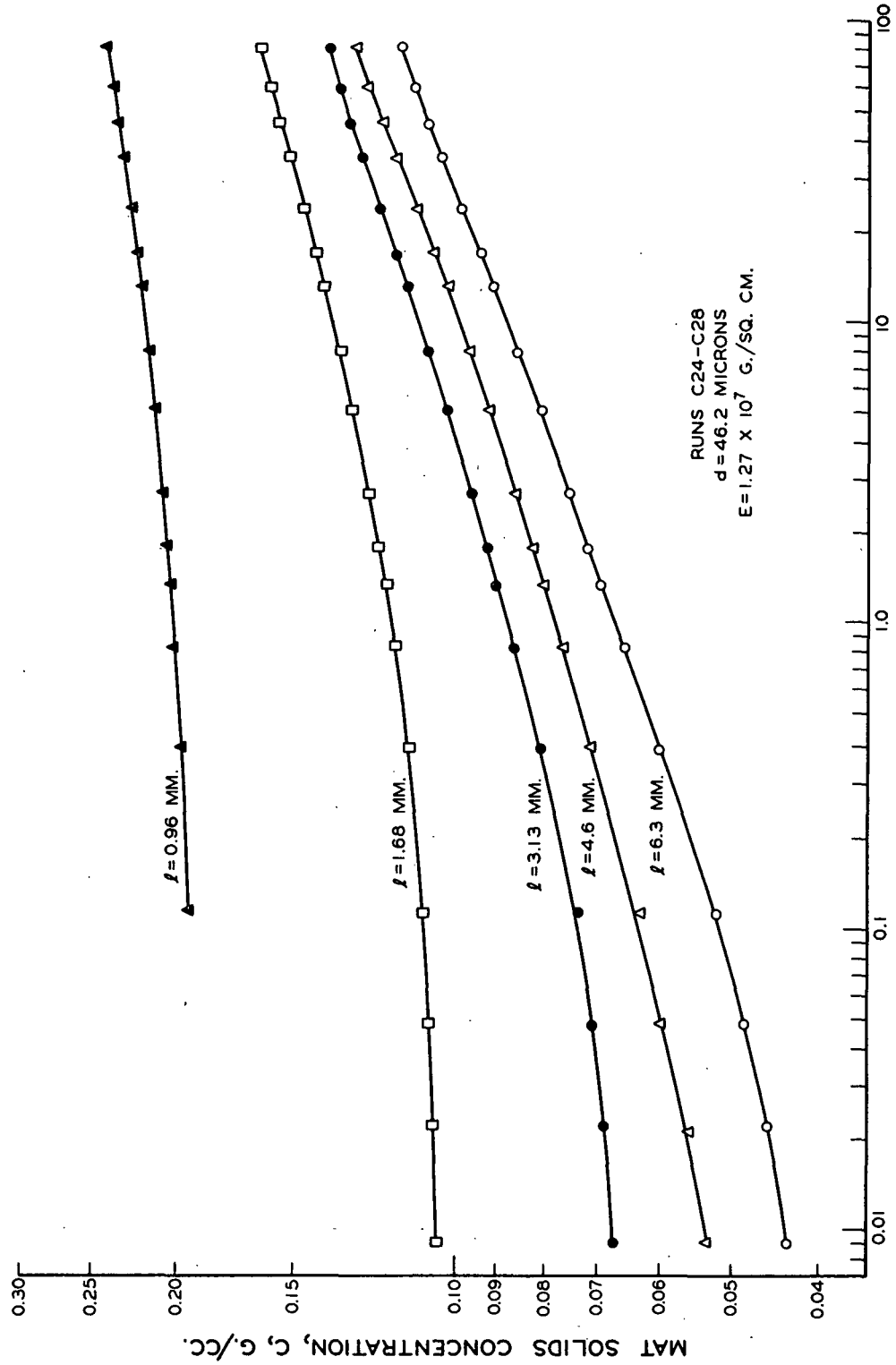

Figure 15. Mechanically Conditioned Recovery Data for a Nylon Fiber Length Study

It may be noted that the mechanically conditioned fiber bed compression data begins at an applied stress of 0.111 g./sq. cm., whereas the recovery data goes as low as 0.009 g./sq. cm. applied stress. The reason for this is that the recovery data were always taken after the compression data and carried out to very low applied stresses in order to obtain an estimate of $\underline{C}_o$, the mat solids concentration at zero applied stress. At this point, the bed structure was usually held together so loosely that if compression studies had been initiated, flow of water out through the sides of the bed would have completely disrupted the structure. Nylon beds were generally mechanically conditioned following the third or fourth compression cycle.

Analysis of a quantitative relationship between fiber length and the position of these curves is deferred to a later section.

During the early portion of this work, it was demonstrated that the curve in the low load portion of the first compression data (see Fig. 13) could be related to the maximum fluid stress applied to the bed during filtration. If this stress was maintained at a lower level during formation, the straight-line portion of the first compression data on a double logarithmic plot of $\underline{C}$ vs. $\underline{P}$ was extended to lower apparent applied stresses. This straight-line portion is represented by the empirical relationship

$$C = MP^N \qquad (1).$$

$\underline{M}$ and $\underline{N}$ are constants, and $\underline{N}$ is the limiting slope. Both theoretically and physically, there must be a lower limit to the applicability of this

empirical relationship since C cannot be equal to zero when P is equal to zero. However, in the present work the equation has been shown to hold down to about 2-4 g./sq. cm. apparent applied stress, if the pressure drop across the pad during formation is not very high. This is shown most clearly in Fig. 28, which contains first compression curves for pulp fiber pads formed under very low pressure drops. As has been mentioned, higher pressure drops during formation do not change the value of the constants M and N for the straight-line portion of the curve.

The results of the nylon diameter-modulus studies, together with the results of the dacron study, appear in Fig. 16-18. The data for the dacron fiber has been converted to an equivalent density of nylon by multiplying the fiber bed weight by the conversion factor (density of nylon/density of dacron). This is equivalent to saying that the data reported represent the results to be expected from a nylon fiber of the same length (ℓ), diameter (d), and elastic modulus (E) as the dacron used, since the only difference between two such fibers is their density.

Another method of representing the nylon-dacron data as well as data for other fibers is to eliminate the density factor by placing the data on the dimensionless solid fraction basis. However, such a technique is hindered by the problem of selecting proper values for the fiber specific volume in order to make the conversion from mat solids concentration to solid fraction. Selected data representing pulp, nylon, dacron, and glass fiber studies are compared as log solid fraction vs. log applied stress in

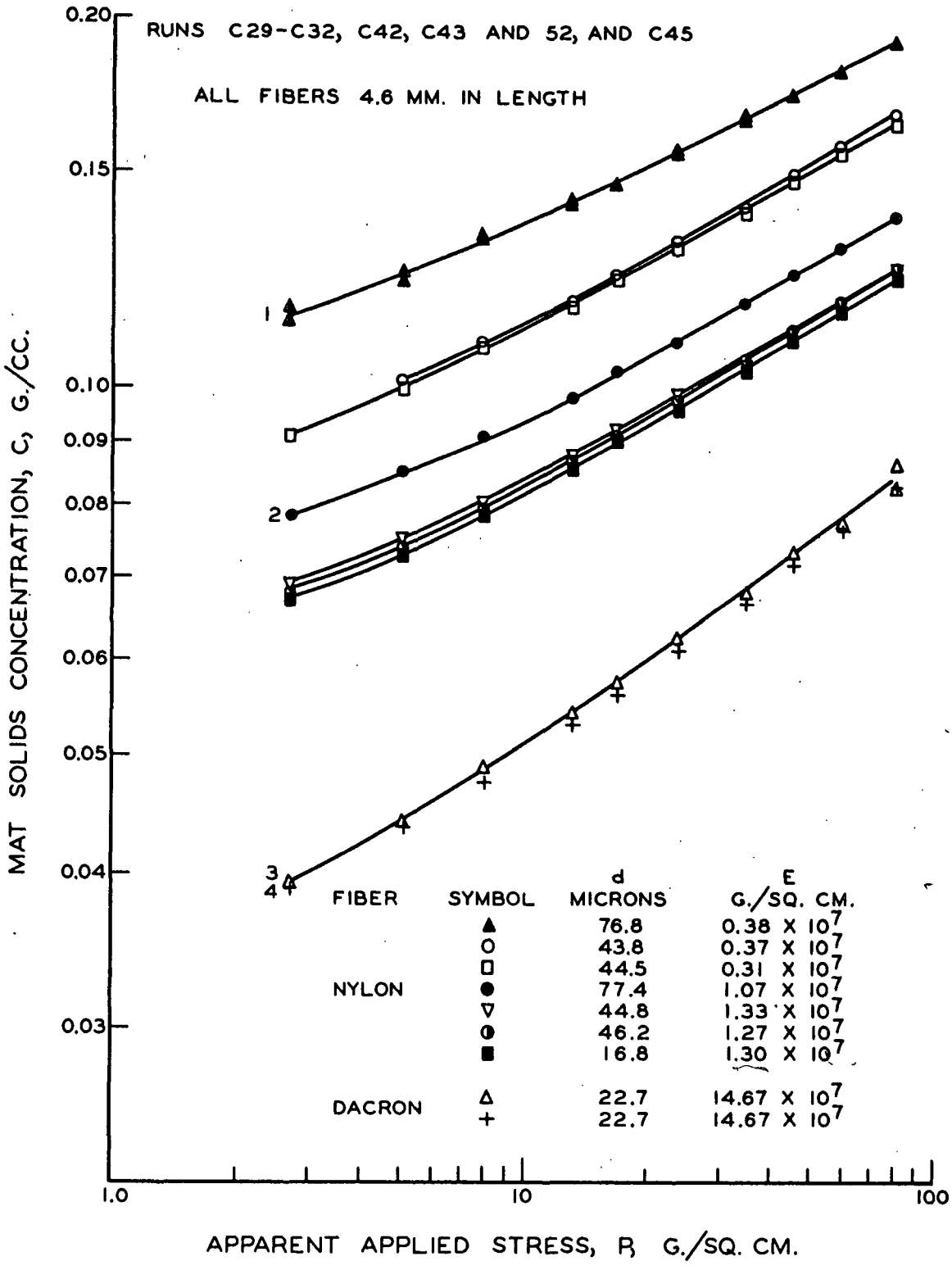

Figure 16. First Compression Data for a Nylon and Dacron Fiber Modulus-Diameter Study

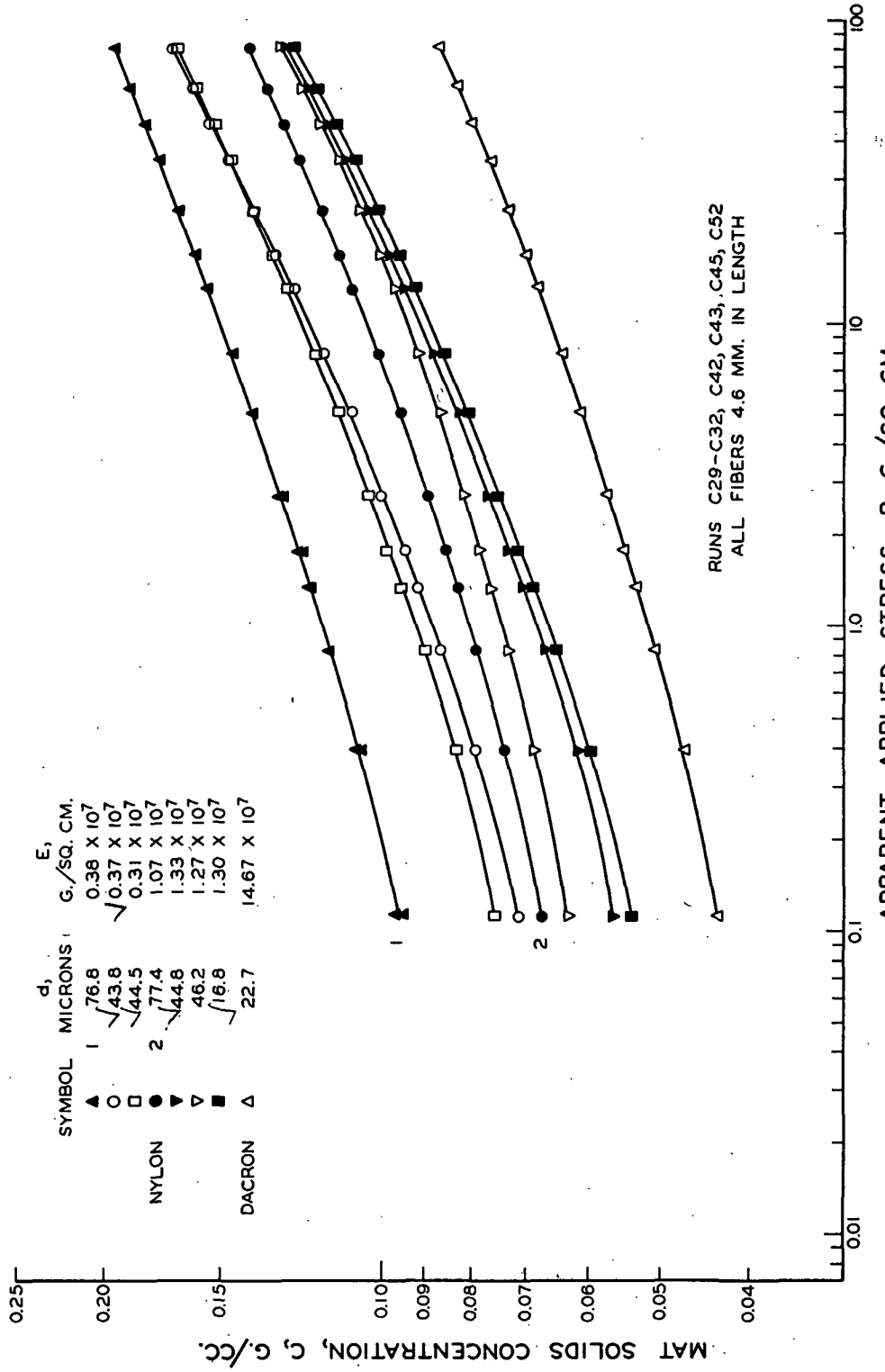

Figure 17. Mechanically Conditioned Compression Data for a Nylon and Dacron Fiber Modulus-Diameter Study

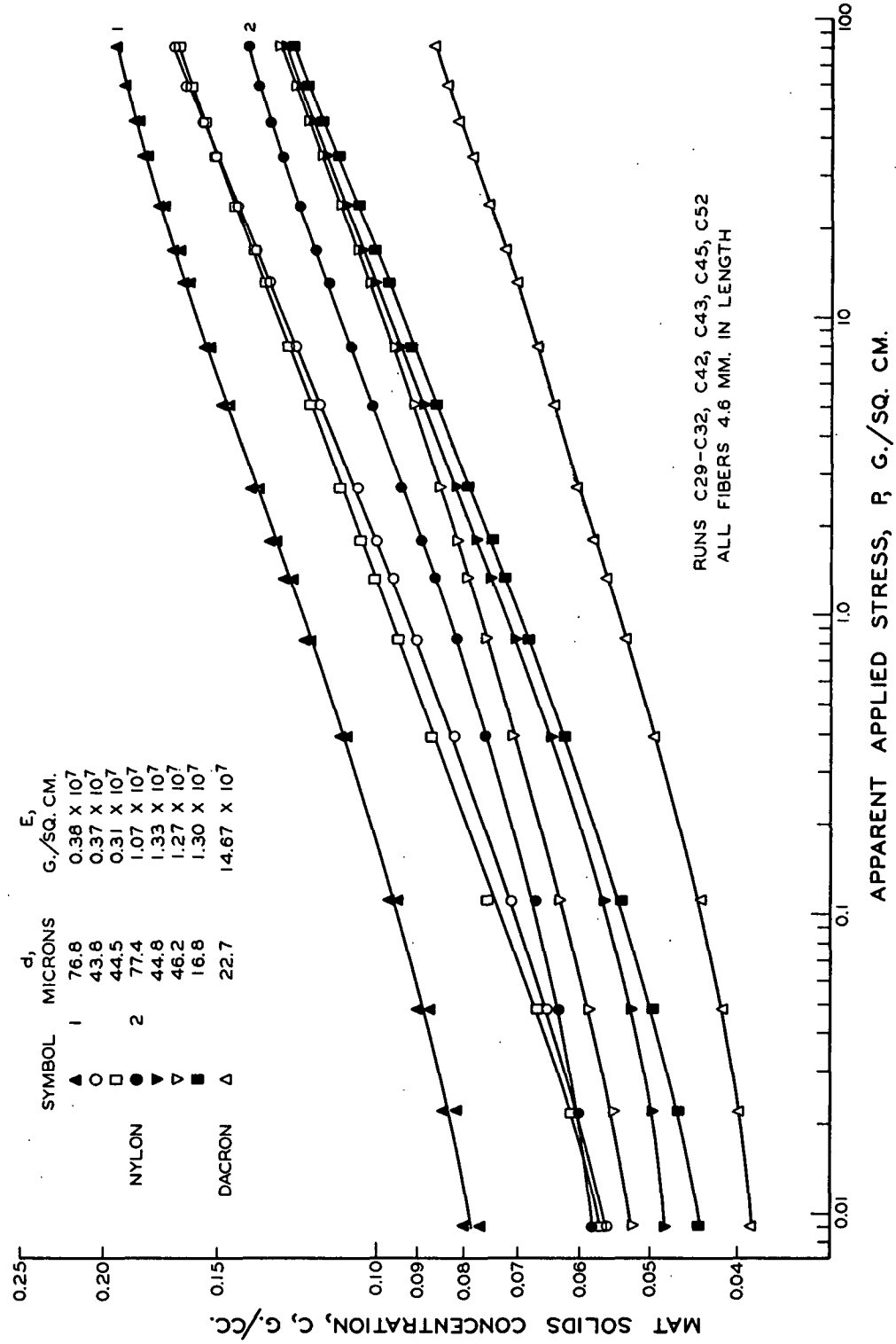

Figure 18. Mechanically Conditioned Recovery Data for a Nylon and Dacron Fiber Modulus-Diameter Study

Fig. 19. The specific volumes of the glass, dacron, and nylon fibers have been computed from the reciprocals of the pycnometric densities. The values are reliable for glass and dacron, which do not swell in water, but nylon swells approximately 3% on the diameter in water. This could result in a sizable error in the value of the specific volume computed from pycnometric density. The specific volume used for the pulp is a hydrodynamic value and carries with it the attendant difficulties of interpretation of that value. However, Fig. 19 does give a reasonable idea of the effect of modulus of elasticity on compression behavior of five different fiber types.

In viewing the data, one observes first that there is an obvious trend to lower solids concentrations, at the same apparent applied stress, as the fiber modulus of elasticity increases. Secondly, it appears that the fiber diameter has very little effect on the C vs. P relationship for fibers of the same modulus of elasticity. Two apparent exceptions to this observation are the two runs made on nylon fiber, 77 μ in diameter, labeled 1 and 2 in Fig. 16-18. However, it has been shown that there is a critical length-to-diameter ratio below which the above observation concerning diameter may break down and be altered. These very large-diameter nylon fibers have a length-to-diameter ratio of 60, which is below the critical ℓ/d ratio of 75-150 found for nylon and therefore they form a more compact mass at the same applied stress. This view will be amplified later in the discussion through an evaluation of these data and the glass fiber data which follow.

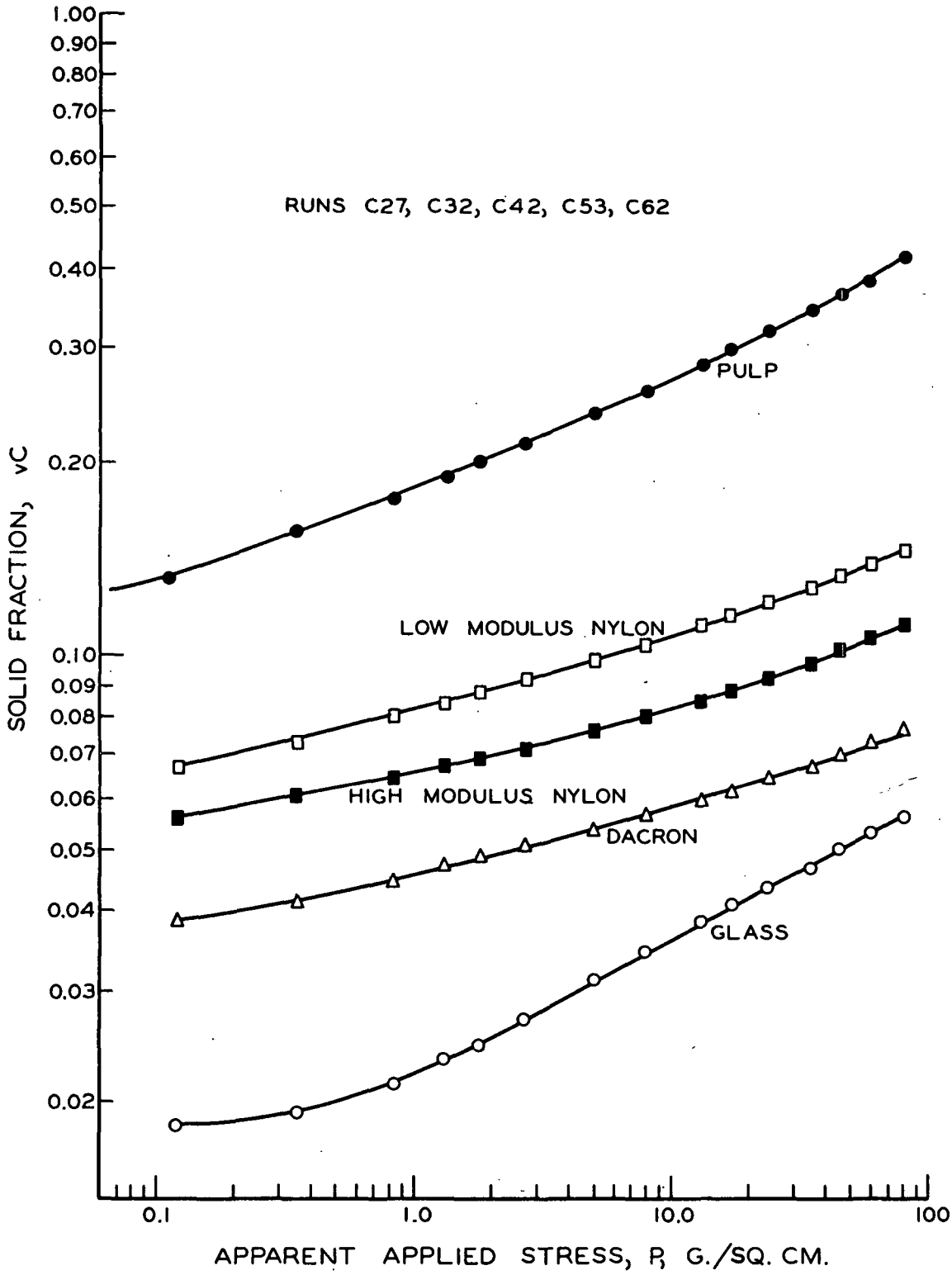

Figure 19. Mechanically Conditioned Compression Data Plotted as Solid Fraction vs. Applied Stress for 4.6-mm. Synthetic Fibers and 2.84-mm. Pulp Fibers

GLASS FIBER STUDIES

Because of the special technique used to obtain data for glass fiber beds, the first compression data will not be reported graphically. However, it was possible to obtain reasonable estimations of the straight lines of limiting slope for these data, and compressibility constants for the empirical equation $\underline{C} = \underline{M}P^{\underline{N}}$ have been computed.

In order to check the reliability of the bed clipping procedure, the dacron fiber was tested with both the 4-inch diameter procedure and the clipping procedure. The comparison of results was excellent, and the first compression results for both procedures are plotted together as dacron data in Fig. 16. The open triangles (Curve 3) are the data for a 5-inch dacron bed which was clipped to 4 inches for testing. The crosses of Curve 4 represent the data taken for the same fiber on a bed formed and tested at 4 in. in diameter.

The compression curves for mechanically conditioned beds of 12.86 and 5.12 μ diameter glass fiber of different lengths are presented graphically in Fig. 20 and 22. These beds were usually conditioned following second compression. The recovery data appear in Fig. 21 and 23. The trends with changes in length for glass fiber are the same as those which are found for nylon. There are some differences between these two sets of data which will be discussed at a later time. Of particular interest is the fact that the limiting slopes at high stresses for the glass data are all greater than those found for nylon. In the special case of the length study on 5.12 μ diameter glass (Fig. 22), it was found that compression studies could be initiated from the lowest recovery load. It

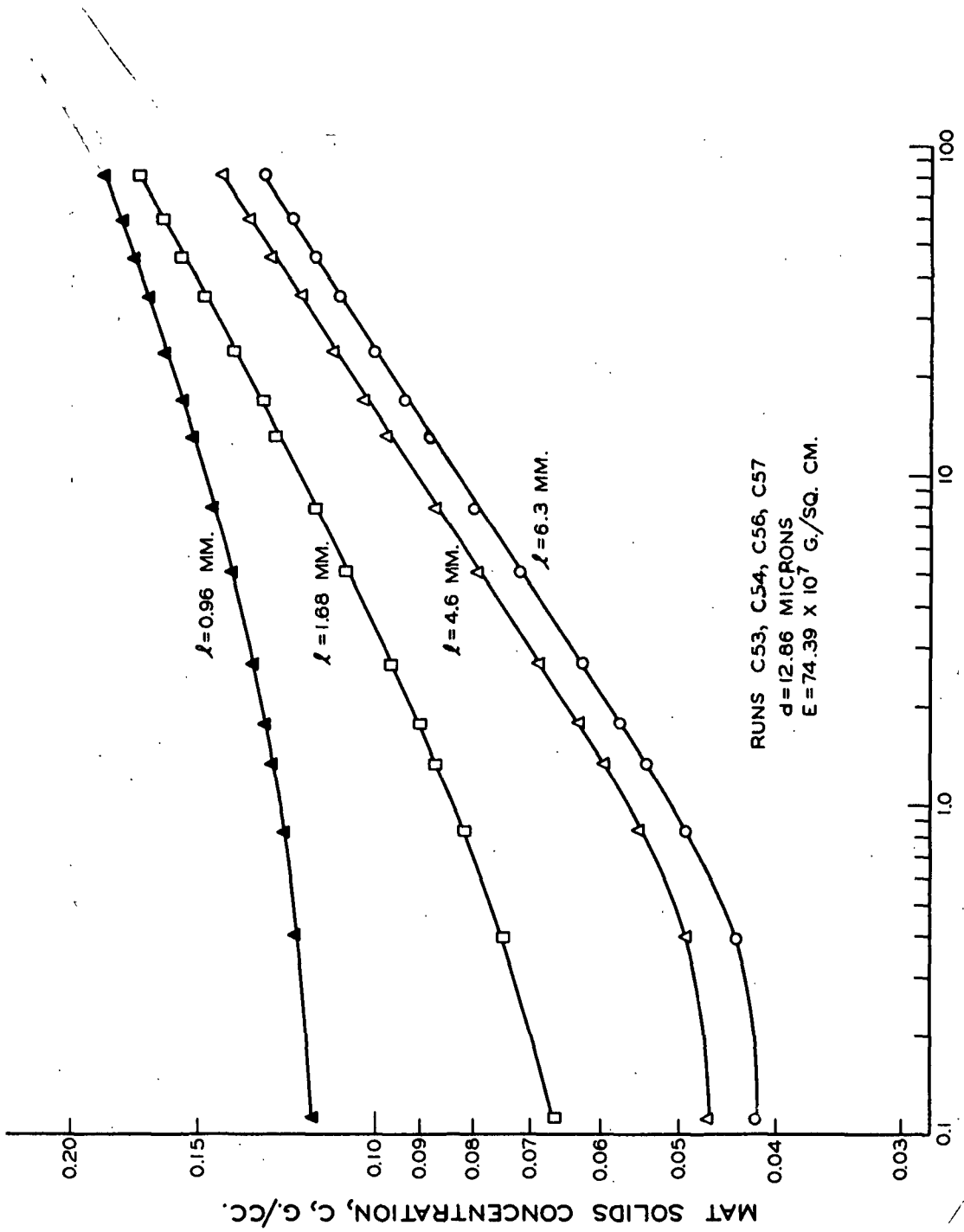

Figure 20. Mechanically Conditioned Compression Data for a Glass Fiber Length Study

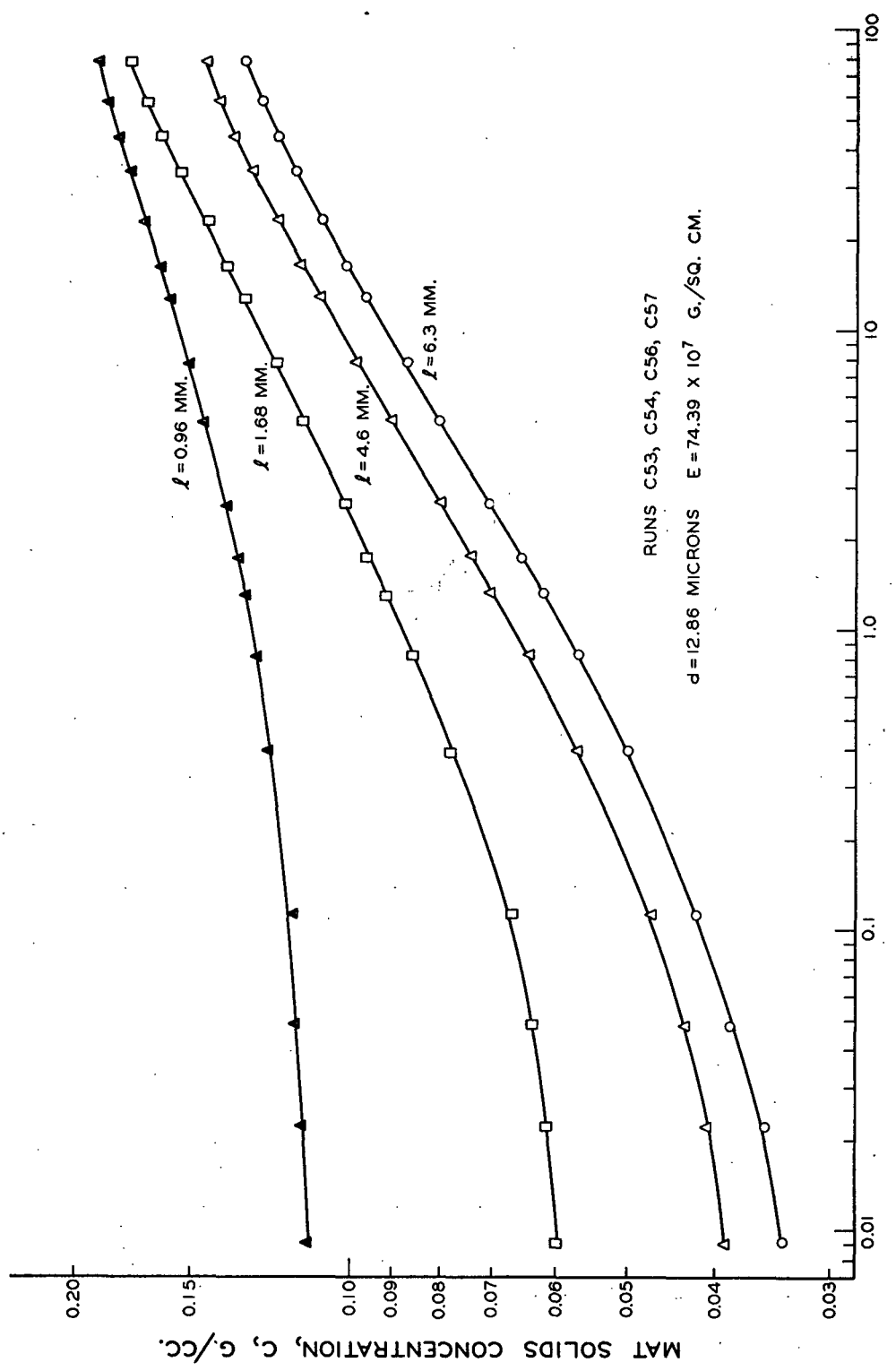

Figure 21. Mechanically Conditioned Recovery Data for a Glass Fiber Length Study

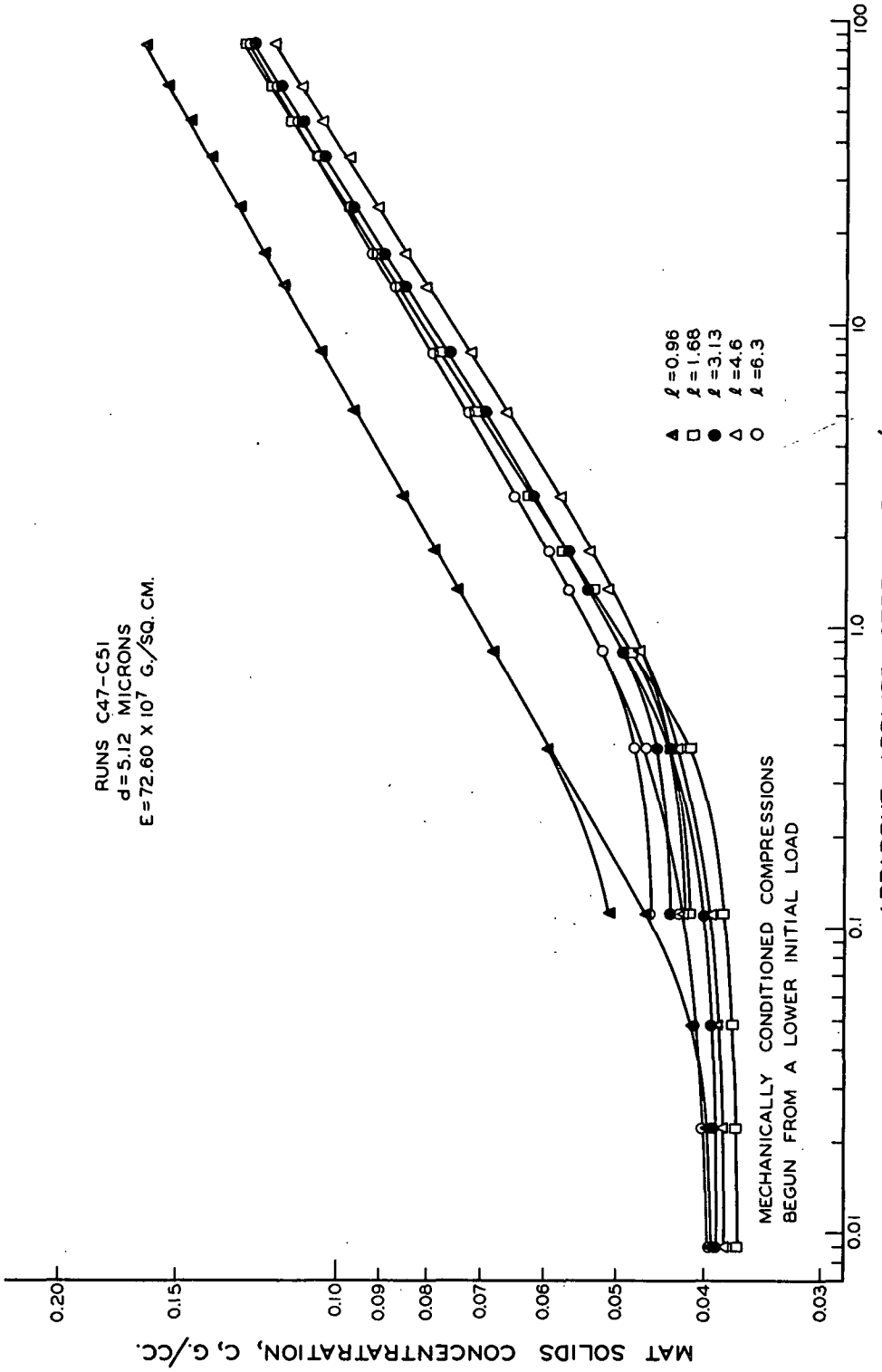

Figure 22. Mechanically Conditioned Compression Data for a Glass Fiber Length Study

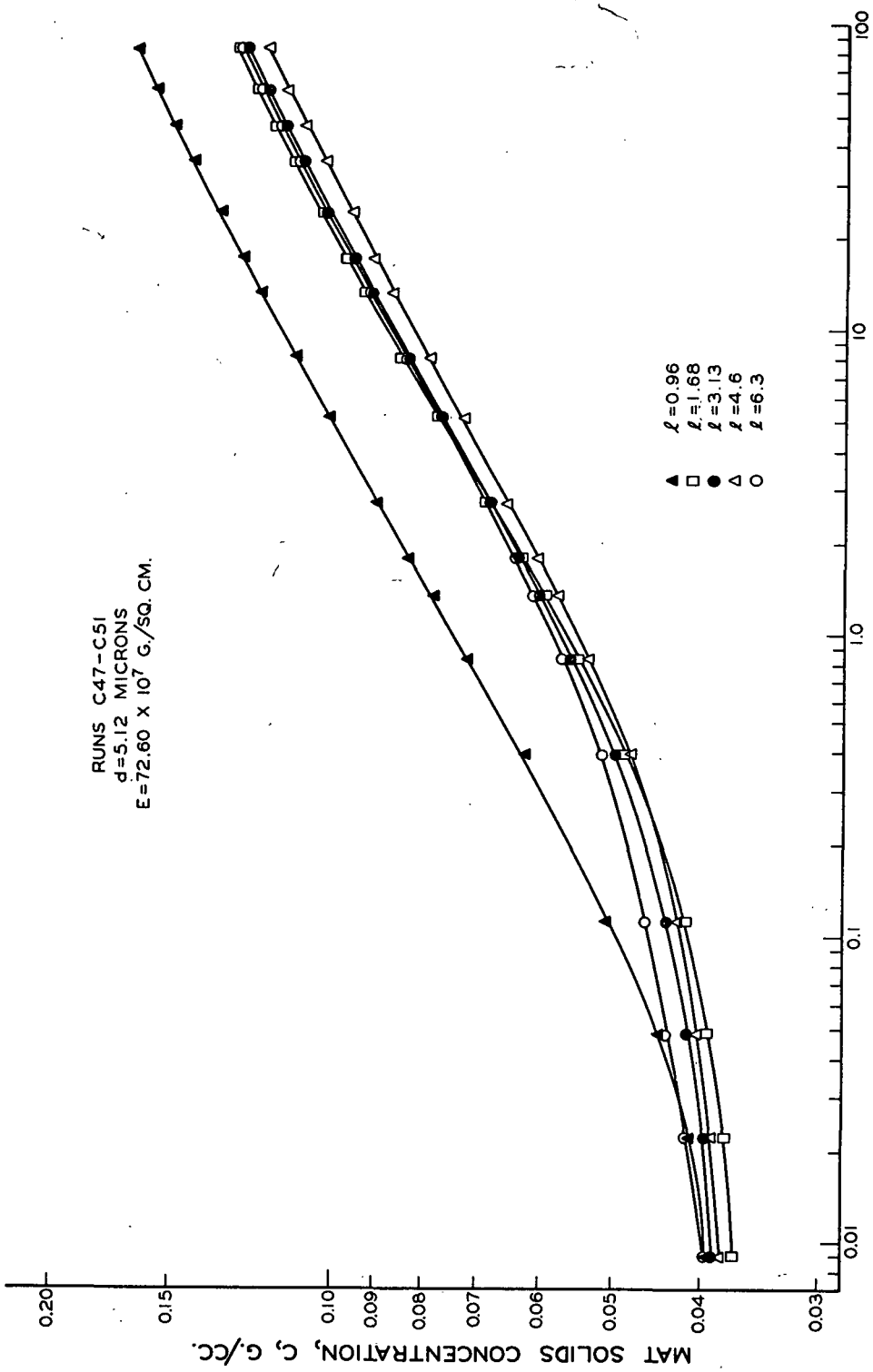

Figure 23. Mechanically Conditioned Recovery Data for a Glass Fiber Length Study

is believed that these beds possessed higher network structure strength than others because of the high length-to-diameter ratios involved and also the interfiber frictional properties of glass. The data are included in Fig. 22 along with the compression data, beginning at 0.111 g./sq. cm. It will also be noted that there is no real order to the position of the data curves representing the four longest lengths of fiber. The lack of continuity here was introduced by minor bed formation difficulties which occurred with fibers of these very high ℓ/d ratios.

Portions of the length study data are combined with other results to create a diameter study for glass fiber. These results appear in Fig. 24 and 25. There is a large effect of change in diameter at the 0.96 mm. length. This will be shown to be definitely due to length-to-diameter ratio effects. The smaller differences brought about in compression-recovery response by changes in diameter at longer lengths (4.6 mm.) are also due to differences in length-to-diameter ratio. The fact that such an effect was not found for nylon is explained in terms of differences in modulus of elasticity and interfiber friction between glass and nylon fibers, but the detailed analysis has been deferred to an appropriate point in the discussion.

The effect of changes in modulus of elasticity for glass fiber is shown in Fig. 26 and 27. Of primary interest here is the fact that very little difference if any is produced in the compression-recovery relationships by a change in modulus of elasticity of the glass. This observation for glass fiber differs from that made on nylon fiber. The apparent inconsistency remains to be clarified in further discussion and will be shown

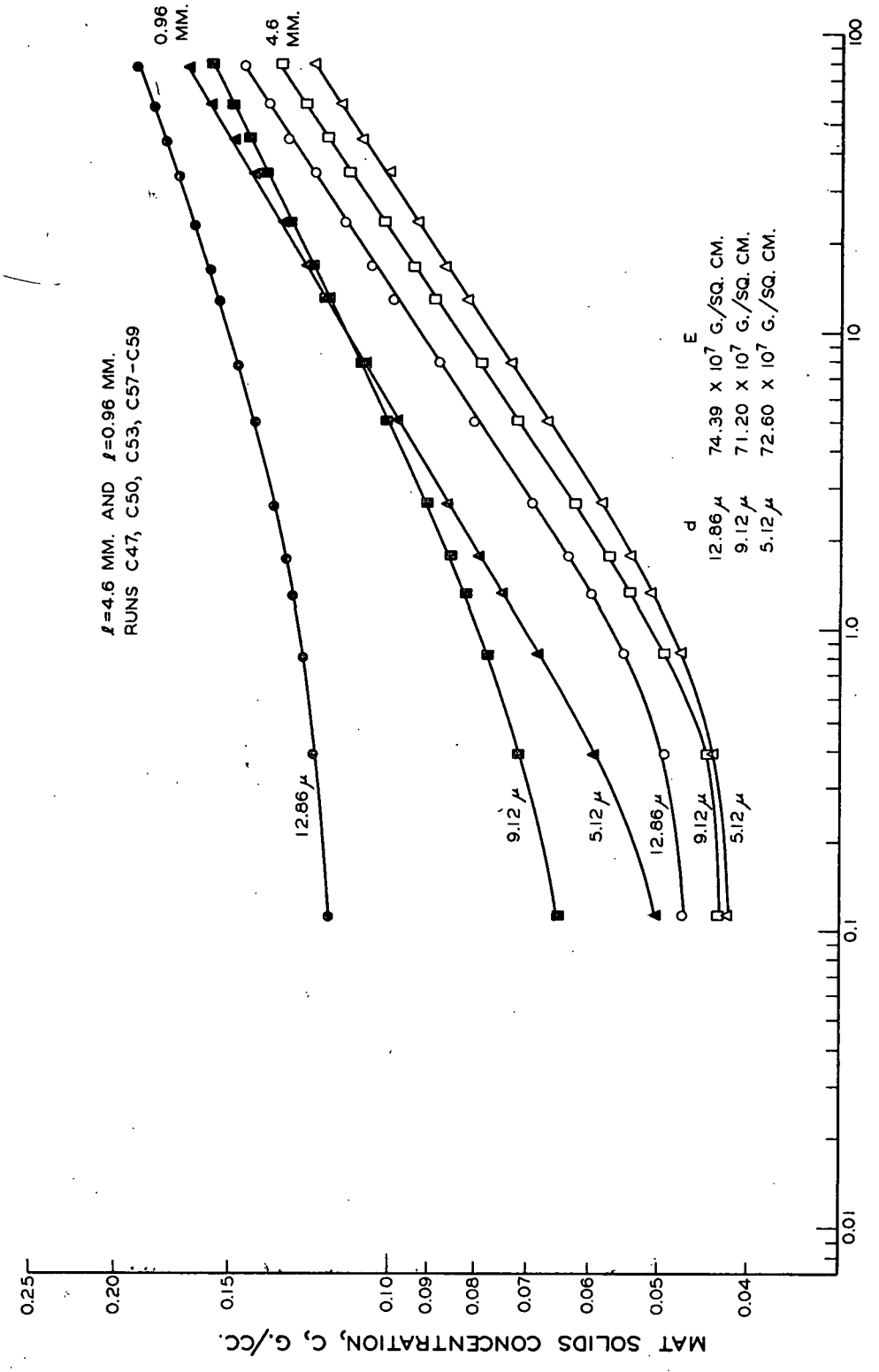

Figure 24. Mechanically Conditioned Compression Data for a Glass Fiber Diameter Study

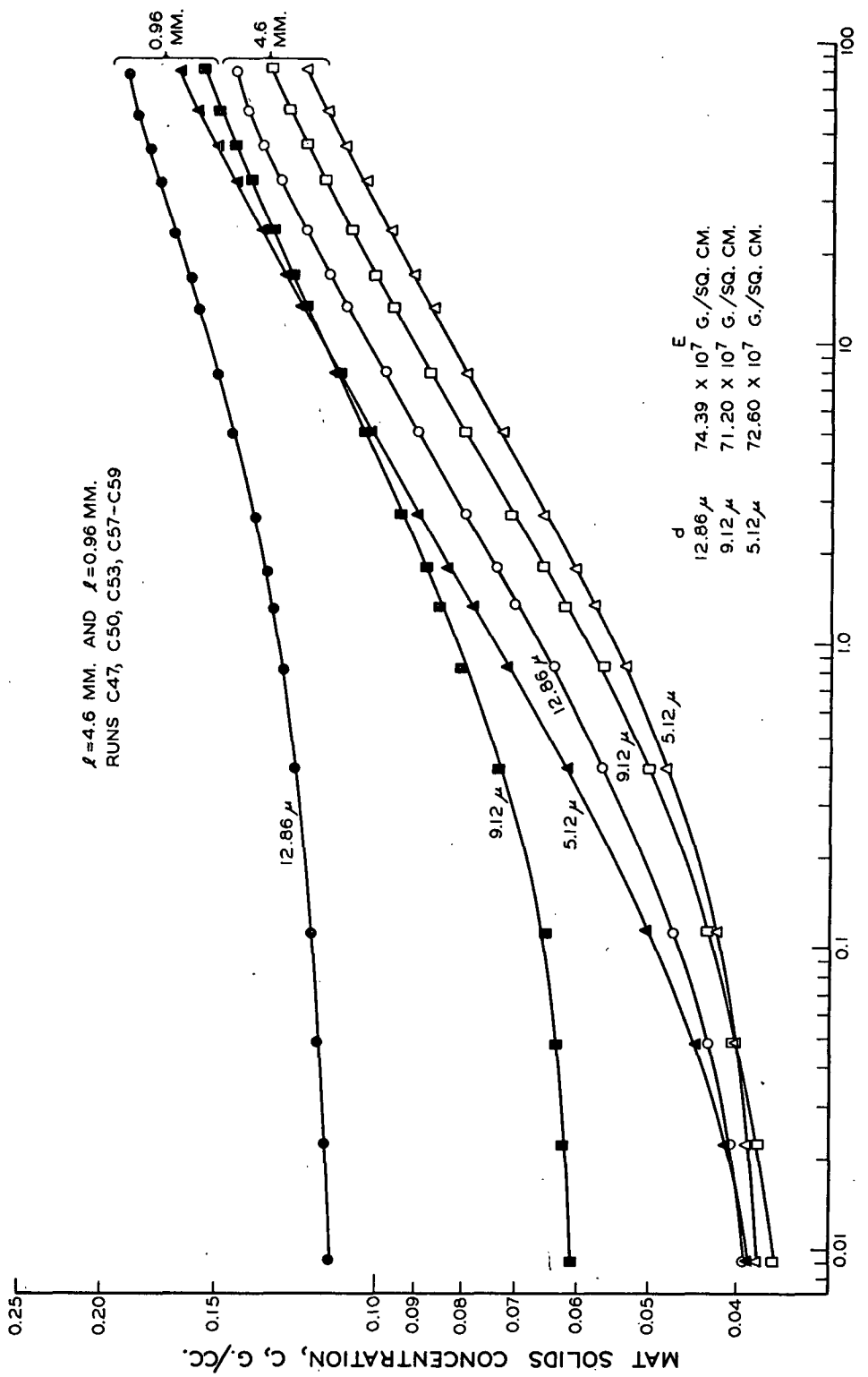

Figure 25. Mechanically Conditioned Recovery Data for a Glass Fiber Diameter Study

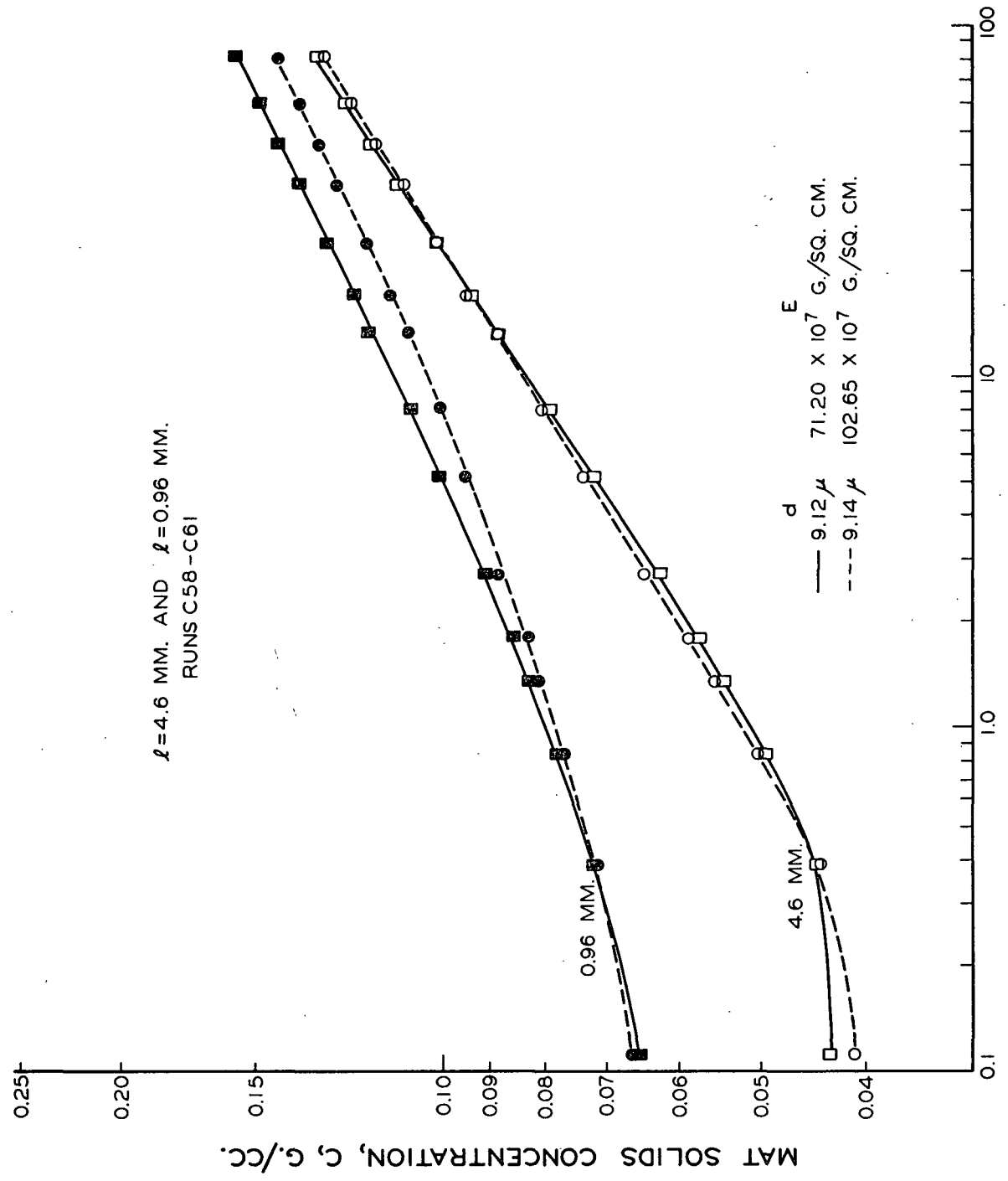

Figure 26. Mechanically Conditioned Compression Data for a Glass Fiber Modulus Study

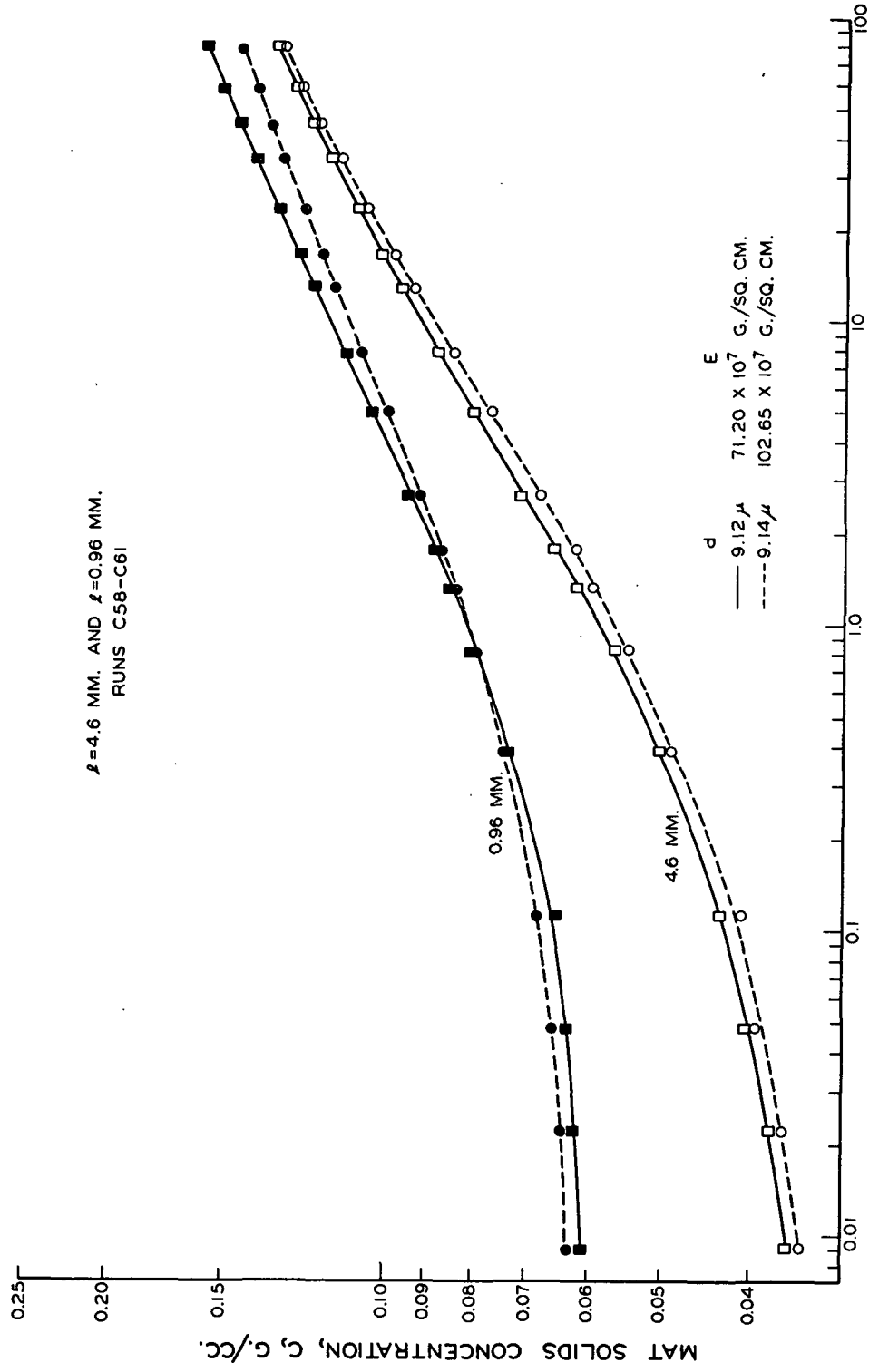

Figure 27. Mechanically Conditioned Recovery Data for a Glass Fiber Modulus Study

to be related to the relatively small difference in the modulus of elasticity of the two glass samples. Since some difficulty was encountered in dispersing the 4.60-mm. sample of "Hi-Modulus Beryllia" glass, perhaps a larger difference in the position of the curves than is shown should be seen between the two samples at this length.

PULP FIBER STUDIES

A limited number of compression-recovery tests have been made with pulp fiber in order to determine whether or not pulp fibers follow the same trends observed with less complicated fibers such as glass and nylon. Figure 28 contains the data for first compression work. The assumption has been made that the bleaching procedure used in this work should alter only the flexibility of the pulp fiber, that is, the bleached fiber would be more flexible than the unbleached fiber. The bed made from bleached fiber has a higher solids concentration at each value of the applied stress than does the unbleached fiber. This is the same trend observed with a decrease in elastic modulus of the synthetic fiber. Bleaching probably reduces the fiber modulus of elasticity and thereby increases fiber flexibility by removing the lignin binding material. However, one cannot be certain that fiber diameter is not increased and fiber surface characteristics changed at the same time in a way that also affects the results. For instance, an increase in diameter would be expected to decrease flexibility. The trend with reduction in length is to higher solids concentration, as is the case with synthetic fibers. Perhaps the most important difference between pulp and synthetic fibers is that pulp fibers have much higher limiting slopes for the first compression curves than do synthetics.

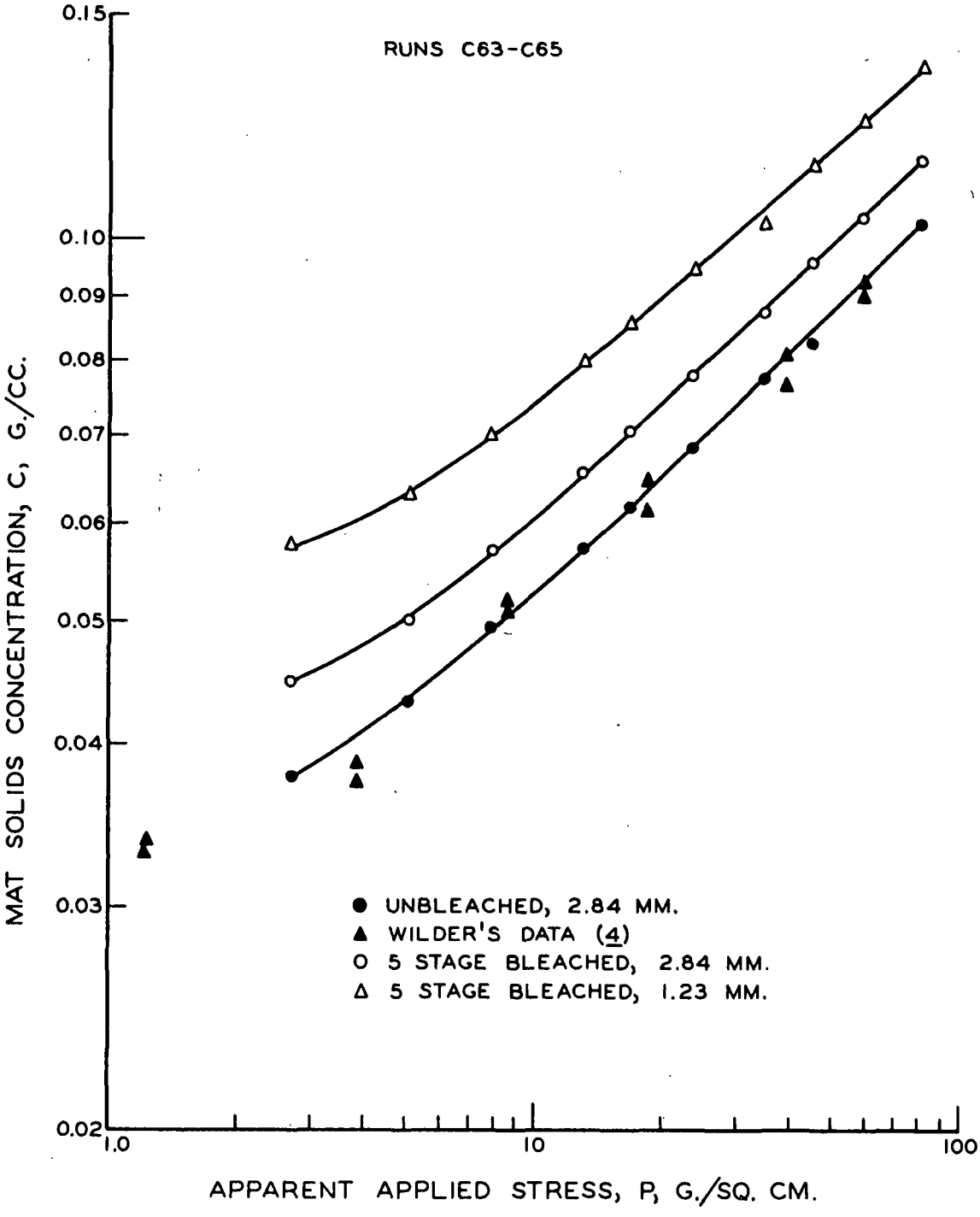

Figure 28. First Compression Data for Loblolly Pine Summerwood Pulp

One pulp fiber bed was mechanically conditioned for comparison with mechanically conditioned synthetics. These data for the sixth cycle are to be found in Fig. 29. The compression-recovery data form a closed hysteresis loop. The size of this hysteresis loop is much larger in the case of pulp than for synthetics as can be seen by comparison to Fig. 12. Also, note the memory effect in the hysteresis character of the bed. When taken through the short cycle shown in Fig. 29, the bed may then be caused to first return to the starting point and repeat the long cycle. This is, of course, true for mechanically conditioned synthetics as well.

In the past all first compression data for pulp fiber beds have been taken when no further change in height of the bed could be detected. Kurath (28) found that if one did not wait for sufficient time to elapse before taking data, a curve rather than a straight-line double logarithmic plot of C vs. P resulted. This was particularly true at higher applied stresses. In this study, the data for first compression in Fig. 29 show that, at least for low applied stresses, the same value of the slope, N, of the log C vs. log P plot is obtained for different durations of loading. The straight lines are merely displaced.

A compressibility curve constructed from Wilder's (4) creep data was not a straight-line log C vs. log P plot. The reason for this situation might be related to repositioning of fibers within the bed. Nonrecoverable fiber repositioning would be expected to be highly dependent upon the loading schedule, i.e., the number of loads used and the magnitude of the difference between loads. If this is the case, one might expect that extremely different loading schedules would give slightly different shapes

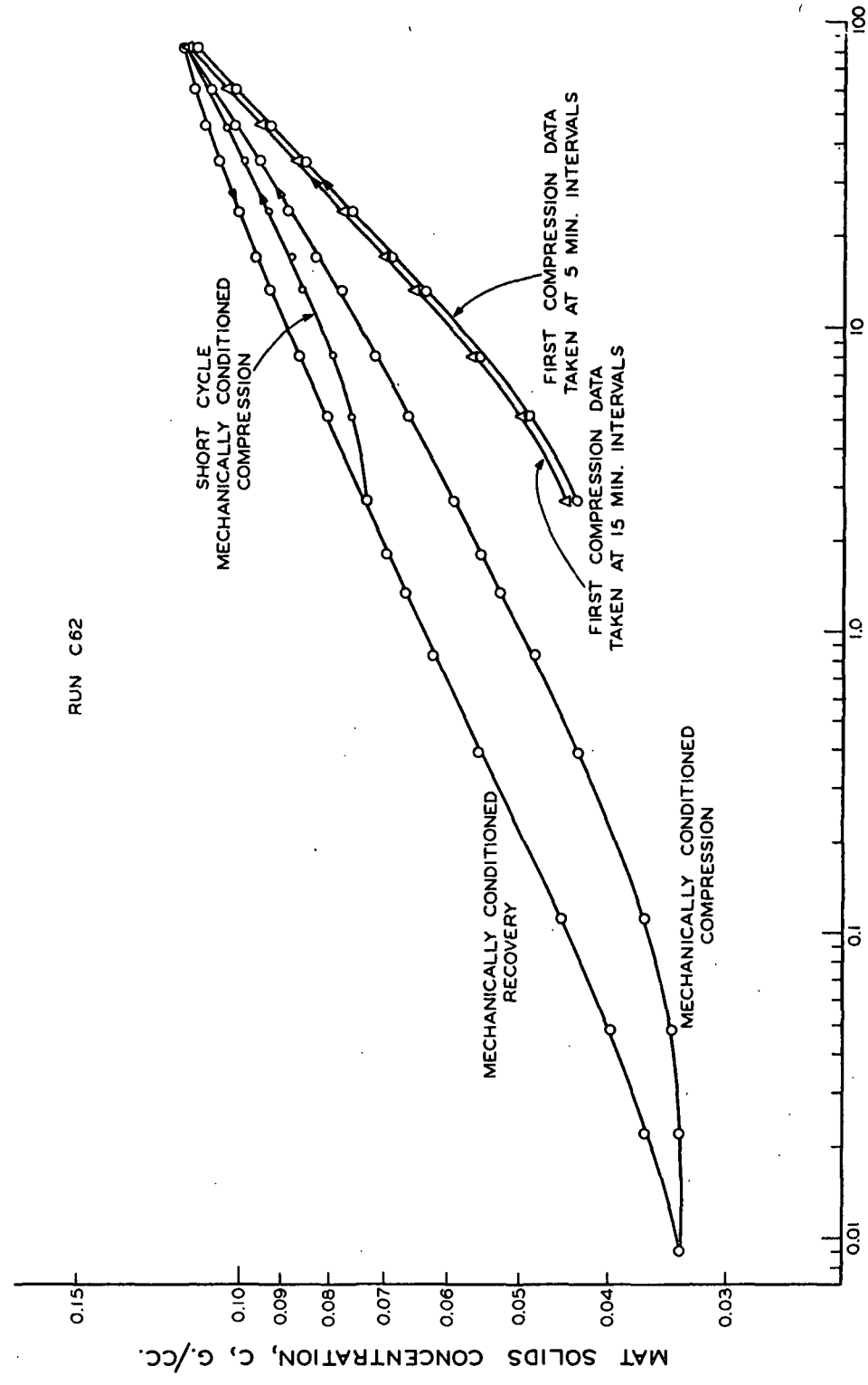

Figure 29. Compression and Recovery Data for Loblolly Pine Summerwood Pulp

to the first compression data. Then the results of Wilder's work might be expected, since in his case each load was applied to a new bed. No information is available to confirm these suppositions.

However, one thing does seem certain: the exponential relationship $\underline{C} = \underline{M}\underline{P}^{\underline{N}}$ which applies so well to much first compression data is merely a result of the testing method. The relationship certainly does not hold true for the low load portions of the mechanically conditioned fiber beds studied in this investigation. The equation can be applied to the high load portions of the data for mechanically conditioned glass fiber beds, but does not apply as well to data for mechanically conditioned pulp and nylon beds.

DATA TREATMENT AND ANALYSIS

EMPIRICAL TREATMENT OF THE DATA

The variation of those fiber structural properties which alter fiber bed compression-recovery response have been carefully measured and controlled in this study. It would be desirable to have at least an empirical expression through which one could relate the position and shape of the $\underline{C}$ vs. $\underline{P}$ curves. This relationship should preferably be simple in form and include constants which may be readily related empirically to the fiber structural properties. When one encounters smooth, curved lines on log-log plots, a standard approach to straighten out these lines is to apply the equation form:

$$C - B = MP^N \qquad (13)$$

where B, M, and N are constants. This form is the same as Equation (3) suggested by Ingmanson and Whitney (26) for compression data. Although the log C vs. log P curves are straightened out rather well by Equation (13), the reasons for the relative positions of the log (C-B) vs. log P curves are not readily apparent. This method of data treatment offers no advantage over the logical arrangement now obtained through the graphical representation which has been used.

Other empirical equations offered in the literature have not been tried. However, they do not appear to present any advantage of simplification in data treatment and presentation over the techniques now used.

ANALYSIS OF DATA IN TERMS OF BULK MODULUS

It was mentioned earlier that Wrist (33) has used bulk modulus considerations to derive an equation of the same form as the empirical compressibility equation, i.e.,

$$C = (C_o/P_o^{1/k})P_2^{1/k} \qquad (2),$$

where C_o is the sedimentation consistency of the slurry and P_o is a compacting pressure of the slurry in sedimentation. P_2 is the sum of P_o and the apparent applied stress, P. The assumption that the bulk modulus K is equal to kP_2 would be expected to hold well for first compression data where $C = MP^N$ holds, and this has been verified through an analysis of the bulk modulus for the first compression data taken on nylon fibers. Wrist's development predicts that a linear relationship exists between log C and log P_2 all the way down to the point where $P_2 = P_o$ and $C = C_o$. He has found reasonable agreement between his

predicted values of $\underline{C}_o$ and the critical consistency for shear flow. With these considerations in mind, it was decided to obtain an estimate of the value of $\underline{C}_o$ in order to experimentally establish the general trend of the first compression curve at low loads and to provide an evaluation of Wrist's equation over an extended range.

In order to estimate $\underline{C}_o$, a special fiber settling study was made. To form a bed, nylon fibers were settled out of a very dilute suspension over a period of four hours. The settling apparatus consisted of a concentric lucite tube arrangement in which the inner tube could be adjusted and maintained several centimeters above the height of the bed all during forming. The purpose of this arrangement was to avoid a building-up of fiber at the tube wall so that the bed height could be measured. In this way, a 3-inch diameter unconfined bed was formed by settling. The height of the bed was measured at four intervals after known weights of fiber had been settled so that the influence of the sedimentation compacting stress could be evaluated and then eliminated. This was done by plotting the data and extrapolating to zero weight, as is shown in Fig. 30. There is a slight effect of sedimentation compacting stress on mat solids concentration.

The value of the solids concentration was determined by draining off the water, punching out a section of the center of the bed and weighing that fiber. Data for both the punched-out center portion and the annulus are reported. This indicates a variation in basis weight across the pad which is undoubtedly due to wall effects on the fibers during settling.

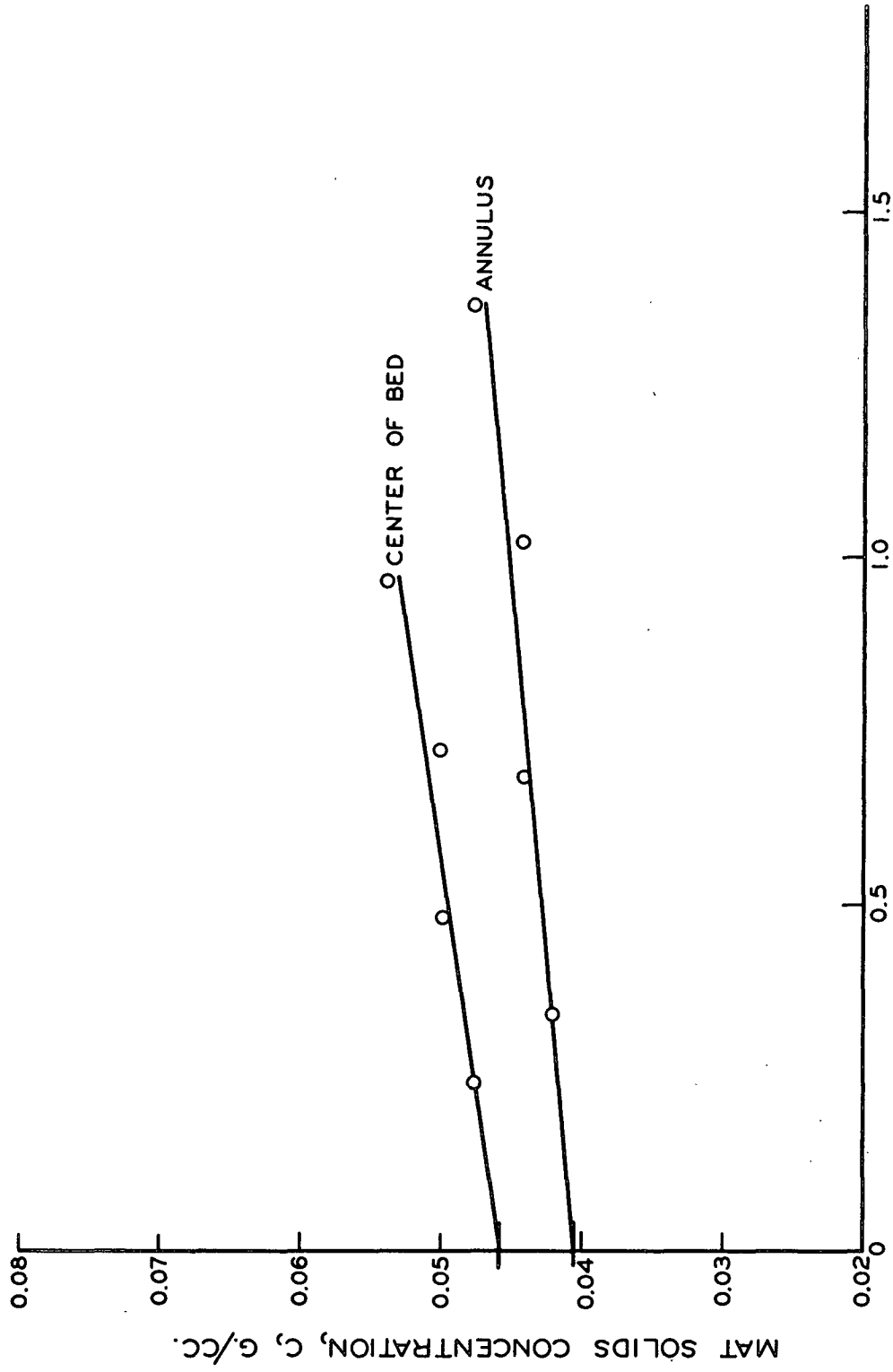

Figure 30. Determination of C_o at Zero Bed Weight in a Fiber Sedimentation Study

In order to evaluate Wrist's Equation (2), a value of the sedimentation compacting stress was estimated for the first compression data of the same fiber used in the settling study. The average sedimentation compacting stress was assumed to be one half of the effective weight of the fiber bed, i.e., $\frac{1}{2}$(fiber bed weight - buoyancy force). The sedimentation consistency, $\underline{C}_o$, taken from Fig. 30 is plotted in Fig. 31 together with the first compression data. The apparent applied stress in this case is $\underline{P}_2$, the sum of the sedimentation compacting stress, $\underline{P}_o$, and the applied stress, $\underline{P}$. The extrapolation of the first compression data does pass through the estimated $\underline{C}_o$ data in agreement with Wrist's hypothesis. Of course, the curve in the first compression data is a result of pressure drop across the mat during forming, a topic which has already been discussed.

Wrist's development also predicts that the mat solids concentration must be zero at zero sedimentation compacting pressure. However, if we assume that the extrapolation carried out in Fig. 30 to find the mat solids concentration at zero sedimentation compacting stress is a valid one, then there must be a change in the linear relationship between log $\underline{C}$ and log $\underline{P}_2$, between $\underline{C}$ at $\underline{P}_2 = 0$, and $\underline{C} = \underline{C}_o$ at $\underline{P}_2 = \underline{P}_o$ not taken into account by Wrist's development.

The value of $\underline{C}$ at $\underline{P}_o = 0$ obtained by extrapolation in Fig. 30 is plotted together with first compression data as $\underline{C}$ vs. $\underline{P}^N$ in Fig. 32 in order to demonstrate this point. The size of the data point at $\underline{C}_o$ represents the extremes of the data in Fig. 30. The expected general trend of the data based on a knowledge of the behavior of mechanically conditioned

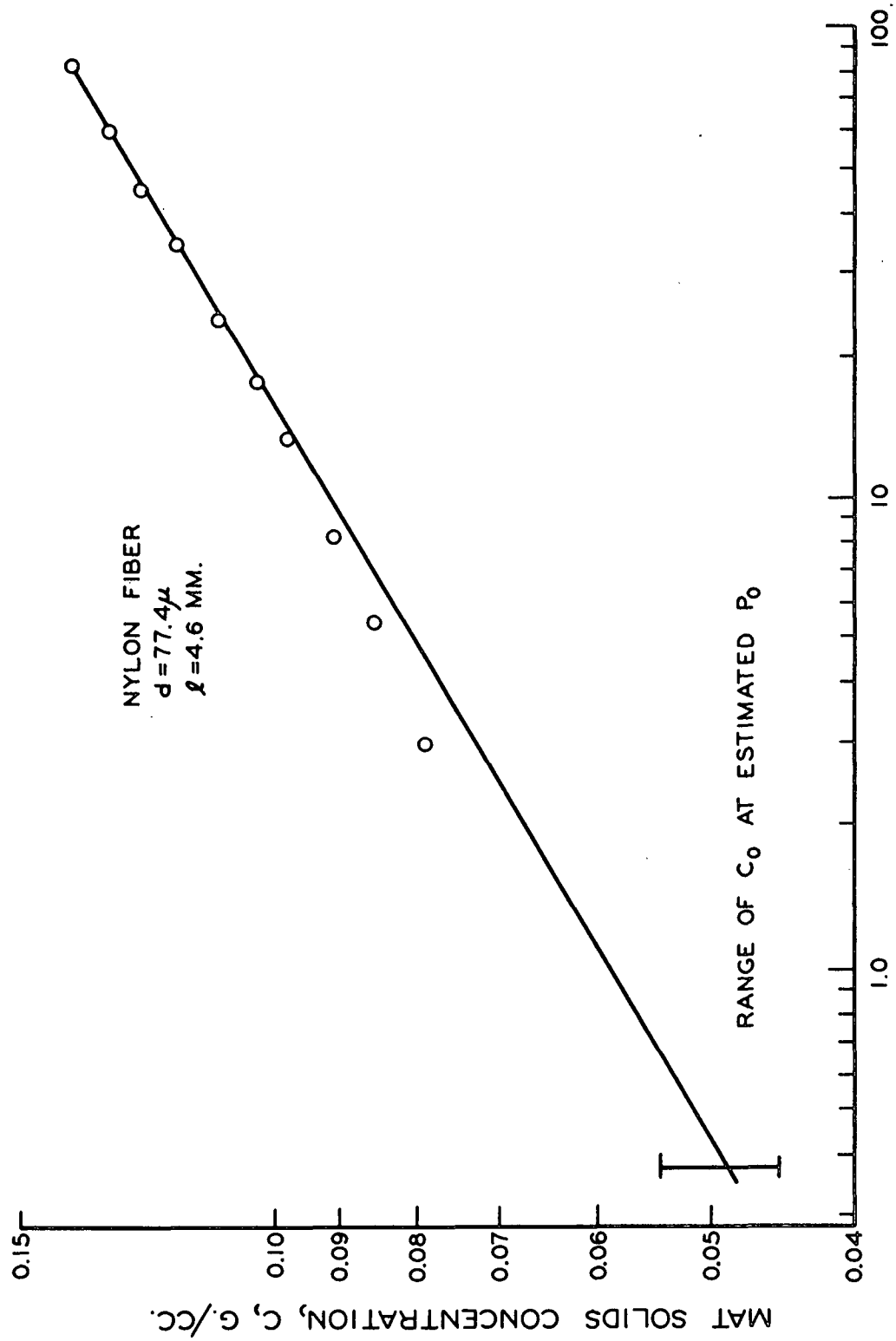

Figure 31. Test of Wrist's Compressibility Equation for First Compression Data

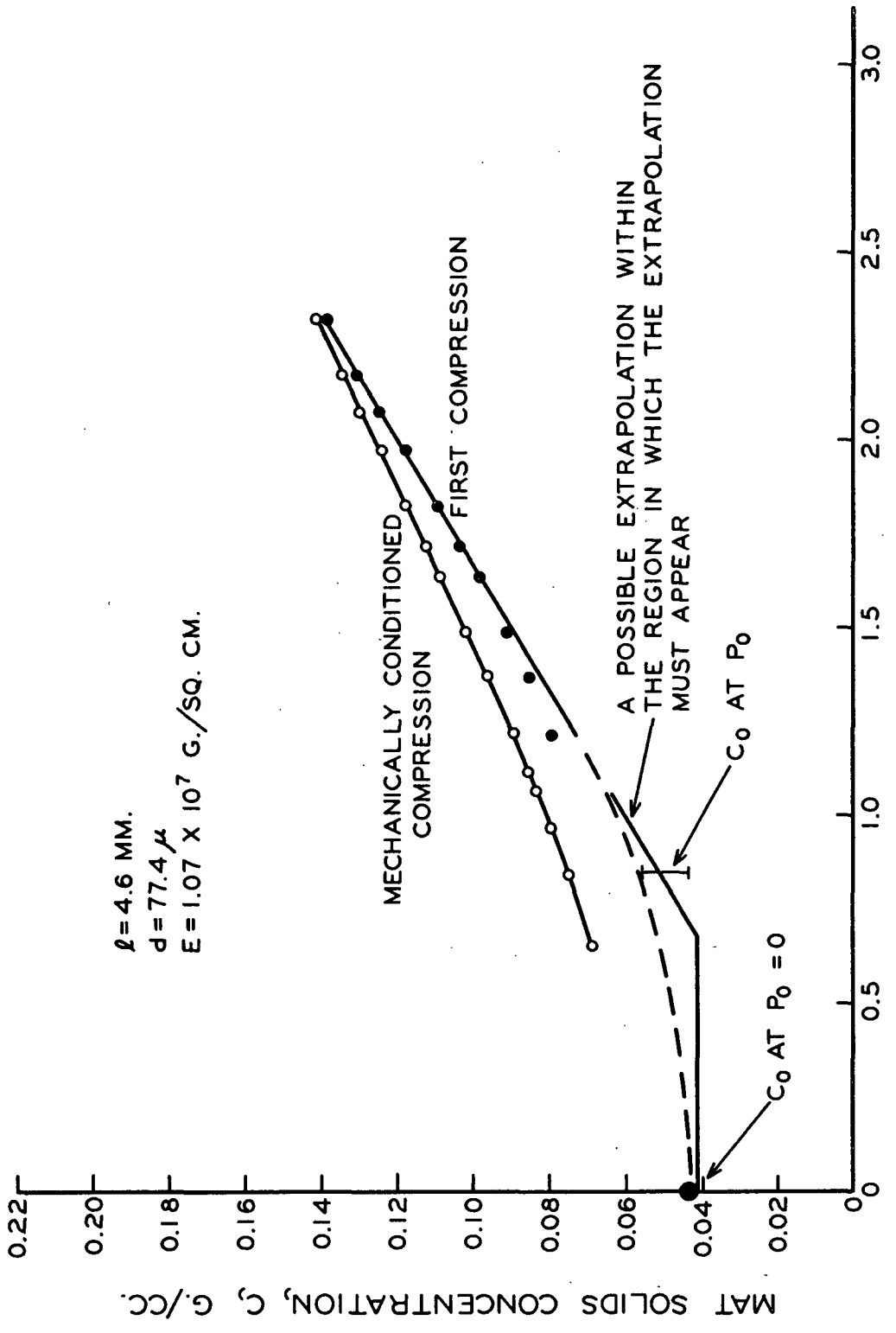

Figure 32. Approximated First Compression Curve for C29 Nylon Plotted at $\underline{C}$ vs. $\underline{P^N}$ Using Sedimentation Value of $\underline{C}_o$

beds is indicated by a dashed line in Fig. 32. It should also be noted that the $\underline{C}$ at $\underline{P} = 0$ which may be predicted for mechanically conditioned beds from this work is higher than that value obtained for first compression studies through the sedimentation work. This is to be expected since in the mechanically conditioned case all nonrecoverable deformation has been removed and the bed structure is entirely different from that for an uncompressed bed.

Wrist's suggestion of considering the moduli properties of a bed has sound basis, and it was decided to apply it to the data for mechanically conditioned beds in an attempt to simplify the data treatment. If an easily defined relationship between bulk modulus and applied stress could be found, the data could be reported in this form rather than as log $\underline{C}$ vs. log $\underline{P}$. Unfortunately, no simple relationship was found, and the $\underline{K}$ vs. $\underline{P}$ graphical representation had no advantage over the one now used. The shape of the $\underline{K}$ vs. $\underline{P}$ curves for two fiber lengths is shown in Appendix II.

DIMENSIONAL ANALYSIS

Early in this work a dimensional analysis was undertaken to obtain a relationship for mat solids concentration as a function of applied stress, and other variables which were expected to be important. The variables chosen were fiber length, fiber diameter, modulus of elasticity, and fiber density, i.e.,

$$C = f(P, \ell, d, E, \rho) = k\ell^a d^b E^c \rho^f P^g \qquad (14).$$

This type of analysis leads to the equation:

$$C = k(d/\ell)^b(P/E)^g\rho \qquad (15).$$

A rearrangement of Equation (15) places it in the form $\underline{C} = \underline{M}P^{\underline{N}}$, and it has a form of $\underline{M}$ similar to, but not identical with, that of Wilder's Equation (10). Wilder's equation does not appear to contain either the length or diameter factor, but more will be said about this later.

ANALYSIS OF FRICTION BETWEEN THE FIBERS

All the mechanically conditioned fiber beds exhibited a hysteresis in their compression recovery response. In dealing with viscoelastic materials, this hysteresis effect can usually be attributed to delayed deformation and delayed recovery of the material. This explanation is unsatisfactory for beds of elastic glass fiber and has been shown in this work through long-term creep studies on mechanically conditioned beds to be not entirely adequate for explaining the hysteresis in the nylon studies. These creep studies showed that although the size of the hysteresis loop could be decreased somewhat by permitting long-term time-dependent deformation and recovery to take place, it could not be eliminated entirely. Some other factor, responsible for the hysteresis loop in glass fiber bed compression response, was apparently also at work in the nylon fiber networks.

It was felt that the energy lost in going around the hysteresis loop might be a measure of the work lost in overcoming friction between the fibers at contact points during compression recovery cycles. This concept has been found to be so valuable to an explanation of much of the

work done in this investigation that it is to be presented here before an analysis of the effect of changes in ℓ, d, and E is undertaken. The viscous drag effect of the fiber moving through the fluid would also dissipate some energy and may affect to some extent the equilibrium position of the individual fibers. However at the present time, one is not in a position to calculate the relative importance of this effect and it has been neglected in this treatment.

The compression-recovery data for mechanically conditioned fiber beds were plotted as bed height vs. applied stress. A typical plot appears in Fig. 33. The area between the two curves, when multiplied by the fiber bed cross-sectional area, is equal to the difference between the work put into the compression and that regained from the recovery, i.e., work lost. The work-lost information was obtained for a number of the glass and nylon fiber runs and was then correlated with fiber length, fiber diameter, and fiber type.

Since all the beds varied in total weight, number of fibers, and change in height, it was necessary to find a common basis through which to compare the work lost. The basis of comparison chosen was the number of fiber-to-fiber contacts. An estimate of this number has been obtained through application of an equation derived by Onogi and Sasaguri (44) for the mat solids concentration of a fiber bed:

$$C = (\pi^3/16)(d\rho/b) \qquad (16)$$

where b is the length of a fiber element between contact points. Equation (16) is of the same form as one derived by Wilder (4). The total number

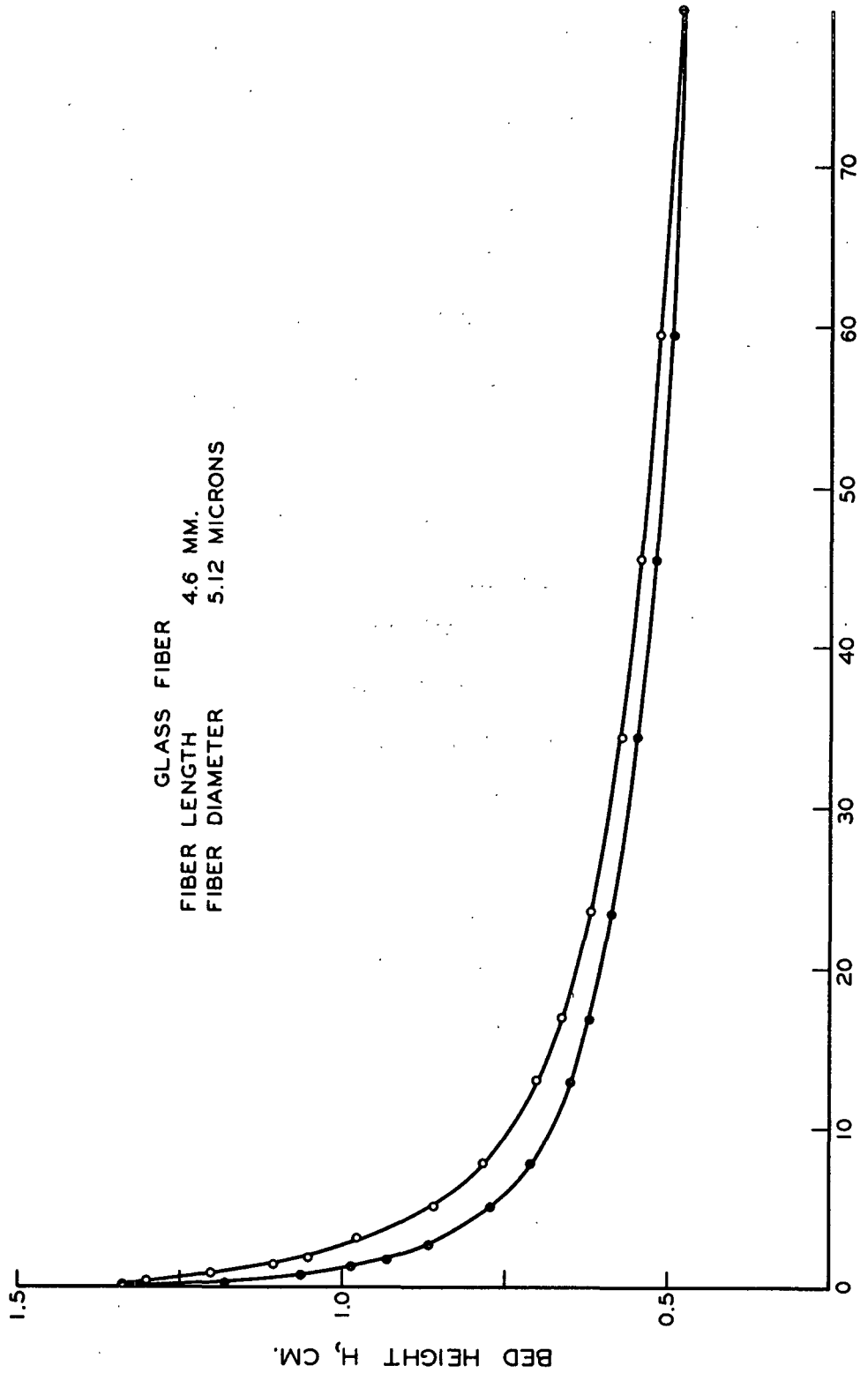

Figure 33. A Typical Hysteresis Loop for a Mechanically Conditioned Bed Plotted as Bed Height, H, vs. Applied Stress, P

of contacts is equal to the total fiber length divided by the segment length, b, where total fiber length is equal to $W/\pi(d^2/4)\rho$, where W is the weight of dry fiber in the bed. The equation which results says that

$$\text{number of contact points, } CP = 64W^2/\pi^4 d^3 \rho^2 HA \qquad (17),$$

where A is the cross-sectional area of the fiber bed. Equation (17) has not been experimentally verified. However, analysis of the approach used in this derivation and the agreement with Wilder's form strongly indicate that Equation (17) is reliable enough to be used for comparison purposes.

Table VIII contains a list of the pertinent data for this analysis. The general trend is that as the number of contact points decreases, the work lost per contact point increases. The total work lost would be equal to the sum of the work lost at each contact point. In turn, the work done at each contact would be the product of the force, F, required to move the fiber and the distance, D, which two fibers slide across each other at the contact point. One would expect that there would have to be less fiber slippage per fiber in order to obtain the same over-all bed deformation for a bed made of many small-diameter fibers than for a bed made of fewer large-diameter fibers. Therefore, the distance through which a fiber would be forced to travel would be less at each contact for small-diameter fibers. Such a situation would contribute to less work lost per contact for these small-diameter fibers.

There is another factor which also works to force the trend toward lower work lost per contact for fibers of small diameter. The frictional force at a contact, F_f, is a function of the coefficient of friction, μ,

TABLE VIII

INTERFIBER FRICTION ANALYSIS

Fiber	Type	Length, mm.	Diameter, μ	Work Lost, g.-cm. ±6.0	Initial No. of Contacts, x 10^{-6}	Final No. of Contacts/Init. No. of Contacts	Bed Weight, g.	Work Done/Init. No. of Contacts, g.-cm. x 10^{9}
Glass	Diameter Study	4.6	5.12	219.2	144.0	2.83	4.535	1.51
		4.6	9.12	204.5	29.7	3.00	5.207	6.92
		A 4.6	12.86	277.2	13.4	3.04	5.968	20.8
Glass	Diameter Study	0.96	5.12	73.8	170.0	2.30	4.510	0.433
		0.96	9.12	109.2	67.0	2.40	7.811	1.62
		0.96	12.86	112.9	66.6	1.62	12.085	1.70
Glass	Length Study	6.3	12.86	235.9	11.4	3.09	5.712	20.8
		4.6	12.86	277.2	13.4	3.04	5.968	20.8
		1.68	12.86	131.6	24.5	2.44	8.016	5.20
		0.96	12.86	112.9	66.6	1.62	12.085	1.70
Nylon	Diameter Study	B 4.6	16.8	156.5	33.0	1.76	5.746	4.75
		4.6	44.8	192.7	2.10	2.42	6.642	91.9
		4.6	77.4	171.9	0.505	2.08	6.823	343.0

and the normal force, N', at that contact point. In the case of large-diameter fibers, there are fewer total contacts and therefore larger normal forces at the contact points. This, too, would contribute to a greater work loss per contact for beds with a few contacts. Therefore, both the frictional force and the distance through which it acts are expected to be greater as the number of contacts is decreased, and so the work lost at a contact is increased. In Table VIII, this is shown to be the case for the synthetic fiber beds studied.

Finally, note that for two fibers of approximately the same diameter there is less total work loss and less work loss per contact point for nylon fiber than for glass fiber. This is interpreted to mean that the coefficient of friction between wet nylon fibers is less than that for wet glass fiber. (See A and B in Table VIII.)

ANALYSIS OF COMPRESSIBILITY IN TERMS OF FIBER STRUCTURAL PROPERTIES

An analysis of the dependence of the constants M and N of the empirical compressibility function $C = MP^N$ for first compression on the fiber structural properties was undertaken. For the mechanically conditioned beds, the values of C at an applied stress of 10 g./sq. cm., C_{10}, and the limiting slope at high stresses of the log C vs. log P compression curves, N_L, were arbitrarily chosen for correlation with the fiber variables. These arbitrary terms correspond to those used to describe first compression data and provide a number for use in this analysis to describe the position and shape of the compression curves of the mechanically conditioned beds. The value of the mat solids concentration at 10 g./sq. cm. was felt to be a representative value to choose for

all the mechanically conditioned beds. The mechanically conditioned compression data approach a straight line on a log $\underline{C}$ vs. log $\underline{P}$ plot at higher applied stresses. Therefore, an $\underline{N}_{\underline{L}}$ corresponding to the $\underline{N}$ for first compression data was felt to adequately express the shape of the curves for comparison with each other and also comparison with first compression data. It was found that the relationships between $\underline{M}$ and $\underline{N}$ for first compression, and $\underline{C}_{10}$ and $\underline{N}_{\underline{L}}$ for mechanically conditioned compression with changes in fiber properties were the same.

The relationship between the slope $\underline{N}$ and fiber length for nylon, glass, and pulp fiber is shown in Fig. 34. First note that both glass and nylon reach a limiting value of $\underline{N}$ that does not change appreciably with further changes in length. This limiting value of $\underline{N}$ is 0.258 for all three diameters of glass fiber. The upper limit of $\underline{N}$ for nylon is lower than that for glass and is 0.198. This lower value for nylon is suspected to be related to the lower value of interfiber friction for nylon fibers. The fact that $\underline{N}$ is generally higher for pulps than for synthetics may possibly be a result of compression of pulp fibers at points of contact, which undoubtedly occurs even at the low stresses used in this study. However, there is some evidence from this work that this higher value of slope may be related to the fact that the pulp fibers are not straight rods like most of the synthetics used. The reader is referred to Appendix III for the data which support this point of view.

It should also be noted that the glass fiber data in Fig. 34 form a family of curves for different fiber diameters. When $\underline{N}$ is plotted

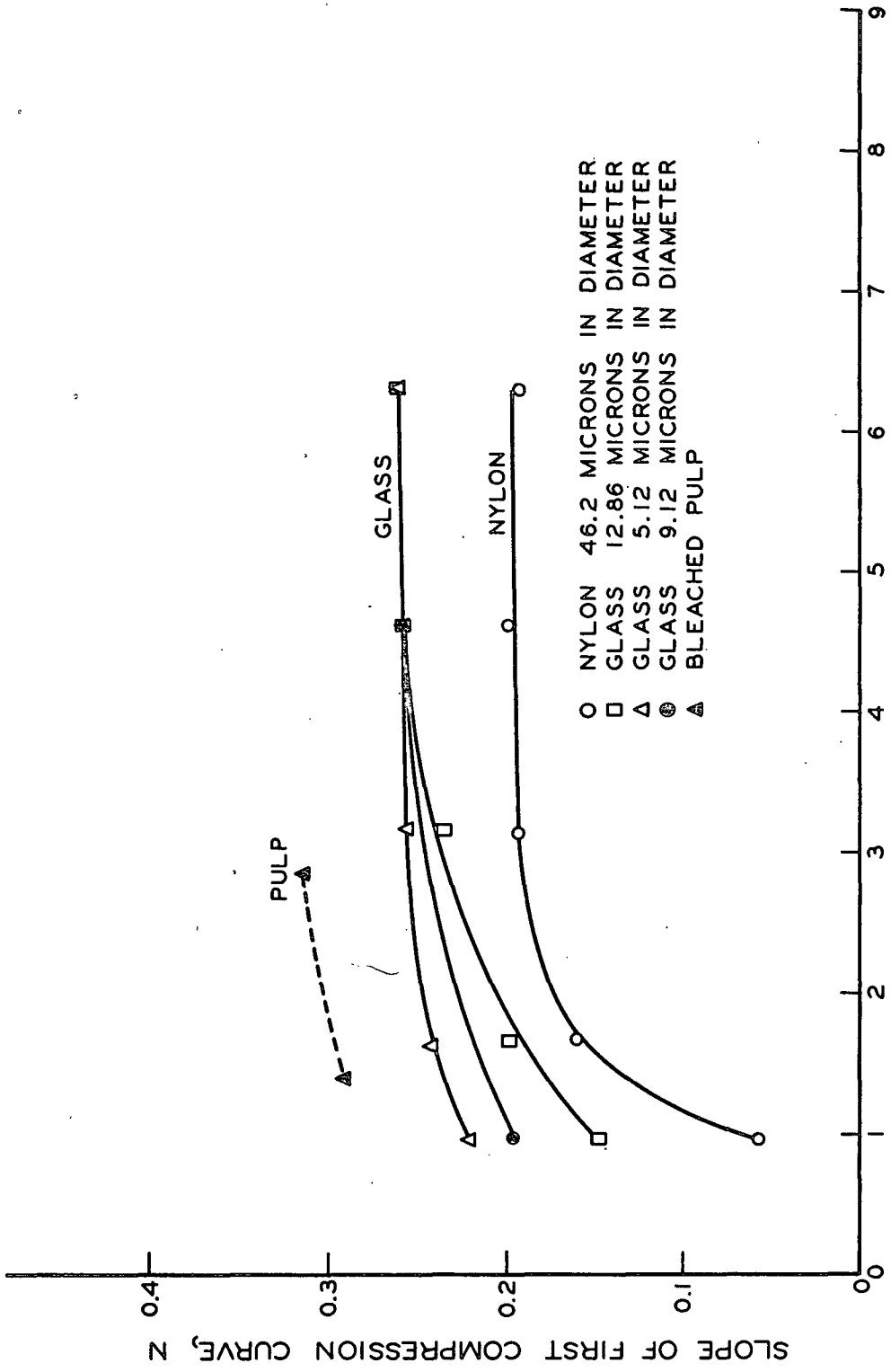

Figure 34. Exponent N of the Empirical Equation $C = MP^N$ vs. Length for First Compression Data of Fiber Length Studies

against the ratio of length to diameter, ℓ/d, as in Fig. 35, the data form one continuous curve. This demonstrates that the structure of a fiber bed and its response to compressive stress are highly dependent upon fiber length-to-diameter ratio and, further, that this dependence on ℓ/d ratio is so minimized as to become unimportant at longer fiber lengths. The range of length-to-diameter ratio where further changes in ℓ/d do not influence the value of N has been termed the "critical" length-to-diameter ratio. The "critical" ℓ/d ratio for glass is 500-600, and for nylon it is 75-100.

The coefficients M and C_{10} also form a family of curves which may be correlated with the length-to-diameter ratio of the fiber, as shown in Fig. 36. It should be noted that M and C_{10} also reach values beyond which further increases in ℓ/d seem to have very little effect on their value.

It has already been stated that the nonrecoverable deformation encountered in mechanically conditioning a fiber bed is a result of the repositioning of the fibers in the bed. It is therefore of interest to determine how the percentage of nonrecoverable deformation changes with fiber length, since this will give one additional insight into the difference in structure of fiber beds brought about by fiber length changes. The percentage of nonrecoverable deformation has been based on first compression and recovery data after the straight-line portion of the log C vs. log P plot is reached. The data are reported as percentage of change in solids concentration which is equivalent to percentage of change in nonrecoverable deformation. (See Fig. 37.)

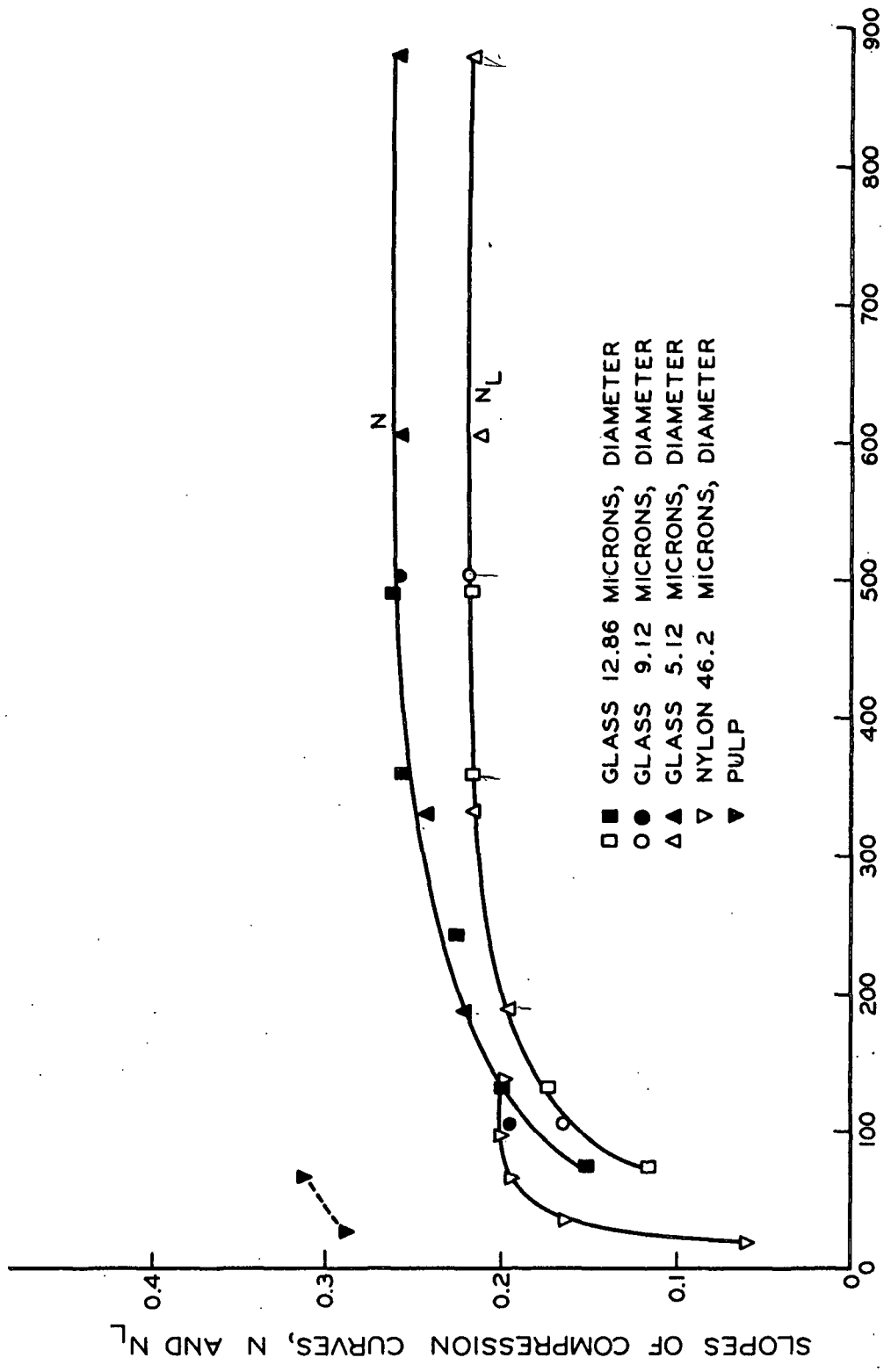

Figure 35. Exponent $\underline{N}$ of the Empirical Equation $\underline{C} = \underline{MP}^{\underline{N}}$ and $\underline{N_L}$ as a Function of Length-to-Diameter Ratio

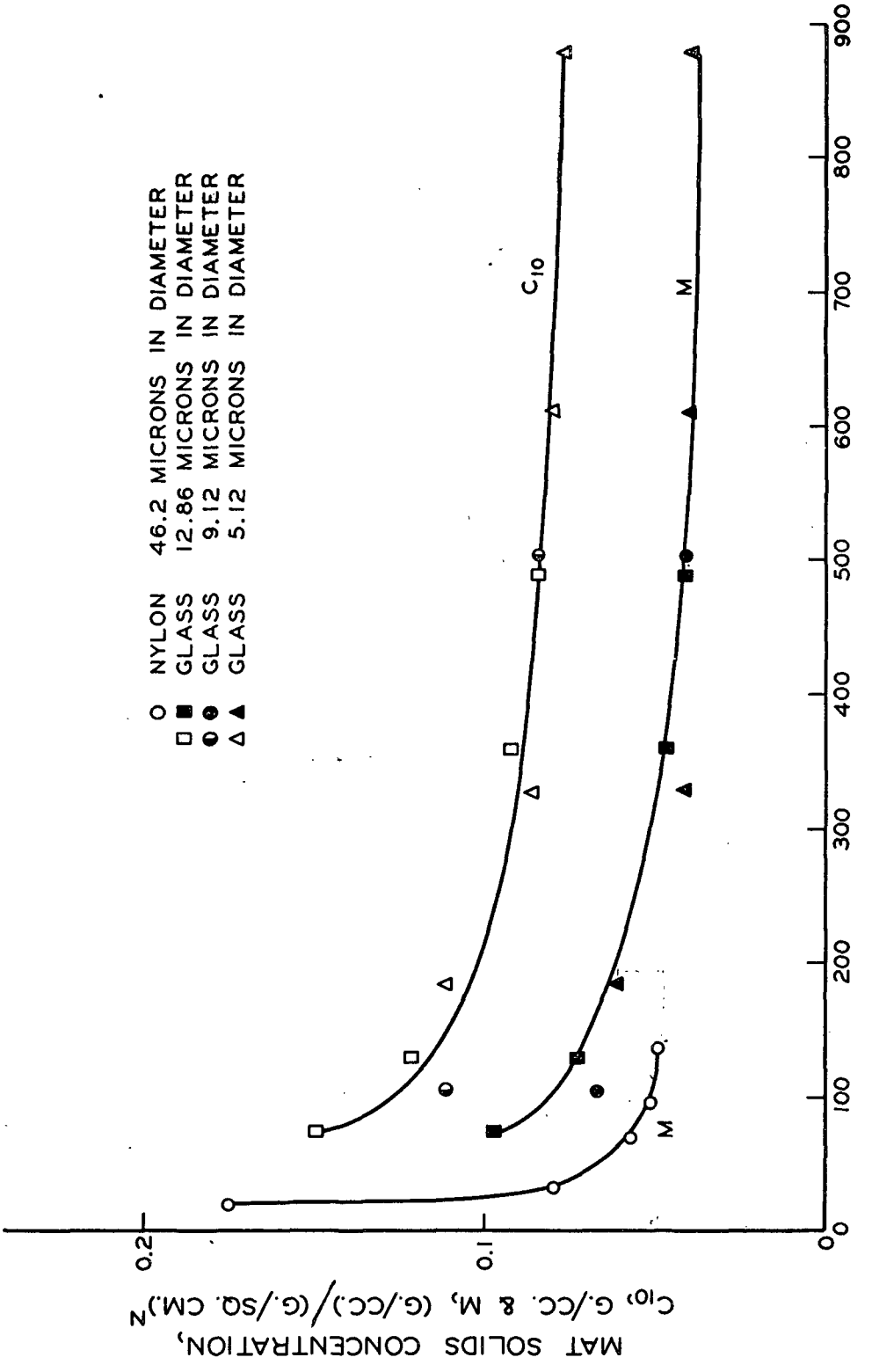

Figure 36. Coefficient M of the Empirical Equation $C = \frac{MP^N}{l}$ and C_{10} for Mechanically Conditioned Beds as a Function of Length-to-Diameter Ratio

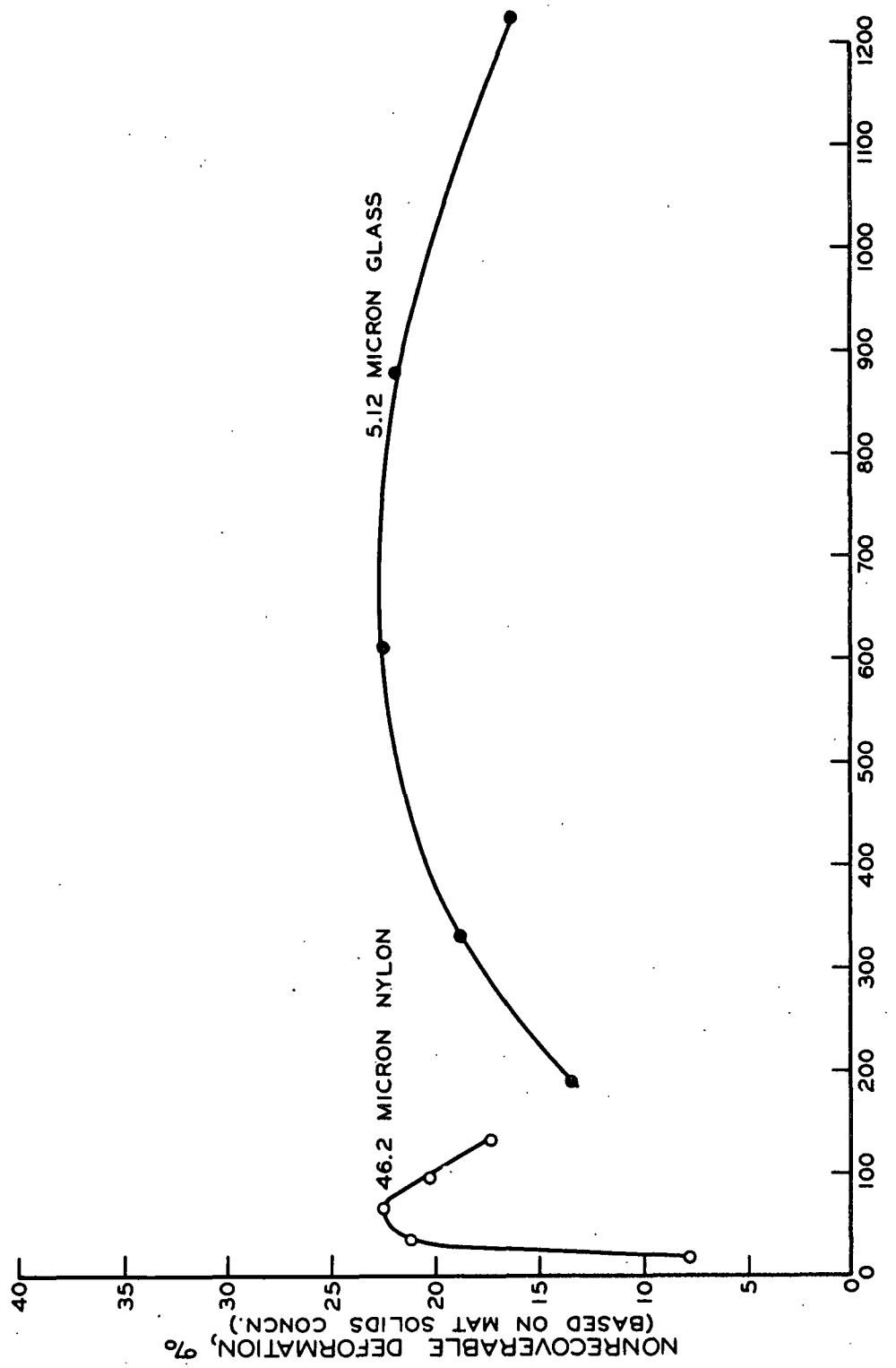

Figure 37. Nonrecoverable Deformation as a Function of Length-to-Diameter Ratio

The percentage of nonrecoverable deformation passes through a maximum at the critical length-to-diameter ratio previously discussed. Again, this critical length-to-diameter ratio is seen to be important to fiber bed compression response. This situation seems to indicate that below the critical ℓ/d ratio the mode of packing of the fibers during formation is very important to the compression response observed. The fibers are small enough to slip past one another and pack together under the low fluid stresses applied to them during formation. For these short fibers, the number of fiber crossings per fiber and the distance between crossings are small. The beds more closely approach the model of small, noncompressible particles than a system of bending beams. In this case, the change in solids concentration brought about by a given change in applied stress would be expected to be far less than that for a system of long fibers supported at a few points. This is, in fact, what is found, and the compressibility curves for short fibers have low slopes. It is not surprising then that the data of Train (31) for compression of powder masses can be plotted as log % solids vs. log applied stress, resulting in a straight line with a very low slope.

The greatest amount of fiber repositioning takes place when the fibers are very close to the critical length-to-diameter ratio. During the formation of the bed, fibers at this length form a loose structure and they are short enough to be caused to rearrange themselves under application of compressive stresses. When the fibers exceed the critical ℓ/d ratio, the compressive response becomes more and more dependent upon the bending characteristics of the fiber elements because it is difficult

for long fibers to be repositioned in the bed. In the case of infinitely long fibers, no nonrecoverable deformation would be expected*, and deformation and recovery would occur entirely through bending of the fiber. This is, in fact, the case as has been verified through the use of model beds of nylon fibers long enough to be considered infinitely long in terms of the test area. The work done on model beds of nylon fibers will be discussed in detail shortly.

The difference between the critical length-to-diameter ratio for nylon and for glass may be related in part to their differences in modulus of elasticity and interfiber friction. A fiber with a low elastic modulus and a low coefficient of friction would slip and bend more easily during the bed-forming stage so that it would pass into the region of low nonrecoverable deformation where bending is most important at lower length-to-diameter ratios. The fact that the glass fiber shows a much broader range of length-to-diameter ratio where considerable nonrecoverable deformation is observed (Fig. 37) would tend to support this view. The glass fibers of high $\underline{E}$ and high coefficient of friction form loose structures over a wide range of $\underline{\ell}/\underline{d}$ ratio where the nylon fibers do not, and therefore nylon passes through the critical length-to-diameter ratio rather abruptly.

Proceeding next to an evaluation of the influence of the elastic modulus, $\underline{E}$, on the relative position of the compression curves, an

*In the work with glass fiber, nonrecoverable deformation is attributed entirely to slippage. Since very few permanently bent nylon fibers were found and there was no evidence of large, permanent deformations at contacts for nylon, nonrecoverable deformation is also attributed to slippage for nylon.

exponential relationship was found between $\underline{M}$ or $\underline{C}_{10}$ and the elastic modulus for fibers above the critical length-to-diameter ratio. This relationship is shown graphically in Fig. 38, and is found to be

$$M \sim 1/E^{0.24}$$

$$C_{10} \sim 1/E^{0.21}$$

The data in this figure are for beds reduced to an equivalent density of 1.14 g./cc. The relative positions of the compressibility curves caused by differences in elastic modulus can be seen by referring to Fig. 19 on page 74, where the compressibility data for the fiber types studied are represented as solid fractions. The fact that the relationship between $\underline{M}$ and $\underline{E}$ is exponential explains why the changes in compression response brought about by changes in $\underline{E}$ were easy to find for the large-moduli differences in the nylon and dacron samples but were not so evident for the small differences in modulus between the two glass systems. In the theoretical equations developed by Van Wyk (17) and Wilder (4) and in the dimensional analysis, Equation (15), the applied stress, $\underline{P}$, and the modulus of elasticity, $\underline{E}$, always appear as a ratio raised to a fractional power. It seems significant, then, that the fractional power in the exponential relationship found between the mat solids concentration and the modulus of elasticity is 0.21-0.24, and very close to that value of $\underline{N}$, 0.20-0.26, found for the relationship between $\underline{C}$ and $\underline{P}$ beyond the critical $\underline{\ell}/\underline{d}$ ratio.

We have already stated that, in general, differences in fiber diameter do not bring about differences in compression response.

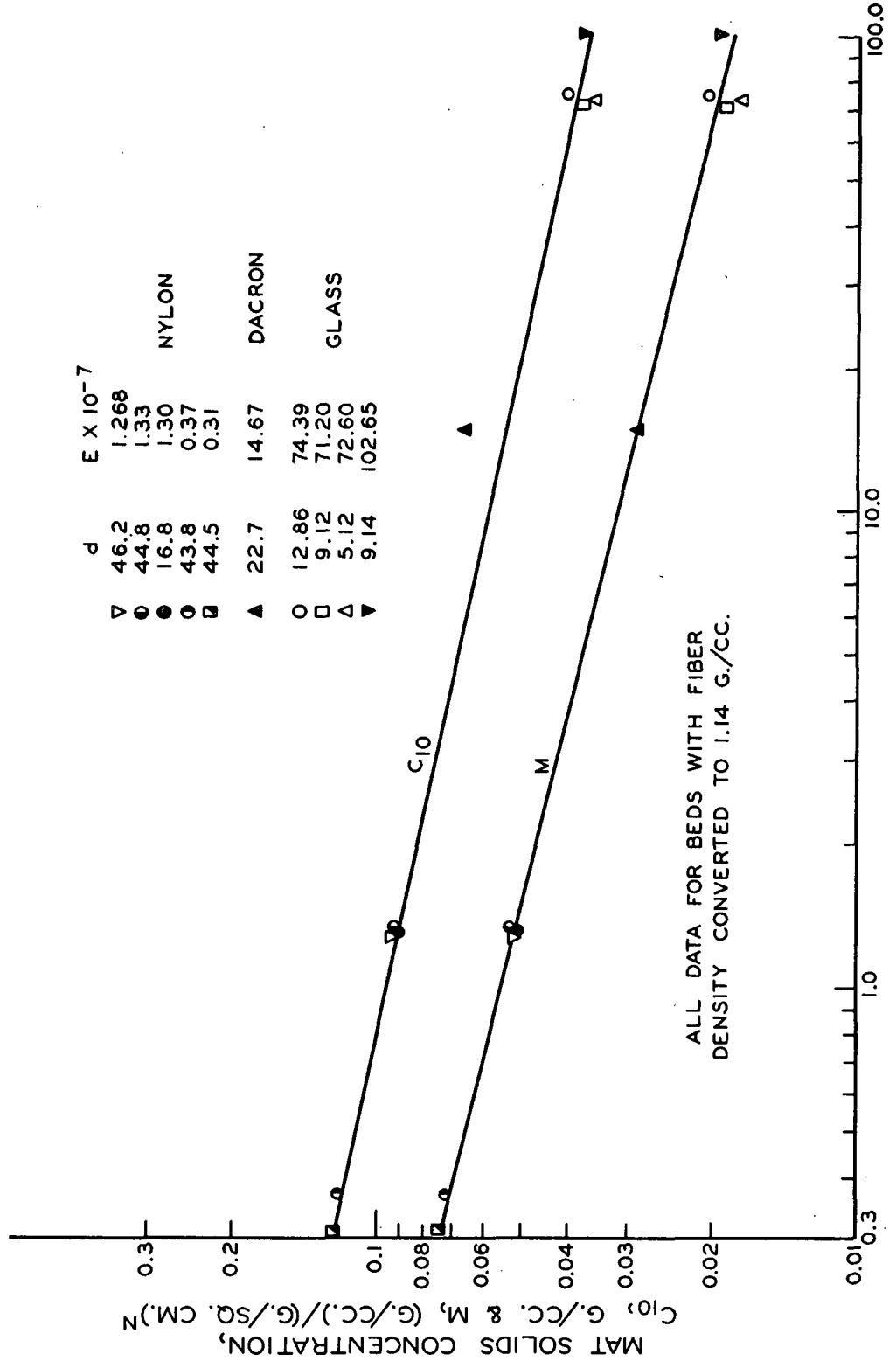

Figure 38. Constant M of Empirical Equation $C = MP^N$ and Factor C_{10} for Mechanically Conditioned Beds vs. Modulus of Elasticity

Consequently, one would not expect to find a relationship between the flexibility, $1/\underline{EI}$, and the terms $\underline{M}$ and $\underline{C}_{10}$ and, in fact, no relationship was found. It is apparent that the fiber diameter so enters into a proper mathematical expression for the fiber bed structure that it counterbalances the important effect of diameter on fiber flexibility, and no over-all diameter effect is observed.

THE SIMPLE BEAM EQUATIONS

A number of equations have been advanced to represent the compression data of both granular and fibrous materials. Some of these are empirical and some are theoretical treatments, both of which have already been discussed. Perhaps the most reasonable approach is that proposed by Wilder (4). It has been mentioned that Wilder's analysis assumed that the primary mechanism through which fibers contribute to bed deformation is fiber bending. The assumption was made at the outset that the amount of fiber slippage and fiber repositioning in the bed during loading is negligible. However, this study has shown that there is considerable nonrecoverable deformation as a result of the first compression, so that Wilder's assumption of no fiber repositioning would rule out the application of his equation to first compression data. It was felt that Wilder's equation (10) might be applicable to mechanically conditioned beds of synthetic fibers where many of the basic assumptions in the treatment might be met.

A trial-and-error solution was applied to the general form of Equation (10),

$$C^{1/N} - C_o'^{1/N} = MP \qquad (18),$$

utilizing the data obtained from several mechanically conditioned beds of glass and nylon fiber. A trial value of N was chosen and a linear regression of $C^{1/N}$ on P performed. The procedure was repeated until the best value of N was obtained. The equation seemed to fit quite well at high values of P. Figure 39 shows the fit of glass fiber compression data to Equation (18). The fit at low values of P was poor, and the values of C_o predicted by the equation were generally higher than those which may be estimated from the mechanically conditioned recovery curves. (The reader is referred to Appendix IV for a more complete discussion of this analysis.)

Evaluation of the data compiled in this study has led to the conclusion that bending is in fact a primary mechanism in compression of synthetic fiber beds. More will be said of this later. The point to be made here is that the consideration of fibers as small, complexly loaded beams is considered to be a fairly sound one.

The good fit of the glass fiber data to Equation (18) at high applied stresses seems to indicate that in the high load region where fiber bending is undoubtedly the controlling factor, Wilder's equation adequately describes the compression response of fiber beds. The fact that Wilder's equations for the bed structure are very much simplified does not adversely affect the fit of the data to the equation. First, the assumptions he used in describing bed structure probably apply fairly well to beds such as those studied because of the preferred orientations of the fibers, and second, his equations for bed structure merely influence the value of the constant M which has been determined empirically

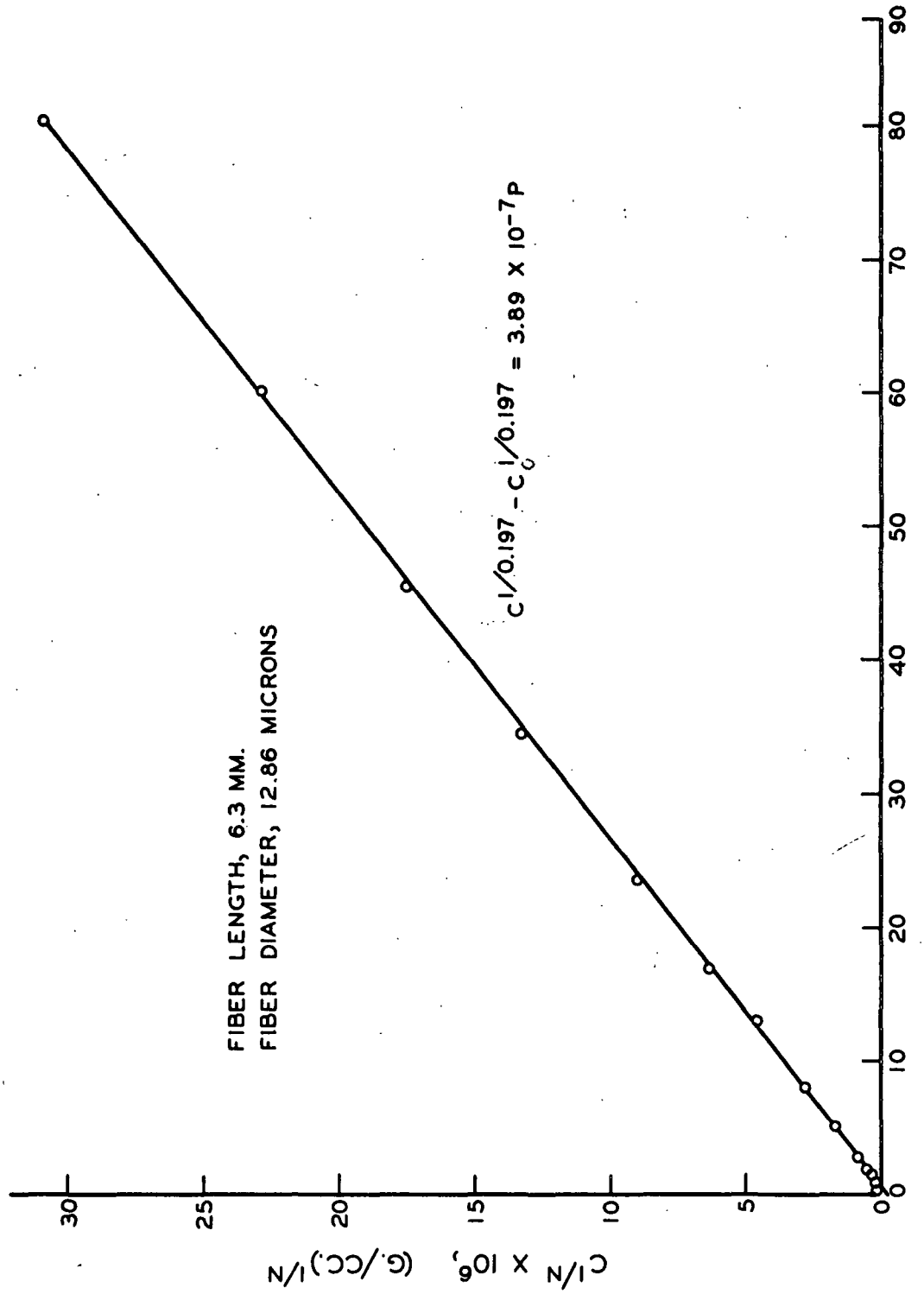

Figure 39. Fit of Glass Fiber Compression Data to Wilder's Equation

here. The lack of fit at low applied stresses is perhaps to be anticipated. In this region one might expect that a fiber repositioning mechanism would be more important than fiber bending and Equation (10) would no longer be expected to apply. It is felt that the shortcomings of Wilder's derivation for low loads may be centered around the expressions for the description of a layer in a fiber bed, and the number of fiber supports which the layer contains at any given applied stress under those conditions. Interfiber friction neglected in Wilder's development could be a very important and serious omission in the analysis, if fiber repositioning is the most important factor in the low load region.

At the present time it is difficult to assess the importance of the term $\underline{C}'_o$ in Equation (10). There is some speculation that it is equivalent to the mat solids concentration at zero applied stress. Calculations based on some of the glass fiber data would tend to support this view. However, the most that can be said about $\underline{C}'_o$ at this time is that the term is a constant of integration for this particular equation.

Treatment of the data taken in this study with Equation (18) indicates that $\underline{C}'_o$ is a function of the length-to-diameter ratio. It has already been demonstrated in this investigation that $\underline{M}$ is a function of $\underline{\ell}/\underline{d}$ ratio, and the above finding explains the absence of the $\underline{\ell}/\underline{d}$ function as such in the constant $\underline{M}$ contained in the brackets of Equation (10). It has also been shown in this study that $\underline{N}$ is a function of $\underline{\ell}/\underline{d}$ ratio, and this simply means that α in Wilder's equation is a function of $\underline{\ell}/\underline{d}$. This is reasonable since α entered into the derivation of Equation (10) in the assumption that $\underline{b} = \underline{k}/\underline{C}^{\alpha}$, and we have already discussed the fact that the

distance between fiber contacts, b, is a function of length-to-diameter ratio.

ANALYSIS OF BED COMPRESSION IN TERMS OF FIBER MECHANISMS

Studies have been made during the course of this work on very idealized, stacked models of fiber beds. These beds were arranged out of rather large fibers prepared from nylon broom bristles so that they were as long as the diameter of the test bed, and therefore they may be considered as infinitely long fibers. Comparisons made between compression response of these fiber beds and those beds made from fibers of "finite" length by filtration have proved very helpful in analyzing the important factors in fiber bed deformation.

The models studied were of three types and are pictured schematically in Fig. 40.

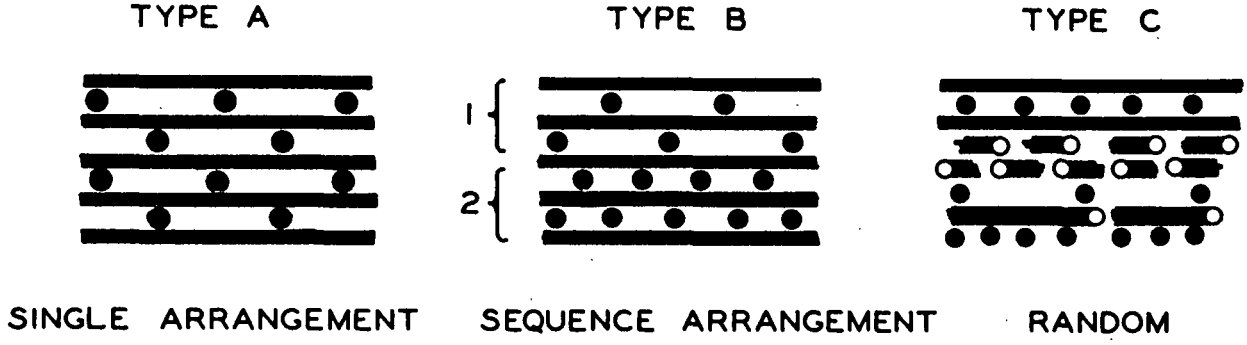

Figure 40. Schematic Representation of Model Fiber Beds

Model Type A had a single arrangement of fiber stacking, and the fibers in succeeding layers were always at right angles to each other. When subjected to compressive stress, the fiber bed exhibited a Hookean

compression response until a log cabin-type structure was set up due to extreme bending of the fiber elements. Further compression was slight and due wholly to compression at points of fiber contact. This type of response is pictured schematically in Section 1 of Fig. 41 and 42. The difference between curves for A_1 and A_2 is that A_2 had a close stacking arrangement, which resulted in a shorter element length between fiber support points. The actual data taken from these model studies is shown in graphical form in Appendix V.

An equation may be derived for this type of bed deformation based on bending of fiber elements as beams. The forms arrived at are:

$$H_o - H = MP \qquad (19a)$$

or

$$(1/C_o) - (1/C) = M'P \qquad (19b)$$

where $\underline{H}$ is bed height. The $\underline{M}$ values consist primarily of a description of the number of fiber contacts per layer and the number of layers. These equations can be fitted to the data taken on a bed of Type A. The derivation of this equation and the two to follow, is shown in Appendix V.

It should be noted that Equation (19b) is merely a special case of Equation (10) in which α is equal to zero, and therefore $\underline{N} = -1$. From Wilder's assumption that $\underline{b} = \underline{k}/\underline{C}^{\alpha}$ it is evident that setting α equal to zero means that the distance between contact points is no longer dependent on solids concentration. This is precisely the case in these model stacked beds of Type A, and in treating the data for these beds with

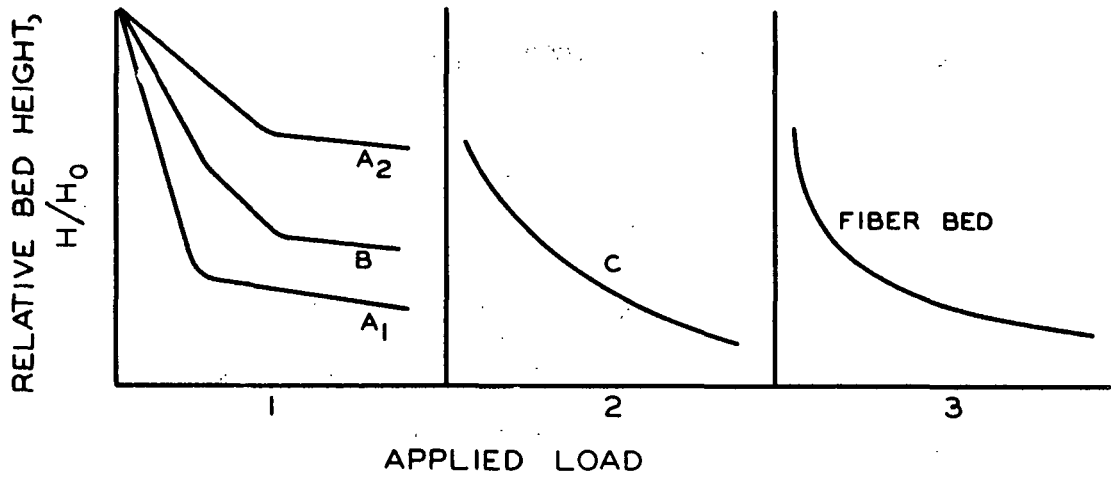

Figure 41

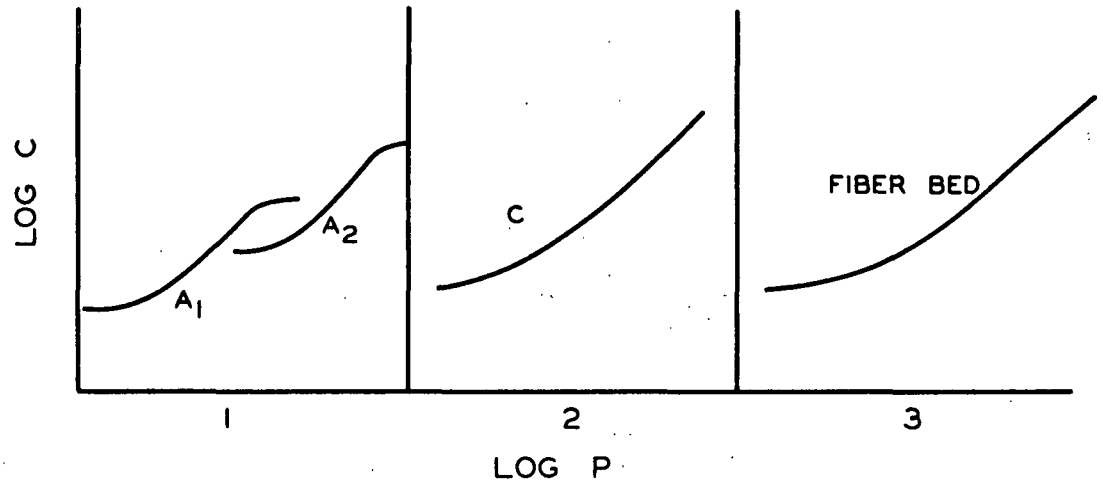

Figure 42

Schematic Representations of the Compression Response of Fiber Beds

Wilder's equation N is found to be equal to -1. That is to say that the data fit Equation (19a) very well as shown in Fig. 43.

A model bed of Type B is a combination of two Type A beds, and gave the second response pictured in Section 1. Note the change in slope of the H/H_o vs. P curve which occurred as first one type of stacking controlled the deformation and then a second type took over. An equation of the form,

$$(1/C_o) - (1/C) = K_a(M_1 + M_2)P \qquad (19c)$$

fits this type of stacking arrangement when both types of stacking are contributing to the bed deformation. At a later time, Equation (19b) fits as only one type of stacking is contributing significantly to deformation.

The random type model C bed had a varied number of fibers in each layer with the fibers in each layer placed at some randomly chosen angle. Each layer would have its own M constant which applied to it, and the compression equation could be written

$$(1/C_o) - (1/C) = K_b(M_1 + M_2 + M_3 \ldots M_n)P \qquad (20).$$

As each layer is collapsed, its associated M drops out of the equation and the slope of the H/H_o vs. P curve changes. When the number of layers is large, one obtains a continuous curve such as is shown in Section 2 of Fig. 41 and 42. There is a strong similarity between the shape of this curve and the shapes of the compression curves for beds of fiber of "finite" length. In the latter case, one would expect the multiplier,

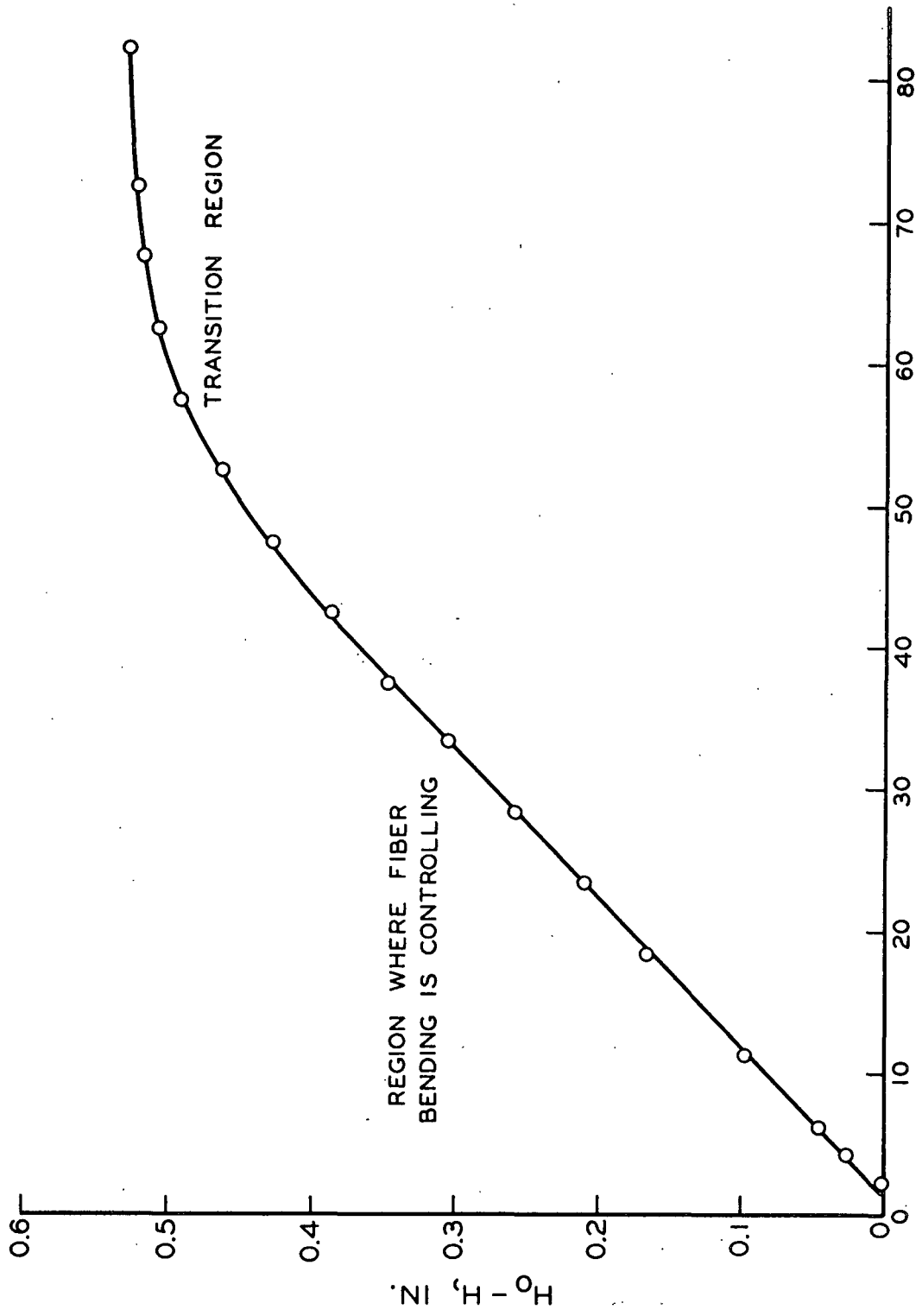

Figure 43. Fit of Data from Model Fiber Bed A_1 to Equation (19a), $H_o - H = \frac{MP}{}$

M, of P to be a function of P and to change continually as the applied stress is increased. This is equivalent to saying that the number of contact points is now a function of applied load and that α in Equation (10) is no longer zero. In treating the data for the random Type C model bed with Wilder's equation N was found to be 0.236, a value which is very close to those values found for fiber beds. The similarity in agreement with Wilder's equation found for fiber beds and these model beds where fiber bending is definitely controlling bed response add strong support to the validity of Wilder's approach in spite of its simplifying assumptions. The agreement of the data for the random stacked Type C bed with Wilder's equation at high loads and the lack of fit at low loads is shown in Fig. 44.

In the model fiber beds, the value N of the limiting slope is not altered by changing the A type stacking to a more tightly packed form (see Fig. 42). Only the C values at a given load are changed. This is a striking similarity to the findings of this study for glass fibers of finite length, where changes in fiber length above the critical length-to-diameter ratio do not alter the limiting slope of the compression curves but do slightly change the value of C_{10} for the plotted data. The changes in over-all bed structure in the two cases are very similar, i.e., the average unsupported length of the fiber is changed (see Appendix V).

The difference in fiber lengths used must necessarily cause marked differences in the structure of a random Type C model bed and a filtration-formed fiber bed. However, there are strong similarities when one views

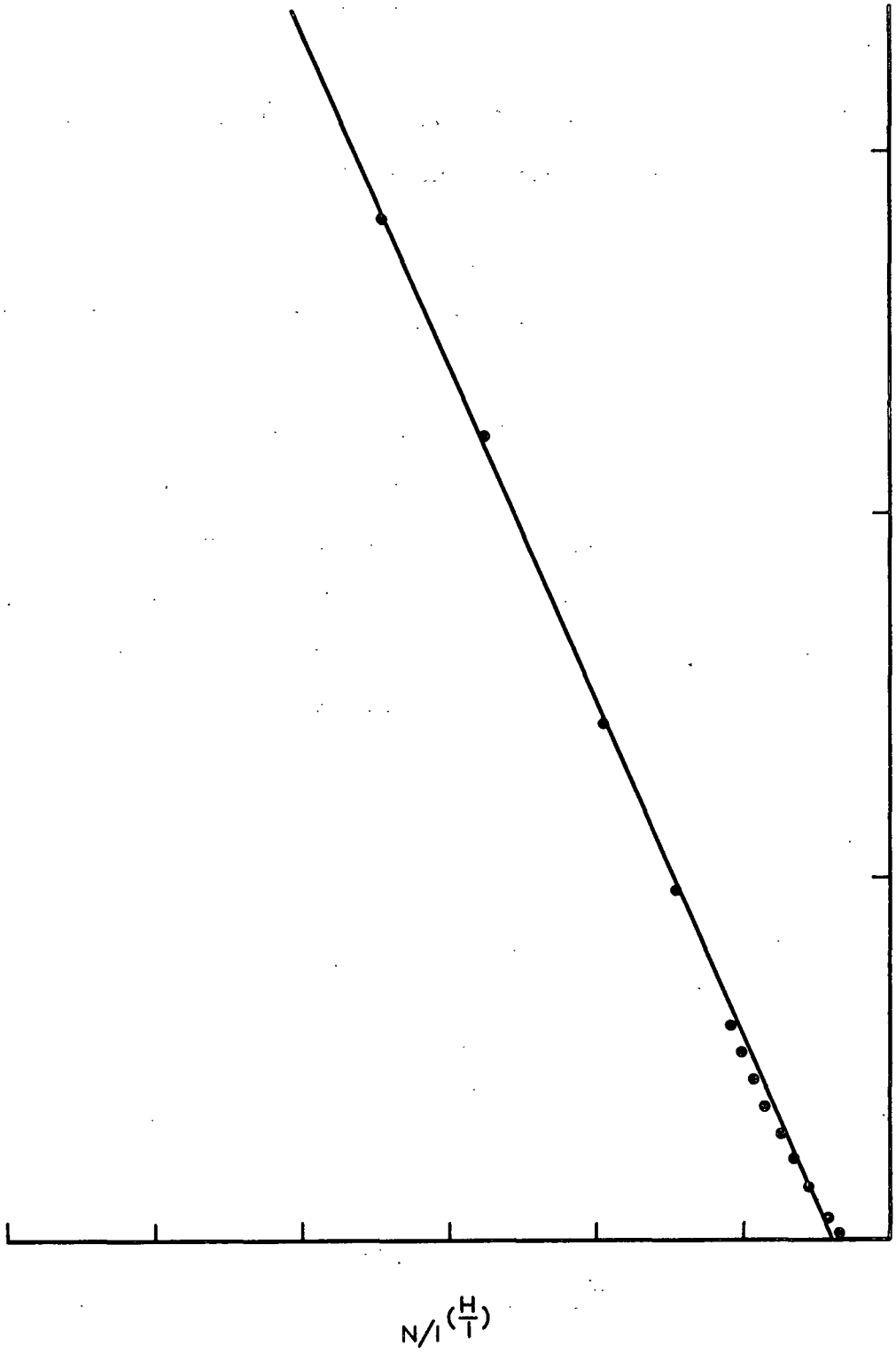

Figure 44. Fit of Compression Data for Randomly Stacked Model Network Type C to the Equation $C_1/N - C_o 1/N = MP$ Plotted as $(1/H)1/N$ vs. F Where $C = W/AH$ and $P = F/A$

only a small section of a filtration-formed fiber bed. Figure 45 is a view of such a section of a glass fiber bed. This figure shows the extremely loose structure found in synthetic fiber beds, and such a structure can now be more easily visualized as a system of fiber elements which bend and slip into contact with one another during compression. The data taken in this study support this concept.

In view of the similarity between glass and nylon fiber data, the changes brought about in compression response through changes in fiber modulus of elasticity can be related only to the bending character of fiber elements. It is true that changes in nylon modulus of elasticity would affect the compression of nylon fibers at contact points in the same way as it affects its bending characteristics. However, the compression of nylon fibers at points of contact is not expected to be important under the loads used in this study. This conclusion is supported by the work of both Finch (36) and Kurath (46), who found that for nylon rather high loads were needed to cause deformation at fiber-to-fiber contacts.

All the above observations on real and model beds would tend to support the conclusion that fiber bending is the most important compression mechanism for mechanically conditioned glass and nylon fiber beds at low applied stress. However, by analogy to the model beds, compression of fibers at points of contact would be expected to become very important at very high applied stresses.

During first compression, fiber slippage and repositioning are very important contributors to fiber bed deformation. The magnitude of this

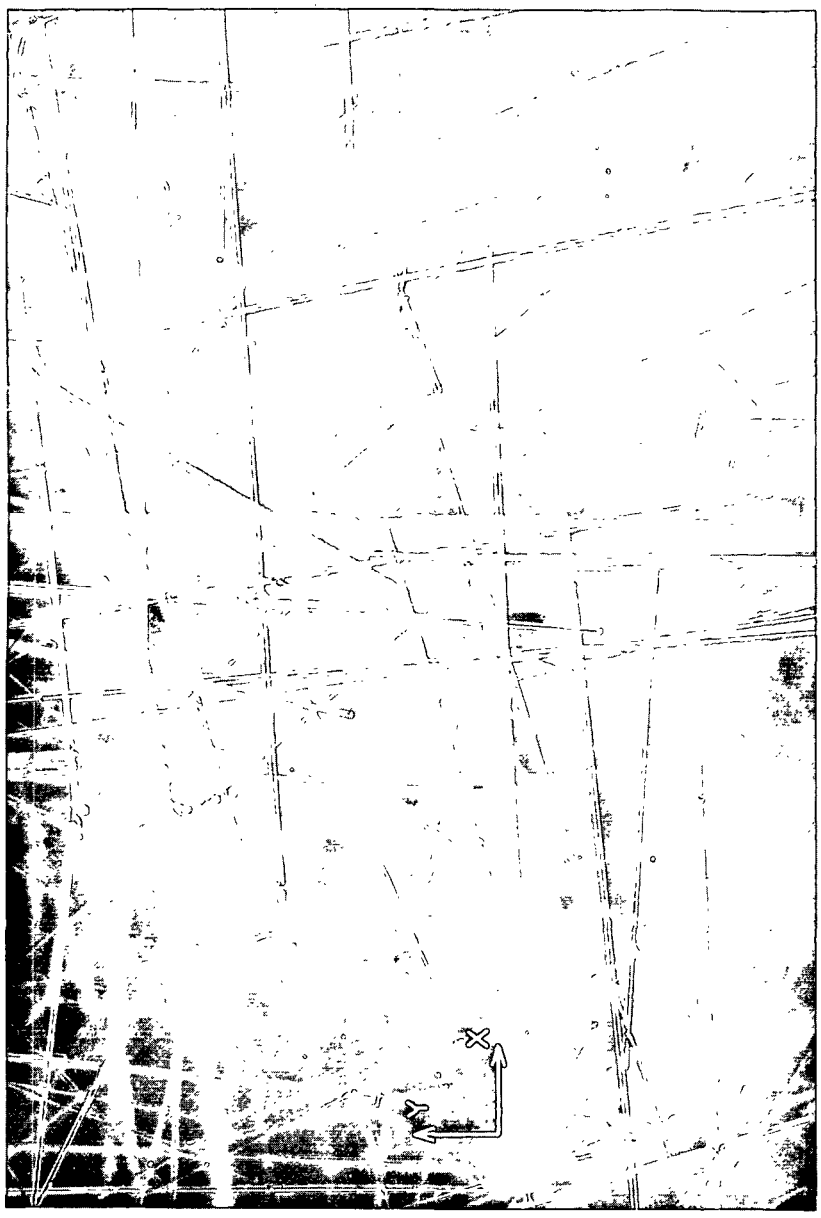

Figure 45. View Into the Interior of a Dry Glass Fiber Bed
Fiber Length 3.13 mm.; Fiber Diameter 12.86 μ; Mat Solids
Concentration ca. 0.15 g./cc.; Porosity ca. 0.985

contribution is dependent upon the fiber length-to-diameter ratio, as has already been emphasized. It seems very reasonable to suppose that the hysteresis loop found in mechanically conditioned fiber beds is the result of interfiber friction developed because of reversible fiber slippage, fiber repositioning, and the passage of fiber ends back and forth over their nearest neighbors. The fact that the model stacked beds exhibited no hysteresis loop in compression-recovery supports this concept. The hysteresis loop for pulps is probably mostly due to time-delayed deformation and recovery rather than to interfiber friction. In addition, part of the nonrecoverable deformation in first compression of pulp is probably due to permanent deformation of fibers, whereas in synthetic fiber beds, nonrecoverable deformation is attributed entirely to fiber slippage.

Some of the most important conclusions to be drawn from this study relate to pulp fiber. First, the effects of changes in fiber moduli and length are the same as those found for synthetic fibers, and it is therefore believed that fiber bending and fiber repositioning are important in the same way to pulp fiber bed compression as they are to synthetic fiber bed compression. However, in the case of pulp, there is the additional factor of compression of fibers at points of contact, even at the low loads used in this study. This is believed to be true because the limiting slopes of the compression curves are always higher for pulp fibers than for synthetic fibers. Other reasons for this higher slope have already been mentioned. The pulp used in this study was all summerwood, and one can assure himself that the fibers were not

collapsed ribbons but actually tubular by looking at Jayme and Hunger's (47) photomicrographs of pulp sheets.

We know from studies on synthetic fibers that the combination of fibers bending and repositioning in the first compression and at higher loads in a mechanically conditioned compression can produce a compression response that is exponential, or nearly so. From theory and in practice, Finch (36) reports that the deformation of fibers at points of contact is also exponential. The sum of the deformations due to all three mechanisms probably would produce a curve of higher slope on a plot of log C vs. log P, and one that, over short ranges, could very well look linear.

The results of this study help to clarify much of the pulp compressibility data taken in the past. The changes brought about in M by pulp bleaching may be due to a change in wet fiber flexibility, the bleached fiber being more flexible. It has also been reported that the constant M changes upon beating of an unbleached pulp, but not upon beating of a bleached pulp. This study has shown that a rather large change in mean fiber length for pulp does not have as large an effect on the compressibility constants M or N as a similar change would have in the case of synthetics. In the case of pulp fibers, there was a wide distribution of fiber lengths. The few very long fibers would be expected to contribute significantly to the over-all bed structure and therefore the changes in compressibility behavior with changes in mean length would not be as great as those observed for synthetics with very narrow fiber length distributions. It is this writer's feeling that the changes

in M observed upon beating pulp may be more closely related to changes in fiber flexibility than to changes in fiber length. That is to say that beating may produce a larger and more noticeable change in fiber modulus of elasticity of the unbleached pulp than of the bleached pulp, which already has a lower modulus. However, observations on pulp reported as solids concentration vs. load are always difficult to analyze. This is because solids concentration does not take into account simultaneous changes in specific volume of the fiber which undoubtedly take place during bleaching and beating and perhaps during loading of the fiber bed.

In view of the considerations presented here it is dangerous to use compressibility or recovery measurements as a general test for fiber flexibility. Although it is true that the changes in fiber elastic modulus strongly influence compression-recovery response, the complications introduced by differences in fiber length-to-diameter ratio make it unwise to compare pulps from different species of wood, different fractions of the same pulp or samples of the same pulp at different degrees of refining. On the other hand, application of a compressibility test as a measure of relative flexibility of samples of the same pulp cooked or bleached to different degrees may be fairly reliable.

SUMMARY

The compression-recovery response of fiber webs is of particular interest to the pulp and paper industry because it has an important effect on the formation and mechanical properties of paper. The present investigation was undertaken to increase our knowledge of the fiber interaction mechanisms that operate in fiber beds placed under compressive stress. In particular, the importance of the variables of fiber length, diameter, and elastic modulus in changing compression-recovery response have been evaluated.

The large number of variables important to the compression response of the very complex system of nonwoven fiber networks of viscoelastic fibers, such as pulp mats, was reduced by studying systems of synthetic fibers--nylon and glass. These results were then compared to results obtained on carefully selected pulp fiber samples. The compressibility test was used to obtain compression-recovery data on relatively thick fiber beds in the 0.009-80.2 g./sq. cm. range of applied stress. The data were interpreted in terms of suspected fiber interaction mechanisms: (1) fiber bending, (2) fiber slippage, (3) compression of fibers at points of contact. Fiber beds were formed by filtration from dilute slurries and studied for first compression and recovery response and mechanically conditioned compression and recovery response. Attempts were also made to determine the mat solids concentration at zero applied stress for both first compression and mechanically conditioned compression. Proposed empirical and theoretical equations used to express compression response were evaluated.

The results of this work may be summarized as follows:

1. Fiber beds can be formed which have their individual fibers randomly distributed in the x-y plane with little or no z orientation.

2. The compression-recovery response of both synthetic and pulp fiber beds is highly dependent upon:

   a. fiber length-to-diameter ratio as it affects the structure of the bed formed;

   b. fiber modulus of elasticity as it affects the flexibility of the fiber; and

   c. degree of fiber flocculation (particularly for glass fibers).

3. Fiber diameter by itself is an unimportant factor in bed compression because its effect on mat structure is apparently counterbalanced by its effect on fiber flexibility.

4. First compression data may be used to compare beds of different fiber types without resorting to the laborious procedure of mechanically conditioning the bed.

5. Wilder's equation based on the mechanism of fibers bending as beams represents compression data quite well at high applied stresses where fiber bending would be expected to be controlling bed deformation, but it does not apply well at very low applied stresses where other fiber interaction mechanisms probably are controlling.

6. Wrist's assumption that the bulk modulus is proportional to the compacting stress applies well over a wide range of first compression

data, but does not seem to be applicable to mechanically conditioned fiber beds.

7. Mechanically conditioned beds of both viscoelastic and non-viscoelastic fibers exhibit the properties of elastic hysteresis and memory.

8. There are strong similarities between the compression response of model beds of infinitely long fibers which involve only fiber bending and the compression response of the filtration-formed beds of short fibers.

CONCLUSIONS

It is felt that this investigation constitutes a significant contribution to the understanding of fibrous bed compression and recovery behavior. Although it has not been possible to make a complete study of all fiber types over a complete range of loads, several important facts have been brought to light. From this investigation, one may conclude that:

1. During first compression, particularly at low loads, fiber repositioning in the bed is probably the most important fiber contribution to fiber bed compression.

2. The importance of fiber repositioning in first compression approaches a situation where it is replaced by fiber compression at very short fiber lengths and fiber bending at very long fiber lengths.

3. Fiber bending is the most important fiber mechanism contributing to the deformation of mechanically conditioned fiber beds at low loads.

4. The importance of bending of fiber elements for mechanically conditioned beds is replaced by compression of fibers at points of contact at extremely high loads, as is shown particularly well by the model network studies.

5. In the case of viscoelastic fibers which swell a great deal, such as the low-modulus wet pulp fiber, compression of fibers at points of contact is probably important at the outset of compression, and may be to some extent recoverable.

6. The hysteresis loop encountered in cyclic compression-recovery of mechanically conditioned synthetic fiber beds is probably largely the result of interfiber friction.

7. The hysteresis loop encountered in cyclic compression-recovery of mechanically conditioned wood pulp fiber beds is probably influenced more by the increased amount of delayed deformation and recovery although friction may still be an important factor.

8. Because of the interference of length-to-diameter ratio and fiber curl, it is dangerous to use compression-recovery response as an indication of fiber flexibility in making comparisons between different types of pulps.

SUGGESTIONS FOR FUTURE WORK

In the field of fiber bed response to compressive stress, there is need for more work on both the theoretical and experimental fronts. In the theoretical area, there is a need to improve the theoretical equation for the relationship between compression response and applied stress by considering other mechanisms besides fiber bending. The real shortcomings here are two:

(1) the lack of an adequate description of the structure of a fiber bed at any single applied load for systems more complex than the beds of preferred fiber orientation studied in this work, and

(2) the lack of a sound expression for the change in number of contact points with change in load.

Of less immediate importance is the need for a method of accounting for reversible slippage and interfiber friction.

Item 2 above appears to be a very promising area for immediate experimental attack. Kurath (46) has made some effort in this direction and his technique of observing permanent deformation on fibers at contact points may prove useful if a fiber can be found which will deform at very low applied stresses.

There is also a need for correlation with structural properties of both creep and compressibility of viscoelastic fibers. This is particularly true if we are to make any further gains in understanding pulp systems. Viscose fibers of various diameters are available in round

cross sections, both with and without a lumen-type structure. These would be ideal for this work.

In order to complete the work that has been initiated in this study, it would be desirable to study the nylon samples used here under a very highly extended load range. What is expected is that compression curves for all lengths and moduli will come together at a value close to the density of nylon. Such a complete load range study would also be of interest with viscose and pulp. In addition, the settling technique introduced in this report might be pursued further to complete the picture of fiber bed compression-recovery behavior. However, all of this work should be directed toward obtaining adequate information to describe mathematically in a very general form the compression response of fiber beds. Further attacks on mathematical descriptions of fiber bed structure might be made by continuing the work initiated in studies of model fiber networks.

All the work done in this investigation has been carried out on relatively thick fiber beds. It would be valuable to extend this work to thin sheets in the range of basis weights normally used in making paper.

ACKNOWLEDGMENTS

It would be a difficult task to list all of those people who have contributed in many different ways to the successful accomplishment of this work. However, a number of these people deserve special mention. In particular, the author would like to express his sincere appreciation to Dr. Harry D. Wilder, the chairman of his thesis advisory committee, and also to Drs. Ingmanson, Nelson, and Kurath, the members of his thesis advisory committee.

The assistance of the following people is also gratefully acknowledged:

Mr. W. T. Myers, Jr., for permission to use both his samples of nylon fiber and the characterization data which he obtained for them.

Mr. Leslie L. Warner, Mr. P. A. Lockwood, and others of the Owens-Corning Fiberglas Corporation for supplying glass fiber samples used in this study, particularly for making available a sample of "Hi-Modulus Beryllia" glass.

Mr. G. D. Campbell of the Pittsburgh Plate Glass Company, also for supplying glass fiber samples used in this work.

Mr. Orlin Kuehl of the Chemical Engineering group and also the members of The Institute of Paper Chemistry Machine Shop and Millwright Shop who had a hand in designing and constructing the apparatus.

I would also like to acknowledge the help of Mrs. Elizabeth Cary in preparing and editing the original manuscript.

The helpful suggestions of Mr. S. T. Han in regard to an evaluation of Wilder's equation are also gratefully acknowledged.

NOMENCLATURE

a, b, c, f, g	=	superscripts in Equation (15), dimensional analysis
a', b', c'	=	constants in Equation (6)
A	=	cross-sectional area of fiber bed, sq. cm.
A_f	=	cross-sectional area of fiber
A', B'	=	constants in Equation (4)
b	=	length of fiber element between contact points
B	=	constant in Equation (13)
C	=	mat solids concentration, g./cc.
C_o	=	sedimentation consistency of the slurry, or mat solids concentration at zero applied stress
C_o'	=	constant in Equation (10)
C_{10}	=	mat solids concentration at 10 g./sq. cm. applied stress
d	=	fiber diameter, microns
D	=	distance two fibers slide across one another at a contact point
E	=	modulus of elasticity, g./sq. cm.
F	=	applied force, g.
F_c	=	vertical force at a contact point
F_f	=	frictional force at a contact
G	=	shear modulus
Δh	=	deflection of a single fiber as a beam
H	=	bed height at any load, cm.
H_o	=	initial bed height
ΔH	=	change in height of a bed
ΔH_t	=	total change in height of a bed of more than one layer
i	=	number of fiber-to-fiber contacts in a layer

i_f = number of fiber-to-fiber contacts per fiber

I = moment of inertia (second moment of the area of cross section)

k = proportionality constant

K = bulk modulus, g./sq. cm.

K_a = constant in Equation (19c)

K_b = constant in Equation (20)

K' = constant in Equations (7)-(9)

ℓ = fiber length

$\Delta\ell$ = elongation

m = mass of dry fibers in a bed

M = constant in the "compressibility equation" (1)

M' = constant in Equation (19b)

n = number of layers in a bed

N = constant in the "compressibility equation" (1) and slope of the straight-line portion of the log C vs. log P first compression curve

N' = normal force at a contact point

N_f = number of fibers in a layer of a bed

N_{ft} = total number of fibers in a bed

N_L = slope of the straight-line portion of the log C vs. log P plot of mechanically conditioned compression data

P = apparent applied stress, g./sq. cm.

P_o = compacting pressure in sedimentation, g./sq. cm.

P_2 = apparent compacting stress, g./sq. cm.

r = fiber radius, microns

R = bed radius, cm.

S = number of fiber support points

t = time

$\underline{V}$ = fiber bed volume, cc.

$\underline{V}_o$ = constant in Equation (7)

$\underline{W}$ = weight of dry fiber in a bed, g.

$\underline{y}$ = difference in weight of slurry-filled or water-filled pycnometer, Equation (11)

α = constant in Equation (10)

μ = coefficient of friction

ρ = fiber density, g./cc.

$\rho_{\underline{w}}$ = density of water, g./cc.

σ = Poisson's ratio

$1,2,3...\underline{n}$ = subscripts used to denote layers of a fiber bed

LITERATURE CITED

1. Leaderman, Herbert. Elastic and creep properties of filamentous materials and other high polymers. Washington, D.C., The Textile Foundation, 1943. 278 p.

2. Brezinski, J. P. A study of the viscoelastic properties of paper by means of tensile creep tests. Doctor's Dissertation. Appleton, Wis., The Institute of Paper Chemistry, 1955. 242 p.

3. Eirich, F. R., Ed. Rheology, theory and applications. Vol. I. New York, Academic Press, 1956. 761 p.

4. Wilder, H. D. The compression creep properties of wet pulp mats. Doctor's Dissertation. Appleton, Wis., The Institute of Paper Chemistry, 1959.

5. Seborg, C. O., Simmonds, F. A., and Baird, P. K., Paper Trade J. 109, no. 8:35-42(Aug. 24, 1939).

6. Seborg, C. O., and Simmonds, F. A., Paper Trade J. 113, no. 7:49-50(Oct. 23, 1941).

7. Seborg, C. O., and Simmonds, F. A., Paper Trade J. 125, no. 15:63-7(Oct. 9, 1947).

8. Christensen, G. N., and Barkas, W. W., Trans. Faraday Soc. 51, no. 1:130-45(1955).

9. Ivarsson, B. W., Tappi 39, no. 2:97-104(Feb., 1956).

10. Ingmanson, W. L., and Andrews, B. D., Tappi 42, no. 1:29-35(1959).

11. Brown, R. B., Paper Trade J. 94, no. 13:35-8(March 31, 1932).

12. Buckingham, S. A., Paper Ind. & Paper World 20, no. 6:629-34(Sept., 1938).

13. Saxl, E. J., Textile Research J. 10, no. 10:425-32(Aug., 1940).

14. Ingmanson, W. L. Personal communication, 1961.

15. Kolb, H. J., Stanley, H. E., Busse, W. F., and Billmeyer, F. W., Jr., Textile Research J. 23, no. 2:84-90(Feb., 1953).

16. Work, R. W., Thorne, A., and Livingston, M. R., Phys. Rev. 70, no. 10:803(Nov., 1946).

17. Van Wyk, C. M., J. Textile Inst. 37:T285-92(1946).

18. Busse, W., Textile Research J. 23, no. 2:77-84(Feb., 1953).

19. Pigeon, L. M., and van Winsen, A., Can. J. Research 105, no. 1: 1-18(1934).

20. Dadswell, H. E., and Watson, A. J. Symposium on Formation and Structure of Paper, Oxford, Eng., Sept. 25-29, 1961.

21. Campbell, W. B., Pulp Paper Mag. Can. 48, no. 3:103-9(1947).

22. Qviller, O., Papir-Journalen 26:312(Dec., 1938).

23. Parker, J. D. Unpublished work. Appleton, Wis., The Institute of Paper Chemistry, 1956.

24. Ingmanson, W. L., Andrews, B. D., and Johnson, R. C., Tappi 42, no. 10:840-9(1959).

25. Andrews, B. D. Personal communication, 1959.

26. Ingmanson, W. L., and Whitney, R. P., Tappi 37, no. 11:523-33(1954).

27. MacLaurin, D. J. Unpublished work, 1951.

28. Kurath, S. F., Tappi 42, no. 12:953-9(1959).

29. Brown, J. C., Jr. Determination of the exposed surface area of pulp fibers from air permeability measurements using a modified Kozeny equation. Doctor's Dissertation. Appleton, Wis., The Institute of Paper Chemistry, 1949. 146 p.

30. Van den Akker, J. A., Wink, W. A., and Bobb, F. C., Tappi 42, no. 4: 340-4(1959).

31. Train, D., Trans. Inst. Chem. Engr. 35:258(1957).

32. Agte, C., and Petrdlik, M., Hutnicke' Listy 7:121-4, 190-4(1952).

33. Wrist, P. E., Tappi 44, no. 1:181A-99A(1961).

34. Eggert, M., and Eggert, J. See Mark, H. Beitrage zur Kenntnis der Wolle und ihrer Bearbeitung. Berlin, 1925.

35. Bogaty, H., Hallies, N. R. S., Hintermaier, J. C., and Harris, M., Textile Research J. 23, no. 2:108-14(1953).

36. Finch, R. B., Textile Research J. 21, no. 6:383-92(1951).

37. Ingmanson, W. L., Chem. Eng. Progr. 49, no. 11:577-84(1953).

38. Sinclair, D., J. Appl. Phys. 21:380-6(May, 1950).

38a. Ilvessalo-Pfäffli, M., and Alfthan, G. v., Paper and Timber 39, no. 11:509-16(1957).

39. Kärrholm, E. M., and Schröder, B., Textile Research J. 23, no. 4:207-24(April, 1953).

40. Myers, W. T., Jr. Unpublished work, 1960.

41. Andrews, B. D. Unpublished work, 1958.

42. Wilder, H. D. Unpublished work, 1958.

43. Arnold, E. Unpublished work, 1961.

44. Onogi, S., and Sasaguri, K., Tappi 44, no. 12:874-80(Dec., 1961).

45. Doughty, R. H., Paper Trade J. 94, no. 9:114-19(1932).

46. Kurath, S. F. Personal communication, 1961.

47. Jayme, G., and Hunger, G. Symposium on Formation and Structure of Paper. Oxford, England, Sept. 25-29, 1961.

APPENDIX I

SAMPLE CALCULATION AND DISCUSSION OF ERRORS

ERRORS

Mat solids concentration, C, is defined as the mass of dry fiber per unit volume of fiber bed. For a circular fiber bed of height H, mat solids concentration is defined by the equation

$$C = \frac{W}{\pi R^2 H} \qquad (21)$$

where W is the weight of dry fiber in grams and R is the radius of the pad test area. The weight of dry fiber could easily be determined to ±0.001 g. Pads ranged in weight from 3 to 17 g. Since the lowest weight of pad studied was approximately 3 g., the largest error that could be introduced due to the determination of fiber bed weight was approximately 0.3%. Initial bed heights could be determined to ±0.0002 in. and deformations to at least ±0.0007 in. over the entire range of the LVDT. Since beds ranged in height from 0.2 in. at the highest loads to 0.8 in. at the lowest loads, the maximum error in measurement of height could be 0.45%. By far the largest possible error in determination of mat solids concentration is introduced in the test area measurements. The bed test area was taken from a measurement of the piston surface area which was 79.01 sq. cm. However, the fiber beds appear to extend slightly beyond the outer edge of the piston, and photographic measurements indicated a possible 1% difference in bed cross-sectional area and piston surface area. This error would be difficult to check accurately, and is probably very close to constant for all beds formed in the 4-in. diameter

forming tubes. Maximum possible errors in the 5-in. diameter clipping process have already been mentioned as 2.5-3%.

SAMPLE CALCULATION

DATA TABLE

Septum position	2.6520 in.
Bed initial point	2.2017 in.
Initial VTVM reading	0.693 v.
Bed weight	5.8261 g.
Bed cross-sectional area	79.01 sq. cm.

Applied stress, g./sq. cm.	VTVM Reading, v.	Septum Deflection Correction, in.
2.70	0.693	0.0
5.04	0.599	0.0006

The initial mat solids concentration at an applied stress of 2.70 g./sq. cm. may be calculated as follows:

$$\begin{matrix}\text{initial}\\ \text{bed height}\end{matrix} = \begin{matrix}\text{bed initial}\\ \text{point}\end{matrix} - \begin{matrix}\text{septum}\\ \text{position}\end{matrix} = 0.4503 \text{ in.}$$

$$C = \frac{\text{bed weight}}{\left(\begin{matrix}\text{initial bed height x}\\ \text{bed cross-sectional area}\end{matrix}\right)\left(\frac{2.54 \text{ cm.}}{\text{per in.}}\right)^2} = 0.0645 \text{ g./cc.}$$

All further calculations are based on the initial bed height. An initial core position for the LVDT is determined from a calibration chart and the initial VTVM reading. The calibration curve is in the

form of a "V" with each branch of the curve at 45°. The core position is plotted on a scale of 0.02 in. per in., covering a range of ±1 in. in core position. The voltage output is plotted on a scale of 0.04 volts per inch, covering a voltage output up to approximately 3 volts. In this case, the initial position of the core was 0.7921 in. on the calibration curve at 0.693 volts.

In order to calculate the deformation caused by increasing the applied stress to 5.04 g. per sq. cm., a new core position is determined from the VTVM output reading, 0.599 volt. This is determined to be 0.7547 in. Therefore, the deformation is the difference between these two core positions or 0.0374 in. The bed deformation is subtracted from the initial bed height to give a new bed height of 0.4129 in. However, this value must be corrected by adding to it a septum deflection caused by the additional load on the septum. In this case, the septum deflection is 0.0006 in. and the corrected bed height is 0.4135 in. Calculating the mat solids concentration as before, one finds a value of 0.07021 g./cc.

APPENDIX II

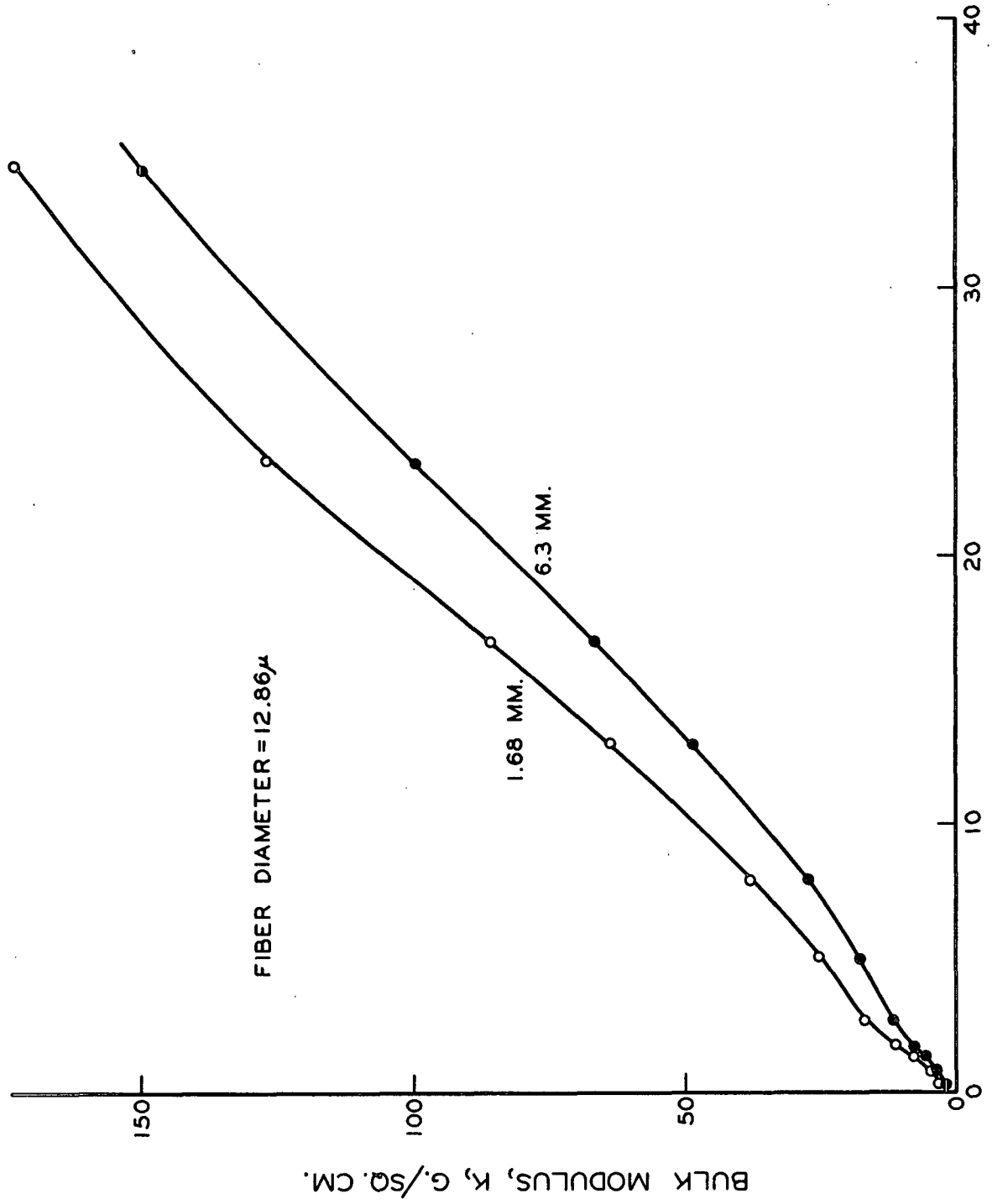

Figure 46. Bulk Modulus, K, vs. Apparent Applied Stress, P, for Mechanically Conditioned Glass Fiber Beds

APPENDIX III

THE EFFECT OF FIBER CURL ON COMPRESSION RESPONSE

It has been suggested that the higher slope, N, of pulp fiber compressibility curves as compared to the slopes of the synthetic fibers may be due partially to the fact that pulp fibers may be curled, unlike the rodlike synthetics studied in most of this work. This view is supported by a compressibility run made on a nylon fiber that curled into closed ringlets when the cut fiber was placed in water. These fibers produced a compressibility curve of higher slope than all other nylon fiber runs, as demonstrated in Fig. 47.

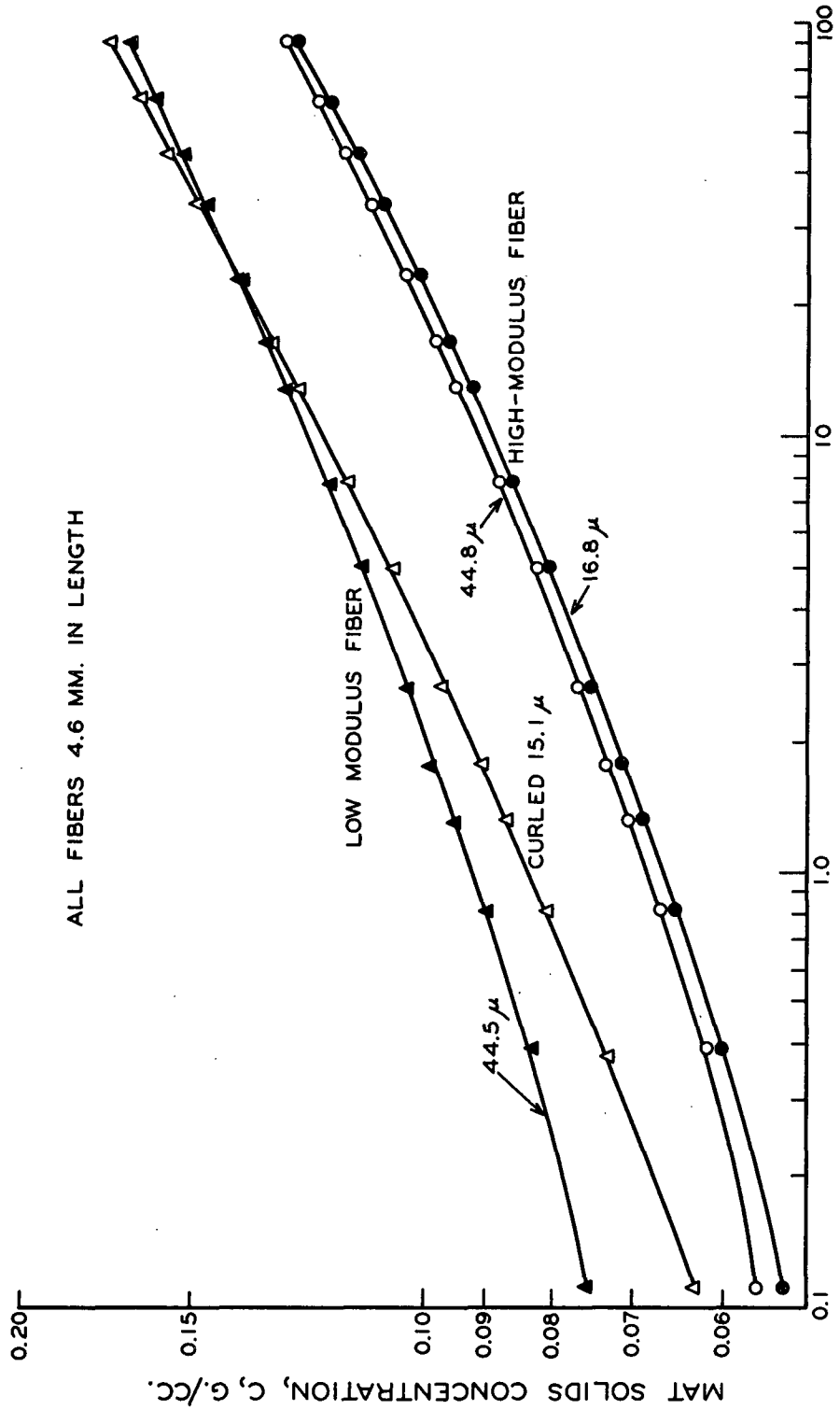

Figure 47. The Effect of Fiber Curl on the Slope of the Compressibility Curve for Nylon Fibers

APPENDIX IV

TESTS OF FIT OF SIMPLE BEAM EQUATIONS

In evaluating the equations based on simple beam theory, this discussion depends quite heavily upon the work done with model fiber networks (page 113 and following). Both the data from model network studies and data from nonwoven bed studies have been treated with a trial-and-error solution of Equation (18). Data taken on mechanically conditioned beds fit Equation (18), $\underline{C}^{1/\underline{N}} - \underline{C}_o^{1/\underline{N}} = \underline{MP}$, quite well over most of the load range, but the agreement is poor in the low load regions where the equation failed to predict the $\underline{C}_o$ values indicated by the data. A closer examination of the data for both model studies and filtration-formed beds showed that the data tended to follow a consistent trend, first to one side of the best straight line through the data and then to the other side over the whole range of loads tested. An example of this is shown in Fig. 39 and 44.

In the case of the nylon studies and the model network studies, the $\underline{C}_o$ values predicted from Equation (18) were all higher than those values indicated from the test data. Figure 44 shows this clearly for the model network, and Fig. 48 shows just the low load region for a nylon fiber bed. The similarity in deviation for the model and nylon fiber networks is interesting because it helps to support the view that there is a strong similarity between the model networks and the filtration-formed fiber beds. The type of deviation from the best straight line may be significant in terms of the mechanisms causing these deviations.

In the case of glass fiber beds, Equation (18) predicted negative values of $\underline{C}_o'^{1/\underline{N}}$ and therefore the corresponding values of $\underline{C}_o$ are meaningless.

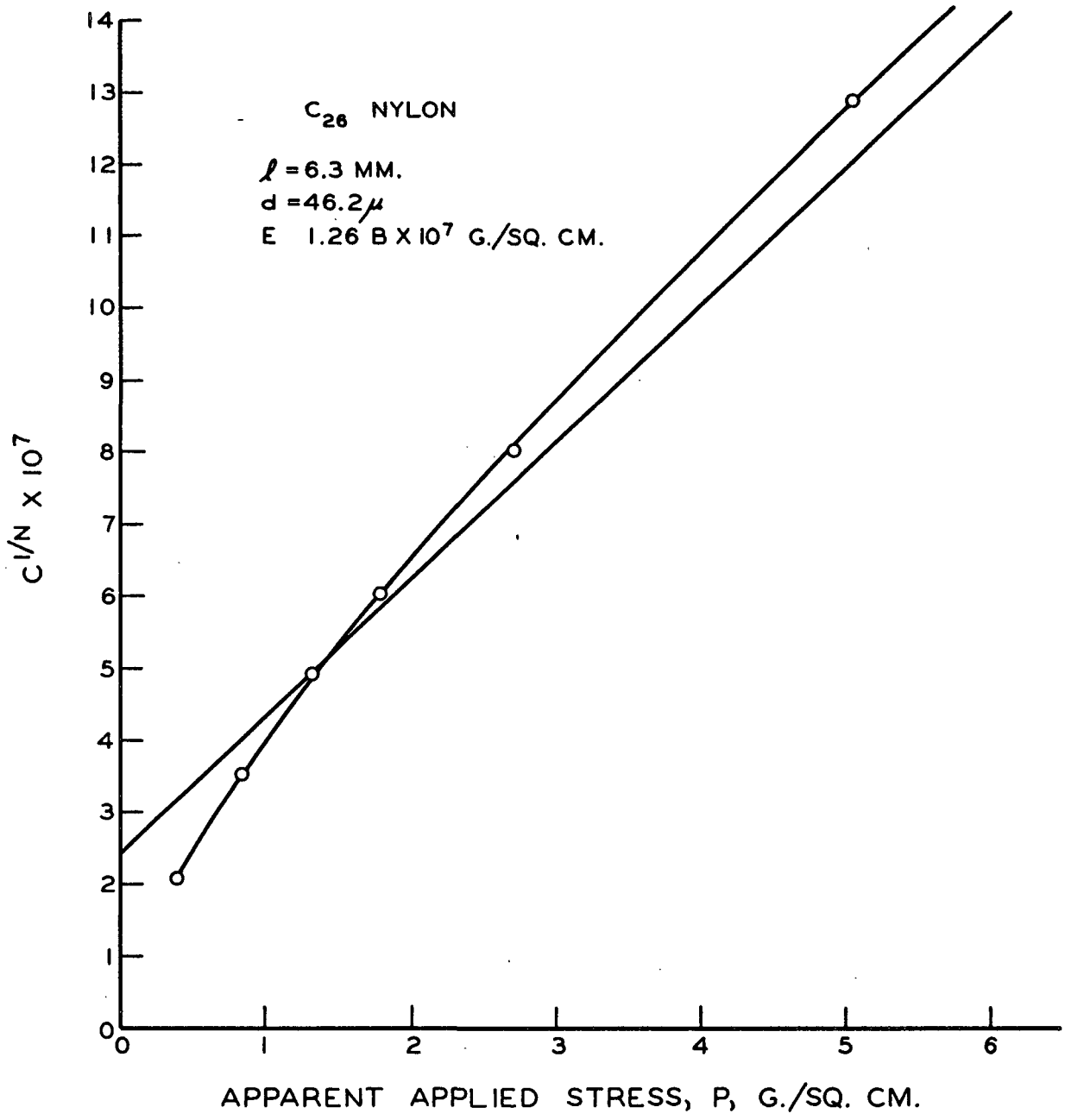

Figure 48. Fit of Mechanically Conditioned Compression Data at Low Applied Stress to the Equation $\underline{C}^{1/\underline{N}} - \underline{C}_o^{1/\underline{N}} = \underline{MP}$

APPENDIX V

MODEL NETWORK STUDIES

The results of the work carried out on model fiber networks has been presented in sketch form in Fig. 41 and 42. The plotted data from which the relative bed height vs. applied load curves were drawn are plotted in Fig. 49. The A_2 model bed had a distance of 1.5 cm. between fiber supports, while the A_1 bed had an element length of 3.4 cm. Bed B was a combination of these two. The fibers were approximately 1.5 mm. in diameter and 12 cm. in length.

DERIVATION OF EQUATIONS (19a)-(20)

Equations have been derived for the deformation of the model structures as a function of the applied stress. Only fiber bending is considered.

Consider a stacked fiber bed of the A type. The total number of fibers, N_{ft}, is given by:

$$N_{ft} = W/\pi r^2 \ell \rho \tag{22}$$

where W is the weight of fiber in the bed, r is the fiber radius, ℓ is the fiber length, and ρ is the fiber density.

The number of layers of fiber, n, may be written

$$n = N_{ft}/N_f = W/(\pi r^2 \ell \rho) N_f \tag{23}$$

where N_f is the number of fibers in a layer and a layer is one fiber

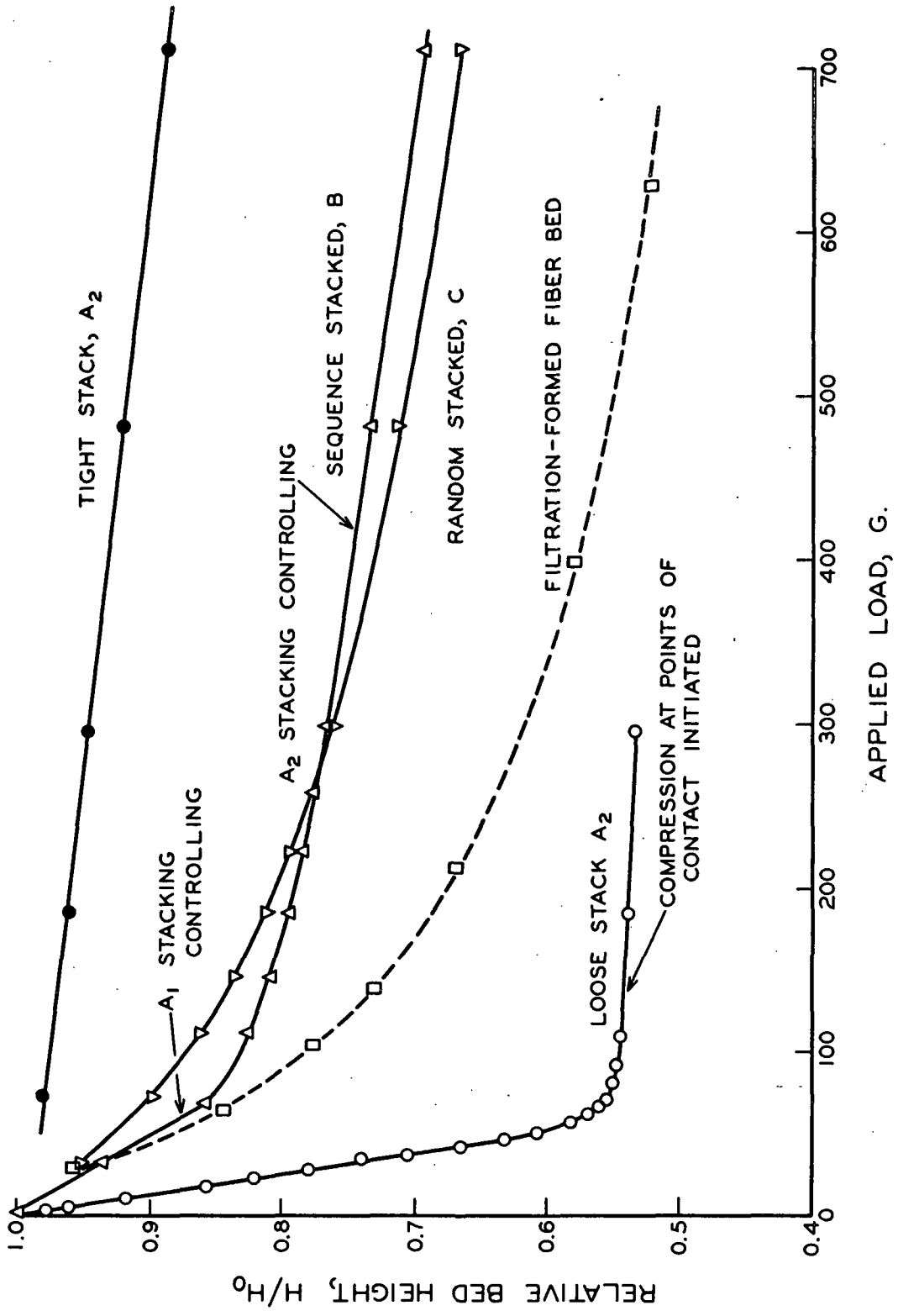

Figure 49. The Effect of Changes in Bed Stacking Type on Deformation Response

thick. The number of intersections, i, between two layers is equal to the number of supports, S, and is given by

$$i = S = N_f^2 \tag{24}$$

Therefore, considering an equal number of fibers per layer, the number of intersections per fibers, i_f, is

$$i_f = N_f \tag{25}$$

The element of fiber length between supports, b, is given by

$$b = \ell/(N_f - 1) \tag{26}$$

In this development, we are neglecting fiber ends.

If the total force applied to the bed is F and the force at a contact is F_c, then

$$F_c = F/N_f^2 \tag{27}$$

Since we know that in the early portions of deformation only fiber bending is taking place, we may write from beam theory

$$\Delta h = -F_c b^3/kEI \tag{28}$$

where Δh is the deflection of a beam, k is a constant depending on the type of beam support, E is the modulus of elasticity and I the moment of inertia.

In our case, the change in height of one fiber layer is the same as the deflection of one beam in the layer, provided the forces are distributed

evenly at the fiber-to-fiber contacts. Therefore, substituting for $\underline{F_c}$ and $\underline{b}$ in Equation (28) we find that

$$-\Delta h = [F/N_f^2][\ell/(N_f - 1)]^3/kE(\pi r^4/4) \tag{29}$$

where $\underline{I} = \pi \underline{r}^4/4$ for circular beams.

The total deformation for the bed, $-\Delta \underline{H}$, is equal to the sum of the deformations for each layer or

$$-\Delta H = n(-dh) = [W/\pi r^2 \ell \rho N_f \ell] \cdot [F/N_f^2] \cdot [\ell/(N_f - 1)]^3/\frac{kE\pi r^4}{4} \tag{30}.$$

Simplifying and remembering that $\underline{P} = \underline{F}/\underline{A}$ where $\underline{A}$ is the cross-sectional area of the bed, we may write

$$-\Delta H = [4W \cdot \ell^2/k\pi^2 r^6 \rho N_f^3 (N_f - 1)^3 E \cdot A] (P) \tag{31}.$$

Now, letting the term in the bracket be $\underline{M}$ and taking a differential change in height with a differential change in applied stress,

$$\int_{H_o}^{H} -dH = \int_{o}^{P} MdP \tag{32}$$

where $\underline{H} = \underline{H_o}$ at $\underline{P} = 0$. Integrating Equation (32), we obtain

$$H_o - H = MP \tag{19a}$$

Now, substituting $\underline{C} = \underline{W}/\underline{AH}$, we find that

$$\frac{1}{C_o} - \frac{1}{C} = M'P \tag{19b}$$

In a sequence-stacked arrangement such as bed B, there would be a different number of intersections per fiber depending upon the layer.

Therefore,

$$S = N_{f_1} \quad \text{for layer 2}$$
$$S = N_{f_2} \quad \text{for layer 1} \tag{33}$$

since the number of intersections between layers must be $\underline{N}_{f_1} \cdot \underline{N}_{f_2}$. The number of layers of each type given by equations similar to Equation (23),

$$n_1 = \frac{N_{ft_1}}{N_{f_1}} = W_1/\pi r^2 \ell \rho N_{f_1} \tag{34}$$

and a similar relationship exists for layer 2. The element length for fibers in layer 1 is given by

$$b_1 = \ell/(N_{f_2} - 1)$$

and in layer 2

$$b_2 = \ell/(N_{f_1} - 1) \tag{35}.$$

Proceeding as before and combining deflections for the two types of layers, we may write

$$-\Delta H_t = (-\Delta H_1) + (-\Delta H_2) = \frac{4\ell^2}{K\pi^2 r^6 \rho E A N_{f_1} \cdot N_{f_2}} \left[\frac{W_1}{N_{f_1}(N_{f_2} - 1)^3} + \frac{W_2}{N_{f_2}(N_{f_1} - 1)^3}\right] P \tag{36}.$$

Simplifying for integration, we obtain

$$-\int_{H_o}^{H} dH_t = K_a(M_1 + M_2) \int_o^P dP \tag{37},$$

and integration would lead to

$$\frac{1}{C_o} - \frac{1}{C} = K_a(M_1 + M_2)P \qquad (19c)$$

K_a, M_1, and M_2 are constants.

Using the same approach, one could write a general equation for many combinations of stacking types which would lead to the integrated form

$$\frac{1}{C_o} - \frac{1}{C} = K_b(M_1 + M_2 + M_3 + \ldots M_n)P \qquad (20).$$

Finally, the reader is referred to Fig. 50 to see the relationships between mat solids concentration and applied stress for two different types of bed stacking. It has already been mentioned that the behavior shown is similar to that brought about by a change in fiber length for filtration-formed beds. These data are sketched in Fig. 42, Section 1.

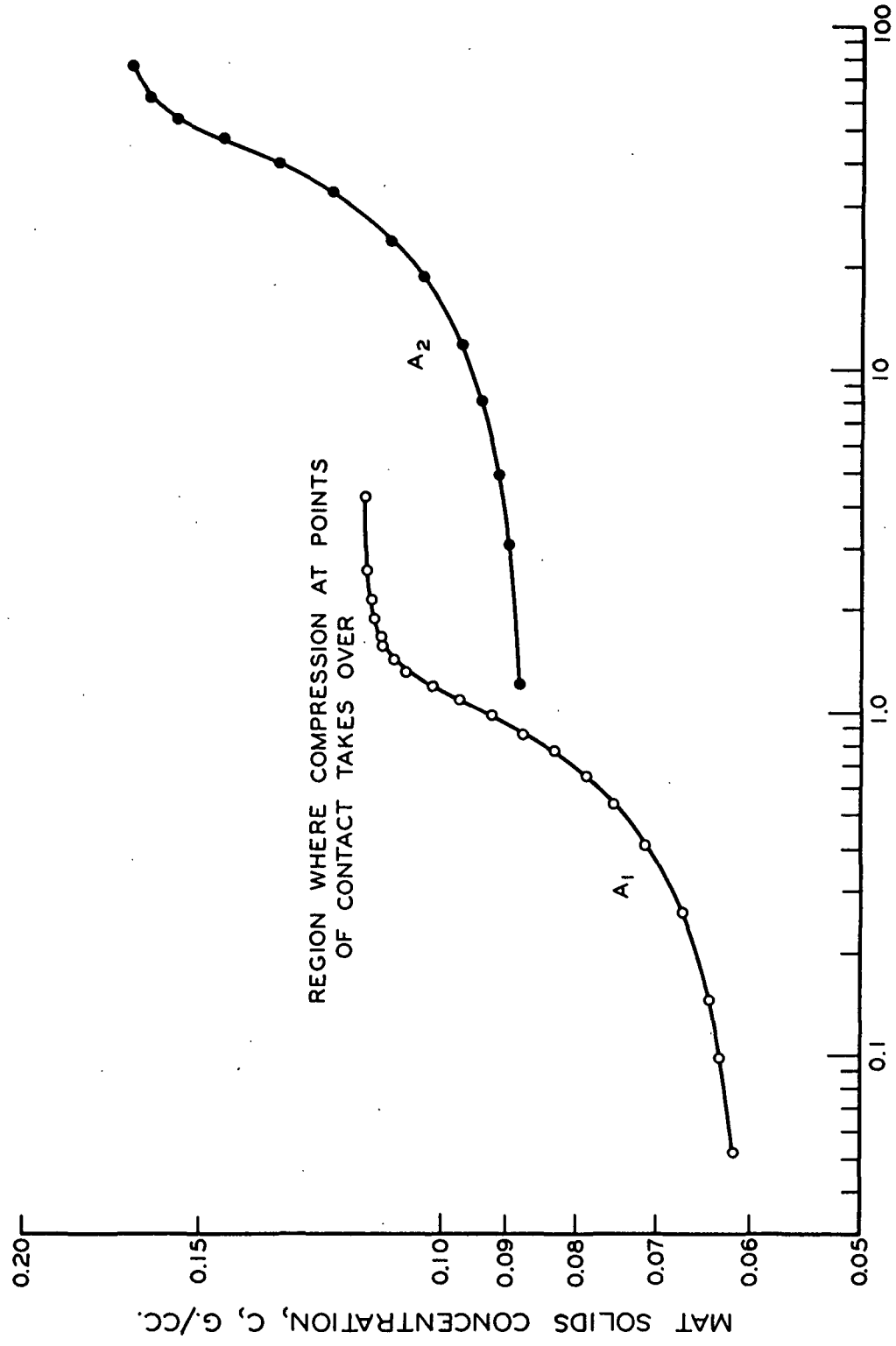

Figure 50. Mat Solids Concentration vs. Apparent Applied Stress for Model Fiber Networks